8-2012

Hydrologic Modeling to Examine Land Use Change Impacts (1970's and 2005) on the Sediment Yield and Flow Regime in Cayuga Creek, Niagara County, New York

Kimly Reth
State University of New York College at Buffalo, rkimly@yahoo.com

Advisor
Dr. Kimberley Irvine, Professor of Geography and Planning
First Reader
Dr. Kimberley Irvine, Professor of Geography and Planning
Second Reader
Dr. Kelly Frothingham, Chair and Associate Professor, Geography and Planning
Third Reader
Dr. Stephen Vermette, Professor, Geography and Planning

To learn more about the Geography and Planning Department and its educational programs, research, and resources, go to http://graduateschool.buffalostate.edu/multidisciplinary-studies.

Hydrologic Modeling to Examine Land Use Change Impacts (1970's and 2005) on the Sediment Yield and Flow Regime in Cayuga Creek, Niagara County, New York

By

KIMLY RETH

An Abstract of a Thesis
in
Multidisciplinary Studies

Submitted in Partial Fulfillment
of the Requirements for the Degree of

Master of Science

August 2012

State University of New York
College at Buffalo

ABSTRACT OF THESIS

Hydrologic Modeling to Examine Land Use Change Impacts (1970's and 2005) on the Sediment Yield and Flow regime in Cayuga Creek, Niagara County, New York

ABSTRACT- This research aims to assess the water quality and the land use change impacts on sediment concentration and flow regime in Cayuga Creek, Niagara County, NY for two land use periods, 1970's and 2005. The 1970's land use, classified by the USGS, had a significant error. Therefore, the scenario of sediment yield and discharge level to land use change is more of a "what if" since the 1970's land use was classified incorrectly. The Soil and Water Assessment Tool (SWAT)was used to simulate flows and sediment concentrations for the two land use scenarios using the same rainfall data at the upstream and downstream sites. The modeling results indicated that the discharges at the downstream site were higher than those at the upstream site for both 1970's and 2005 land uses. The sediment concentration was higher at the downstream site than the upstream site for 1970's land use and the result was in an opposite direction for 2005 land use. Hydrolab Datasonde 4a's were installed at an upstream and downstream site for a ten week period in order to assess water quality. The parameters monitored were: dissolved oxygen, pH, conductivity, turbidity, and temperature. Grab samples were taken in order to examine total suspended solids levels and establish a relationship with turbidity.

Kimly Reth

August, 2012

State University of New York
College at Buffalo

Hydrologic Modeling to Examine Land Use Change Impacts (1970's and 2005) on the Sediment Yield and Flow Regime in Cayuga Creek, Niagara County, New York

A Thesis in
Multidisciplinary Studies

By

Kimly Reth

Submitted in Partial Fulfillment
of the Requirements
for the Degree of

Master of Science
August 2012

Approved by:

Kim Irvine, Ph.D.
Professor, Department of Geography/Planning
Thesis Advisor

Kevin Railey, Ph.D.
Associate Provost and Dean of the Graduate School

ACKNOWLEDGMENTS

I would like to dedicate the success of this thesis to my family back home in Cambodia for their support and encouragement. I would like to thank Dr. Irvine, my supervisor and my academic advisor for his invaluable advice and his kind supervision throughout my academic program and this research. I would like to thank dearly Dr. Fredericks for his advice and mental support throughout the difficult times and for never stopping to believe in me. Last but not least, I would like give my gratitude to Mary Perrelli for providing me assistance with GIS and modeling processes. I also would to dedicate this thesis to Mrs. Eleanor Blackburn for her warmest love and support for me and other international students.

TABLE OF CONTENTS

LIST OF FIGURES

LIST OF TABLES

LIST OF ACRONYMS

Units of Measure

°C	Celsius
Cfs	Cubic ft per second
cm	Centimeter
°F	Fahrenheit
L	Liter
mg	Milligram
msl	Mean sea level
NTU	Nephelometric Turbidity Unit

Others

AGWA	Automated Geospatial Watershed Assess
AHPS	Advanced Hydrologic Prediction Service
AOC	Area of Concern
BASINS	Better Assessment Science Integrating Point and Nonpoint Sources
BOD	Biochemical Oxygen Demand
CSO	Combined Sewer Overflow
DDT	Dichloro-Diphenyl-Trichloroethane
DEM	Digital Elevation Model
DO	Dissolved Oxygen
ENCRPB	Erie and Niagara Counties Regional Planning Board
EURSEM	European Soil Erosion Model
FAO	Food and Agriculture Organization
GIRAS	Geographic Information Retrieval and Analysis System

HRAP	Hydrologic Rainfall Analysis Project
HRU	Hydrologic Response Unit
HSPF	Hydrological Simulation Program Fortran
BMPs	Best Management Practice
NCDPDT	Niagara County Department of Planning, Development & Tourism, now called Niagara County Department of Economic Development
NCSWCD	Niagara County Soil and Water Conservation District
NFARS	Niagara Falls Air Reserve Station
NHD	National Hydrography Dataset
NOAA	National Oceanographic and Atmospheric Administration
NPP	Niagara Power Project
NRCS	Natural Resource Conservation Service
NYPA	New York Power Authority
NYSDEC	New York State Department of Environmental and Conservation
NYSDOH	New York State Department of Health
NWS	National Weather Service
OAR	Ocean and Atmospheric Research
OMOE	Ontario Ministry of the Environment
OPG	Ontario Power Generation
PAH	Polynuclear Aromatic Hydrocarbon
PCB	Polychlorinated Biphenyl
PCS	Permit Compliance System
PEC	Probable Effects Concentrations

PLOAD	Pollutant Loading Model
RAP	Remedial Action Plan
RCRA	Resource Conservation and Recovery Act
RF1,3	Reach File Version 1, 3
RIBS	Rotating Intensive Basin Survey
SAV	Submergent Aquatic Vegetation
SDR	Sediment Delivery Ratio
SSO	Sanitary Sewer Overflow
STATSGO	State Soil and Geographic Database
SVAP	Stream Visual Assessment Protocol
SWAT	Soil and Water Assessment Tool
TAES	Texas Agricultural Experiment Station
TEC	Threshold Effects Concentration
TMDL	Total Maximum Daily Load
TNT	Trinitrotoluene
TRI	Toxics Release Inventory
USACE	U.S. Army Corps of Engineers
USDA	U.S. Department of Agriculture
USEPA	U.S. Environmental Protection Agency
USFWS	U.S. Fish and Wildlife Service
USGS	U.S. Geologic Survey
WEPP	USDA Water Erosion Prediction Project

CHAPTER 1

1 INTRODUCTION

1.1 Background

Prediction of effects of land use and land cover change on water quantity and water quality are related to a number of issues, for instance the possible effects of land use changes on soil erosion. Urbanization is the prevalent factor contributing to the disturbance of the natural environment, landscape dynamics and eventual replacement of vegetated surfaces with impervious surfaces. Increasing population, inequality in societies, and deforestation has resulted in practices unsuitable for crop production and which ultimately results in soil erosion. Global climate change and variability of precipitation patterns are direct and indirect factors contributing to soil erosion. Soil erosion is considered a potential cause of pollution of water bodies (Lorup and Styczen, 1996).

Soil erosion models are commonly used to simulate erosion rates by examining various factors involved, e.g. crop rotation, runoff, to determine the consequences and the alternatives that may reduce this soil loss (Almoza et al., 2007). Chemicals transported on sediment, such as fertilizers and pesticides, are controlled by regional land uses in dominantly agricultural areas, and other processing chemicals, heavy metals, and other manufacturing wastes in dominantly industrial areas (Toy et al., 2002).

1.2 Objectives

The aim of this study was to examine the impacts of land use change on the sediment yields and flow regime of the Cayuga Creek watershed, Niagara County, New York by using a watershed hydrologic modeling tool called Soil and Water Assessment Tool (SWAT) model.

There are two different land use scenarios in this study: the 1970's as classified by U.S. Geological Survey and the land use data for 2005.

In this research project, the Soil and Water Assessment Tools (SWAT) was used to model the soil erosion of the Cayuga Creek watershed. The approaches to the problem were: (1) delineate the watershed boundary using the automatic delineation tool in BASINS, (2) collect water quality data of the Cayuga Creek watershed using Hydrolab datasondes, (3) evaluate land use change from the 1970's and 2005 using GIS and air-photo imageries, (4) construct the SWAT model and simulate the flows and sediment yields for the 1970's and 2005 land use and assess the impact of land use change.

CHAPTER 2

2 STUDY AREA

2.1 Description of Study Area Physical Characteristics

Cayuga Creek is one of the tributaries to the upper Niagara River in Niagara County, western New York. It is approximately 10.5 miles (16.9km) long and has a drainage basin area of approximately 35 mi^2 (91 km^2). Its headwaters originate in the Town of Lewiston, NY. The creek flows southwest through the Tuscarora Indian Reservation, and into the Town of Wheatfield. It then flows across the Niagara Falls International Airport-Air Force Base Complex, and subsequently is joined by Bergholtz Creek downstream of Niagara Fall Boulevard. Ultimately it enters the Little Niagara River (Figure2-1).

The Natural Resource Conservation Service (NRCS) and the New York State Department of Environmental Conservation (NYSDEC) include Cayuga and Bergholtz Creek in the Niagara River-Tonawanda Creek watershed, which is located in Western New York State approximately covering an area of 514,810 acres (2083 km^2) over part of five counties: Erie, Niagara, Genesee, Wyoming and a small part of Orleans (NYPA, 2005).

Information related to the Cayuga Creek watershed was assessed during the relicensing effort for the Niagara Power Project. In 2005, the New York Power Authority (NYPA) assessed the ecological condition of Fish, Gill, and Cayuga Creeks for the Niagara Power Project. A summary report on the Cayuga Creek watershed assessment was done also by the NYPA for the Buffalo Niagara Riverkeeper.

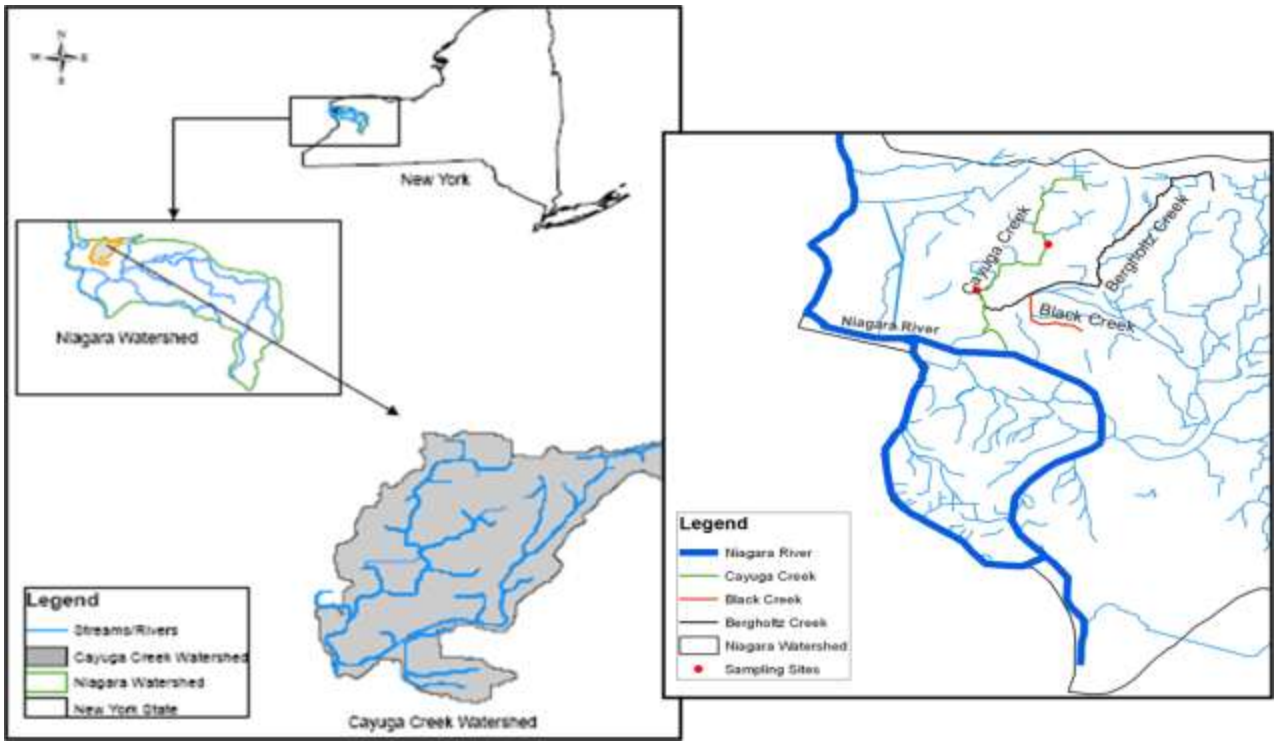

Figure 2-1. Cayuga Creek watershed in Niagara County, NY.

2.1.1 Geology

The bedrock consists of Lockport Dolomitic Limestone, the Queenston and Rochester Shale (USDA, 1972). The surficial geology of the watershed was formed in the glacial material that was deposited during and shortly after the ice age. Final deglaciation of the Great Lakes region began approximately 17,000 years ago and by 14,500 years ago the first of many large meltwater lakes (Lake Maumee) formed in the western half of the present Erie basin (Chapman and Putnam, 1973; Prest, 1981). Small parts of the Cayuga Creek watershed contain glacio-lacustrine silt and clay deposits, but most of the watershed consists of loamy glacial till deposits above the bedrock. The maps of surface geology and bedrock of the Cayuga Creek watershed are represented in Figure 2-2 and Figure 2-3.

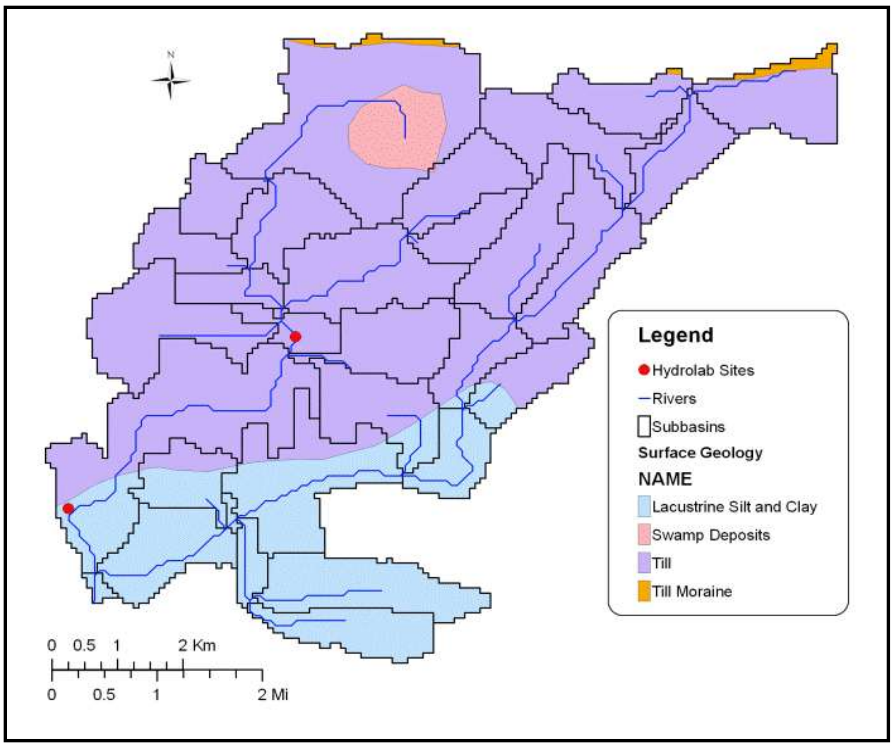

Figure 2-2. Map of surface geology, Cayuga Creek watershed.

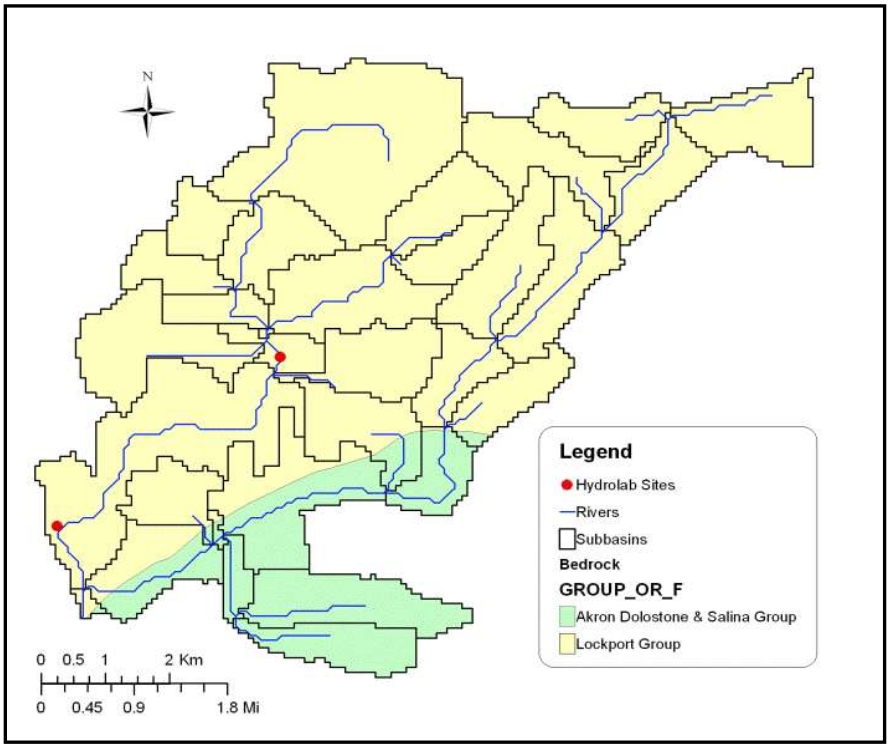

Figure 2-3. Bedrock map of Cayuga Creek watershed, Akron Dolostone & Salina Group- 400 to 700 ft (120-210m) thick and Lockport Group-150 to 200 ft. (45-60m) thick.

2.1.2 Soils

Soils of the Cayuga Creek watershed consist of the Hilton-Ovid-Ontario association, the Odessa-Lakemount-Ovid association, and the Canandaigua-Raynham-Rhineback association. The Hilton-Ovid-Ontario association consists of soils that are deep, moderately well-drained and medium textured. These soils formed in calcareous glacial till containing sandstone and limestone fragments (USDA, 1972). The Odessa-Lakemount-Ovid association consists of deep, somewhat poorly drained, moderately fine texture soils. These soils formed in lacustrine deposits in which calcareous clay is dominant. The Canandaigua-Raynham-Rhineback association includes soils that are deep, poorly drained and very poorly drained and have dominantly medium-textured to fine-textured subsoils. These soils formed in lacustrine deposits of silt, very fine sand, and clay. They are level or depressional and occupy areas where water ponds or runs off very slowly (USDA, 1972).

The U.S. Department of Agriculture Soil Conservation Service has mapped these soils and classified them as to permeability (Higgins et al. 1972). Most of the soils in the Cayuga Creek basin are derived from glacial lake sediments and are characterized by high density, poor tilth (tillability), and very poor drainage (NYPA, 2006). Map soil classification based on State Soil Geographic (STATSGO) database for Cayuga Creek watershed is shown in Figure 2-4.

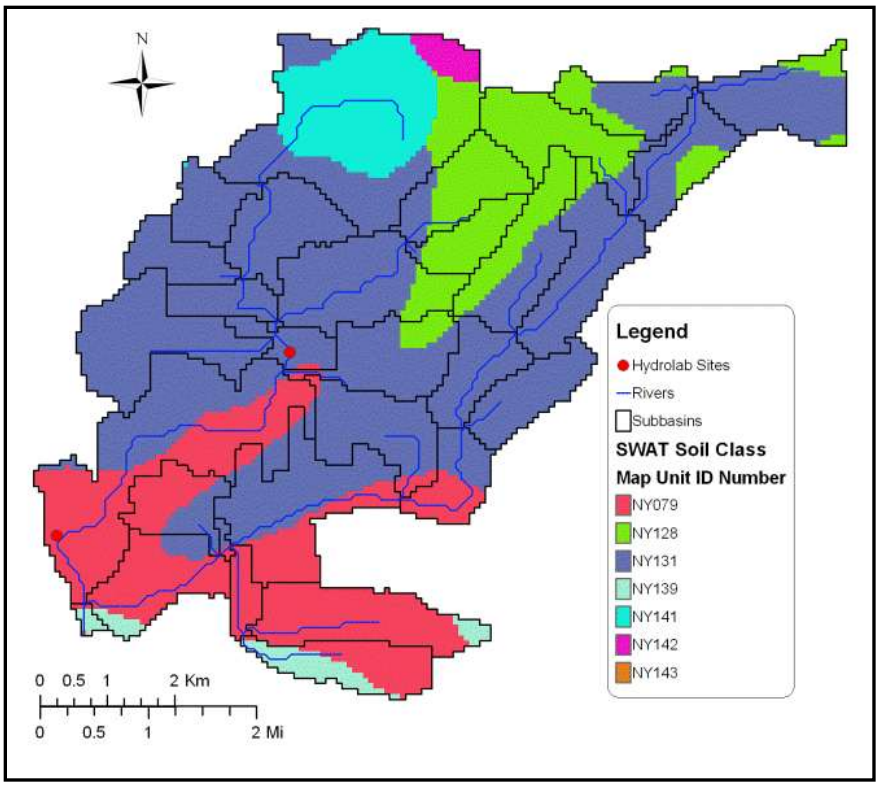

Figure 2-4. Map of soil, Cayuga Creek watershed (STATSGO).

2.1.3 Topography

According to ENCRPB (1975), the Cayuga Creek drainage basin is quite flat. The average gradient along Cayuga Creek is 8.6 ft/mi (1.6 m/km). Much of this relief is traversed in the upper 2 miles (3.2 km) of the watershed, so that lengthy stretches in the lower basin exhibit gradients of less than 4 ft/mi (0.76 m/km). This low relief is attributable to the geologic history of the basin. The creek headwaters flow off the Niagara Escarpment across the Huron Plain, which has at various times been inundated by glacial lakes. Massive deposits of dense, extremely fine-grained lacustrine (lake-derived) clays blanket the area, leveling irregularities in the bedrock (ENCRPB, 1975). The Digital Elevation Model map of Cayuga Creek watershed is shown in Figure 2-5.

Cayuga Creek is a slightly meandering system originating in flat topography at an elevation near 625 ft (190 m) mean sea level (msl). Progressing southward the creek continues into relatively level topography and it takes on characteristic flows as it meanders through a relatively defined main channel and a mosaic of lowland floodplain landscapes. The creek courses through this level landscape where it eventually converges with the Little River approximately 10 miles (16 km) from its source. Elevations range from approximately 625 ft (190 m) at the headwaters to approximately 560 ft (171 m) at the Niagara River confluence in the City of Niagara Falls (USACE, 2002).

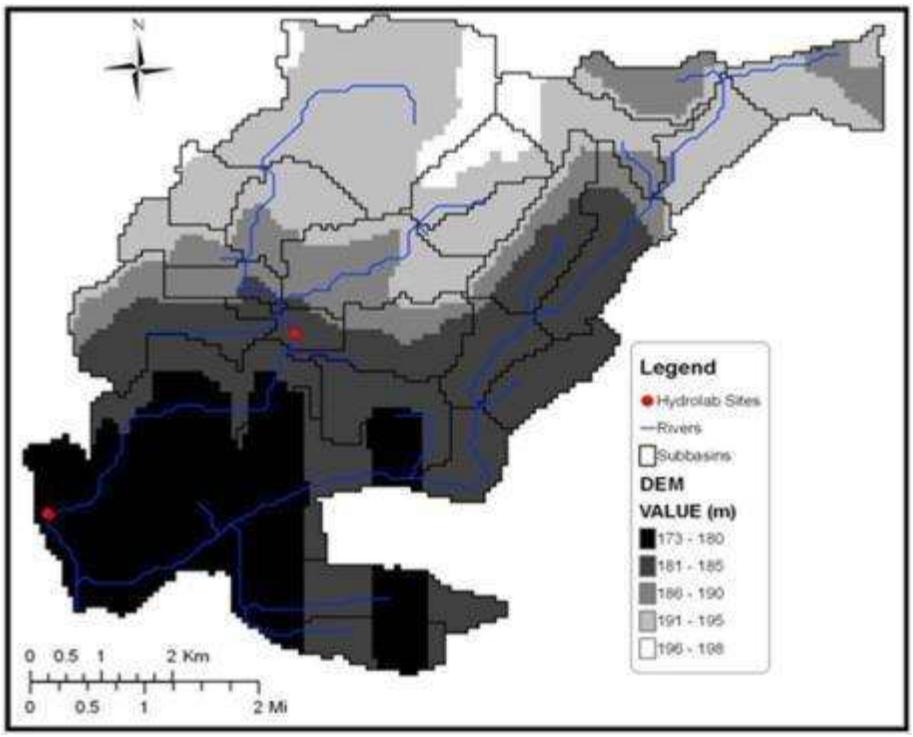

Figure 2-5. Digital Elevation Models of Cayuga Creek watershed, USGS 300 Meter Resolution, 1-Degree DEM (Originator- U.S. EPA Agency).

2.2 Wetlands

The Cayuga Creek watershed had experienced the loss of wetlands due to the historical channel alterations of Cayuga and Bergholtz Creeks. Federal and NYSDEC jurisdictional depressional and riverine freshwater wetlands are located throughout the watershed. The most notable New York state and Federal wetlands are located at the creek headwaters west of Bridgeman Road and north of Saunders Settlement Road in the Town of Lewiston. There are two types of GIS layers of wetlands (Figure 2-6 and Figure 2-7), those identified by the U.S. Fish and Wildlife Service and regulated by the U.S. Army Corps of Engineers, and those identified by the New York State Department of Environmental Conservation (NYPA, 2005).

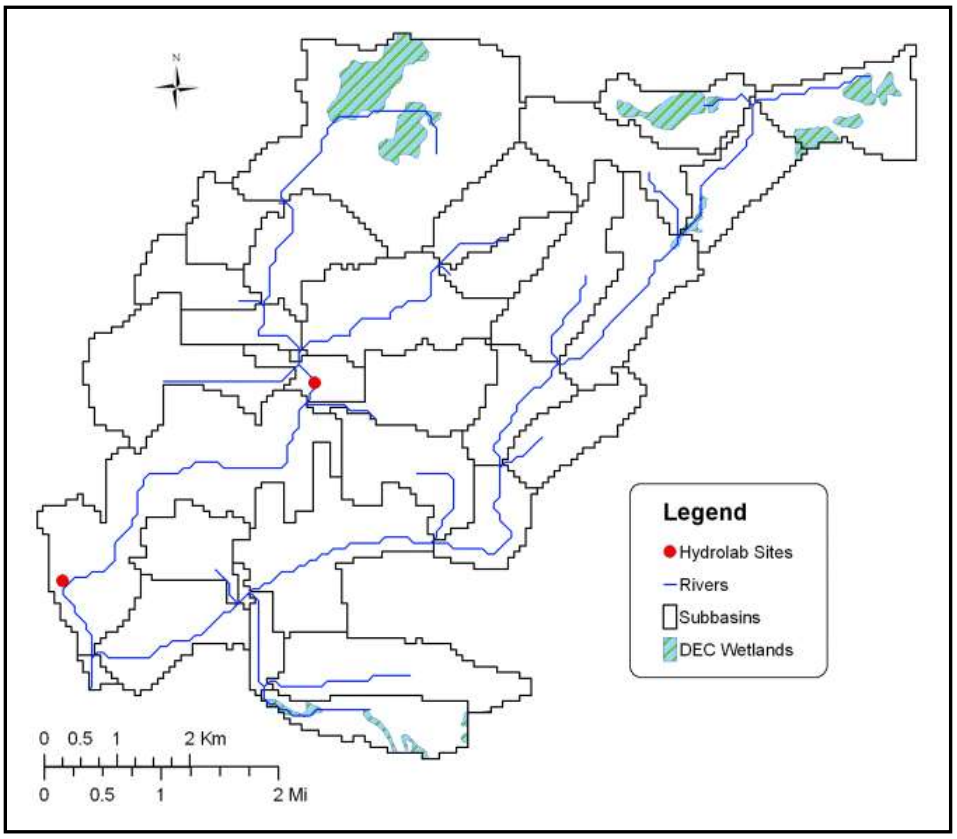

Figure 2-6. NYSDEC wetlands, New York State Department of Environmental Conservation.

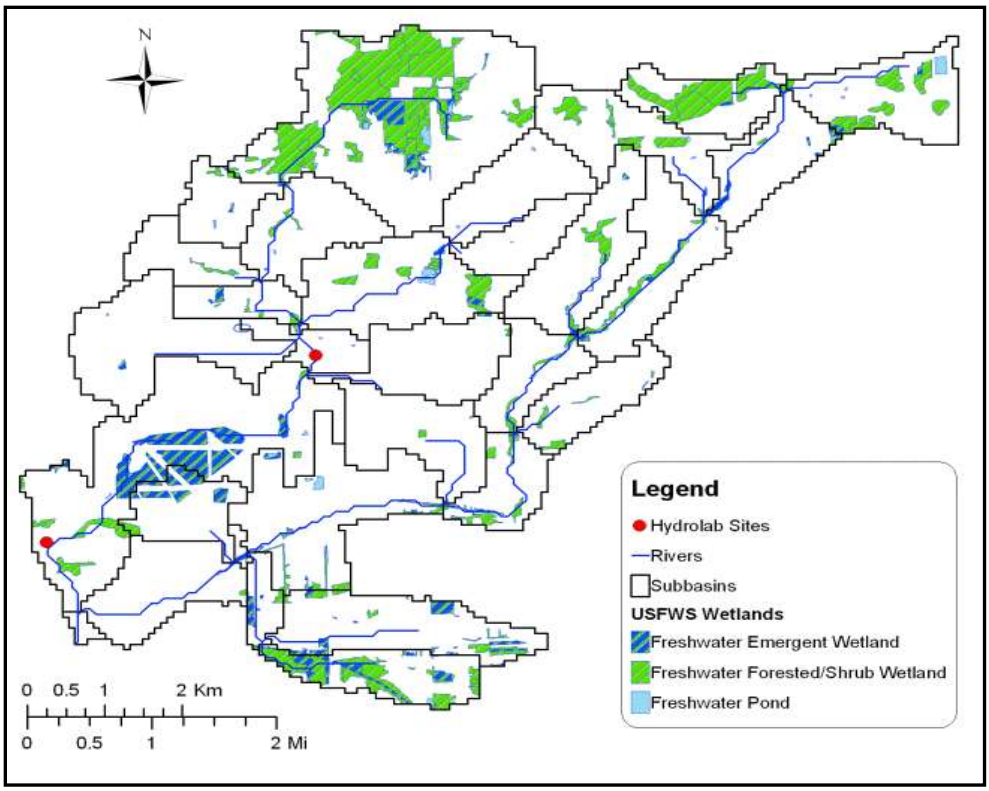

Figure 2-7. Map of USFWS wetlands located within Cayuga Creek (Originator: U.S. Fish and Wildlife).

2.3 Climate

Based on a first-order weather station, which is located at the Buffalo-Niagara International Airport at about 16 miles southeast of the watershed, the mean annual precipitation is 36.19 inches (995.43 mm). The maximum monthly average is 3.28 inches (83.31 mm) in December. The mean monthly rainfall data from 1920 to 1995 and from 1961 to 1990 are listed on Table 2-1. The average annual snowfall is 91.1 inches (2.31 m) at this station. The highest average monthly snowfall is 24.2 inches (614.68 mm) in January. The average temperature, as recorded at the Buffalo Weather station, is 47.4 ºF (8.5 ºC). The warmest month is July and the coldest month is February, with the mean monthly temperature of 70.5 º F (21.3 ºC) and 24.8 ºF

(-4 ºC) respectively (USACE 2002). The average maximum, average minimum and 24-hours average temperature data from 1961 to 1990 are shown in Table 2-2.

Table 2-1. Average Rainfall at Weather Station Lockport 2 Ne, Niagara County (NCDC Cooperative Station).

	Jan	Feb	Mar	Apr	May	Jun	Jul	Aug	Sep	Oct	Nov	Dec	Year
From 1920-1995													
mm	60.9	57.2	63.9	72.4	77.5	77.3	74.9	83.0	82.4	70.2	79.4	69.0	869.0
inches	2.4	2.3	2.5	2.9	3.1	3.0	2.9	3.3	3.2	2.8	3.1	2.7	34.2
From 1961-1990													
mm	61.4	58.6	67.8	80.0	75.1	85.8	72.3	98.8	92.7	71.8	92.4	84.5	941.8
inches	2.4	2.3	2.7	3.1	3.0	3.4	2.8	3.9	3.6	2.8	3.6	3.3	37.1

Table 2-2. Average Temperature at Weather Station Lockport 2 Ne, Niagara County (NCDC Cooperative Station).

Average Maximum Temperature from 1961-1990													
°C	-0.6	0.6	6.1	13.5	20.1	24.8	27.4	26.0	21.9	15.7	8.8	2.1	13.8
°F	30.9	33.1	43.0	56.3	68.2	76.6	81.3	78.8	71.4	60.3	47.8	35.8	56.8
24-hr Average Temperature from 1960-1990													
°C	-4.7	-3.9	1.1	7.6	13.8	18.8	21.6	20.5	16.5	10.6	4.6	-1.6	8.7
°F	23.5	25.0	34.0	45.7	56.8	65.8	70.9	68.9	61.7	51.1	40.3	29.1	47.7
Average Minimum Temperature from 1961-1990													
°C	-8.8	-8.5	-3.8	1.7	7.6	12.7	15.7	14.9	11.1	5.5	0.5	-5.4	3.6
°F	16.2	16.7	25.2	35.1	45.7	54.9	60.3	58.8	52.0	41.9	32.9	22.3	38.5

2.4 Hydrology, Hydraulics of Cayuga Creek Watershed

The Cayuga Creek basin does not have a stream flow gauging station. Hence historical flow data are not available for the Cayuga Creek. ENCRPB (1975) conducted a comparison with

similar creeks in a hydrologically similar basin in order to estimate flows in Cayuga Creek. The prorated estimated flow was done using the Cayuga Creek drainage basin of 34.1 square miles (88.3 km^2) compared to the Little Tonawanda Creek flow statistics. The details are described in the ENCRPB (1975).

The annual and monthly (10%, 30%, 50%, 70%, and 90%) flow exceedances for Cayuga Creek were established using a multiple regression approach based on drainage area, precipitation data and observed daily mean flow from the USGS gauge stations located on unregulated streams in the Niagara River region (URS et al., 2005a). Estimated annual median flow (50% flow exceedance) using the multiple regression approach for Cayuga Creek is 27.5 cfs (0.78 m^3s^{-1}) and the monthly median flow ranges from 7.1 cfs (September) to 91.3 cfs (March), (0.2-2.58 m^3s^{-1}) (Table 2-3). This estimation includes the estimated flow from Bergholtz Creek that enters Cayuga Creek approximately 5,600 ft(1.7 km) upstream of Cayuga Creek's confluence with the Upper Niagara River (Table 2-4). The estimated annual median flow of Cayuga Creek upstream of Bergholtz Creek confluence using the multiple regression method is 10.7 cfs (0.302m^3s^{-1}). Annual median flow at Bergholtz Creek is 17.7 cfs (0.5 m^3s^{-1}) and the monthly median flow ranges from 4.4 cfs (September) to 59.6 cfs (March), (0.12-1.68 m^3s^{-1}). These flows would indicate the total amount of runoff at the mouth of each creek without input from wastewater discharges or other man-made inputs (URS et al., 2005a).

Table 2-3. Estimated flow exceedances (cfs) for Cayuga Creek determined using multiple regression analysis (between drainage area and precipitation), (URS et al.,2005a).

Month	10% Flow Exceedance	30% Flow Exceedance	50% Flow Exceedance	70% Flow Exceedance	90% Flow Exceedance
January	157.0	62.6	42.1	31.5	21.2
February	210.6	78.9	46.8	36.3	23.5
March	278.9	143.8	91.3	58.3	41.9

April	193.1	93.6	62.9	49.0	37.9
May	76.0	37.4	28.7	22.3	19.2
June	41.3	18.7	15.5	13.9	10.0
July	19.4	13.0	10.4	8.1	6.3
August	19.3	11.2	8.7	6.8	4.7
September	23.9	9.4	7.1	5.9	4.4
October	44.0	14.5	7.9	6.1	5.6
November	87.9	38.2	22.3	15.0	9.3
December	142.3	64.9	40.8	28.4	16.6
Annual	120.1	47.1	27.5	13.9	6.5

Table 2-3. Estimated flow exceedances (cfs) for Bergholtz Creek determined using multiple regression analysis (between drainage area and precipitation), (URS et al.,2005a).

Month	**10% Flow Exceedance**	**30% Flow Exceedance**	**50% Flow Exceedance**	**70% Flow Exceedance**	**90% Flow Exceedance**
January	103.1	40.9	27.7	21.1	14.5
February	142.1	53.5	31.4	24.9	16.5
March	178.9	93.5	59.6	38.1	28.6
April	119.9	57.3	38.5	30.7	24.5
May	45.1	22.3	17.6	13.8	12.5
June	24.3	11.1	9.6	9.0	6.6
July	11.3	8.0	6.6	5.2	4.2
August	11.9	7.1	5.6	4.4	3.1
September	14.7	5.7	4.4	3.8	2.9
October	27.2	8.7	4.7	3.8	3.7
November	55.3	23.6	13.7	9.4	6.1
December	93.8	42.2	26.2	18.4	10.9
Annual	76.3	30.0	17.7	8.9	4.2

The ENCRPB (1975) conducted a flow measurement study for Cayuga Creek. The channel was cross-sectioned at selected locations including 10 of 11 water quality sampling points and three significant segments of constriction. Flow velocity measurements were conducted at various sites. The discharges were derived from the measured velocities and calculated cross-sectional areas. The results indicated that the flow in Cayuga Creek is approximately 8cfs (0.226 m^3s^{-1}) at Porter Road Bridge; the flow in Bergholtz Creek was estimated to be approximately 14

cfs (0.396m^3s-1) at the upstream of the confluence (91st Street Bridge). These two flows with additional downstream drainage yielded an estimated flow of 25 cfs (0.707 m^3s^{-1}) at the mouth on the day of sampling.

Erosion and sedimentation issues were stated in the NYPA (2006) report. The issues associated with erosion occurred particularly in the Niagara Falls area. The major factors contributing to these issues are the channelization, channel modification, concentrated point source discharges, loss of riparian zone and vegetation cover, altered hydrological characteristics and fluctuations of water level due to the development of the Niagara River.

Water and sediment quality of Cayuga, Bergholtz and Black Creek is primarily affected by the discharge from Love Canal as has been documented for example by NYSDEC,1993; 1996; 2002; 2006); Ontario Ministry of Environment, (1997); USEPA, (1982; 1999). The Cayuga and Bergholtz Creeks are classified as Class C waterbodies by the NYSDEC, which is best used for fishing. The section from Walmore Road to its mouth is listed on New York State's Priority Waterbodies List (NYSDEC, 1998).

The NYPA (2006) stated that the hazardous waste sites are noted as the main factor contributing to historical sediment contamination. Dioxin contaminated sediment was dredged from Cayuga and Bergholtz Creeks in 1989. Irvine and Perrelli (2006) conducted dioxin mapping for the Cayuga Creek. The dioxin map is represented in Figure 2-9. The dredging process of dioxin contaminated sediment from Bergholtz Creek was performed in the late 1980's. The dredging began at Bergholtz Creek's mouth and extended upstream about 1.5 miles and the dredged materials were disposed at an offsite commercial disposal facility (NCDPDT, 1997).

Since 1980, the Ontario Ministry of the Environment (OMOE) has conducted biomonitoring in the Niagara River to assess long-term trends in contaminant loadings to the Niagara River. The sampling in 1997 showed that dioxins and furans detected in mussels deployed near the 102nd Street Landfill were low and revealed the success of the site remediation and removal of the contaminated sediment. At this site, dioxins and furans were not detected in the sediment samples (Richman, 1999).

Figure 2-8. Dioxin map (ng/g) of Cayuga Creek (Irvine and Perrelli, 2006).

CHAPTER 3

3 SOIL EROSION

3.1 Introduction

Soil erosion is recognized as a serious environmental issue, caused not just by agriculture but all forms of land disturbing activities (Toy et al., 2002). As the population of the United States has increased and shifted from rural to urban residential, commercial and industrial land use with corresponding increases of highway construction, the natural land surface has been disturbed. These disturbances have caused the temporary increase of erosion and sedimentation rates in waterways and the increase of runoff rates and volumes by increasing the proportion of the impervious surface (Wolman and Schick, 1967; Schueler,1994; Arnold and Gibbons, 1996). Contaminants such as heavy metals, PCBs, PAHs and some pesticides also may be adsorbed to eroded sediment (Kelly et al.,1996; Mielke et al., 1999; Ottesen and Langedal, 2001; Mielke et al., 2004).

Constituents of runoff may adversely impact rivers, lakes, and aquifers. For example, soil losses from unprotected construction sites are reported to be 150-200 tons per acre per year(5044 - 6725kg per m^2per year), while the average natural rate of soil erosion is approximately 0.2 tons per acre per year (6.7kg per m^2 per year)(Smoot et al., 1992). Soil and water conservation planning requires knowledge of the relations between factors that cause loss of soil and water and those that help to reduce such losses.

Soil erosion is increasingly being recognized as a hazard in European countries, in particular in the Mediterranean area and on the loamy, sandy loamy, and sandy soils of northern Europe (Refsgaard, 1996).In the1930s, erosion caused by wind and water was recognized as a

national problem that required intervention at the federal level in the United States (Toy et al., 2002).

Erosion causes harm for instance, at the location where erosion takes place because infiltration rates, crop production, and the water holding capacity of soil are reduced via the removal of organic matter and plant nutrients. Moreover, the transported materials affect water quality, increase eutrophication and decrease life time of reservoirs due to siltation (Lorbup et al., 1996). Environmental legislation and regulations have focused on short and long-term impacts of soil erosion and sedimentation (Toy et al., 2002). Erosion is responsible for sedimentation, which is known as the most common water pollution problem in the United States and in other parts of the world. Erosion results in off-site environmental degradation due to sediment movement, sediment storage, chemicals absorbed to sediments and biota response to sediment and chemicals (Osterkamp et al., 1998). Thus, it decreases the recreational value of waterbodies, increases flood damage, and increases water treatment costs. The costs of water pollution by sediment in the United States were estimated at about 16 billion USD per year in one recent study (Osterkamp et al., 1998).

3.2 Factors Influencing Soil Erosion

Factors controlling the rates of erosion are (1) climate, (2) topography, (3) soil, (4) land cover and land use. The major forces driving these processes are shear stresses generated by raindrop impact and surface runoff over the land surface. Hence, water erosion is a function of the forces of raindrop impact on a soil surface and surface runoff relative to the resistance of the soil to detachment (Toy et al., 2002). When soil particles are set in motion, they are referred to as sediment. The amount of eroded material that is transported to a particular location is referred to as sediment delivery, whereas sediment yield is the amount of sediment delivered at the outlet of

the watershed at a specified time (Patra, 2001). Runoff transporting sediment capacity is related to the shear stress as well as the transportability of the sediments for example the size, nature and density of the particles. When the availability of sediment for transport is greater than the transport capacity, deposition occurs, which results in accumulation of sediment on the soil surface (Toy et al., 2002).

3.2.1 Climate

Precipitation, among other variables of weather conditions, is the most important variable affecting water erosion (Toy et al., 2002). Climate determines rainfall erosivity, which estimates the forces applied to the soil to cause water erosion. Rainfall results in ecosystems prone to erosion, particularly in the semi-arid regions where the amount of rainfall impedes the establishment of good groundcover (Lorup and Styczen, 1996). Raindrops loosen the soil particles and water transports them down the hill. Raindrop energy includes three important factors: (1) soil detachment; (2) its beating tends to destroy granulation; (3) its splash, under certain conditions, produces an appreciable transportation of the soil. The force exerted by the rain loosens the soil granules and also mechanically breaks the soil into pieces. Under such hammering, the aggregation of a soil so exposed practically disappears.

Different soil properties determine its inherent resistance to erosion. However, climate affects soil erosion in direct and indirect ways. In a direct way, the erosion process by rainfall occurs from raindrops striking soil, and rainwater flowing over the soil. The parameters involved can be the amount of rainfall, kinetic energy, momentum and intensity (Wischmeier, 1959). The average annual rainfall distribution in the United States from 1961 to 1990 is shown in Figure 3-1. Most rainfall appeared to occur in the West Coast and along the shoreline in the East Coast.

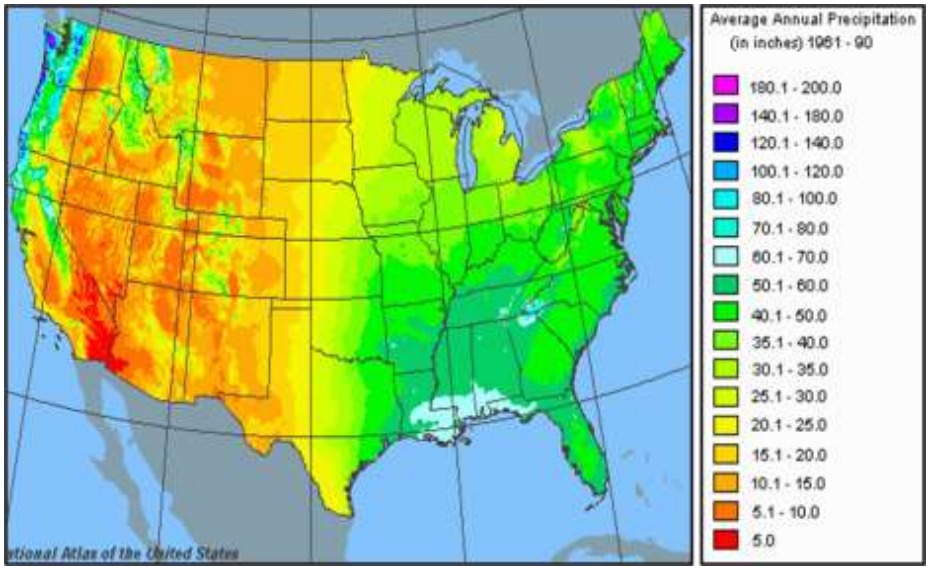

Figure 3-1. Average annual rainfall in the United States, 1961-1990 (NRCS, http://www.nationalatlas.gov/mld/prism0p.html).

Two important rainfall variables for determining storm erositivity are rainfall amount and rainfall intensity. Thus, rainfall amount may be used to estimate the amount of total erosivity for a given storm by multiplying rainfall intensity with the amount of rainfall (Toy et al., 2002). Apart from raindrop impact, erosion by surface flow is related to the amount and rate of runoff. The amount of runoff is a function of rainfall amount, less amount of infiltration, and peak runoff rate is related to peak rainfall intensity, less infiltration rate and surface storage. Therefore, a simple measurement of rainfall erosivity for erosion by raindrop impact and surface runoff is obtained by multiplying rainfall amount and rainfall intensity (Horton, 1933). Another factor that should come into consideration is raindrop size as it influences the force applied to the soil surface. A small raindrop size exerts very low force on soil and causes very little erosion regardless of rainfall amount and intensity. This is because of the effect of kinetic energy of the raindrop striking the soil surface, which is one half of the product of the mass of the drop and the square of the impact velocity. Raindrop size and impact velocity are closely related and thus a small raindrop has very low impact energy (Toy et al., 2002). Miller (2006) mentioned raindrops

in a high-intensity rainfall usually reach a maximum size of 6mm and terminal velocity of about 9m/s. Its impact can displace a 10mm diameter soil particle into the air.

The kinetic energy for a single rain storm is the sum of kinetic energies of individual raindrops (Sharma et al., 1993). The sum of kinetic energy for all storms in a year is an index of rainfall erosivity that can be calculated from a rainfall map (Wischmeier and Smith, 1978). Meyer (1991) stated that the total energy of 30-in (760mm) annual precipitation occurring over 1 square mile (2.6 km^2) is equivalent to the energy of 10,000 tons (9100 metric tons) of TNT. Raindrops, with the influence of gravity accelerate until their force is equal to the frictional resistance of the air and they reach the ground at terminal velocity (Miller, 2006). Factors influencing the speed of raindrop strike are wind pattern, turbulence and drop size (Laws, 1941; Moss and Green, 1987;Sharma et al., 1993).

Climate affects soil erosion indirectly for instance, through temperature influencing the form of precipitation, the capacity of the atmosphere to hold the water vapor, air pressure that controls the density of air, as well as wind speed and wind direction resulting in rainfall location. Temperature also controls soil moisture (hence it does control chemical reactions) conditions and the interaction between soil and precipitation such as infiltration rate, which is related closely to runoff rate. Runoff occurs when the precipitation rate exceeds the infiltration rate (Ward, 1990). Snowfall and rainfall on frozen soil do not produce erosion, but runoff from snowmelt and rainfall on thawing soil can produce very high erosion rate (Renard et al., 1997).

Climate controls vegetation cover on the ground that protects soil from raindrop impact and surface runoff by interception (Miller, 2006). Climate variables such as precipitation, temperature, evapotranspiration, and soil moisture affect the vegetation growth and decomposition within soil profile (Lavelle et al., 2001).

Evaporation and infiltration has impact on surface runoff and therefore erosion since a portion of incoming rainfall that does not infiltrate into soil or return to the atmosphere by evapostranspiration drains as surface runoff (American Meteorological Society, 1984).

3.2.2 Soil

Soil is a naturally occurring loose material mantling the surface of the earth, as distinct from solid rock (Govers and Poesen, 1986). Soil nourishes and supports growing plants. It becomes sediment that can fill water reservoirs and water channels when erosion processes take place, thus can degrade water quality. Production of soil is through chemical and mechanical weathering processes. Initially, in areas where glacial occurs, glacial deposits weather to unconsolidated mineral debris that serve as the parent material for soil development.

A vast array of carbon compounds found in the soil profile, known as organic matter, affects soil function as it provides good soil structure by enhancing water holding capacity and improving soil structure (USDA, 2001). Soil organic matter improves soil function by binding soil particles together into stable aggregates, therefore enhancing porosity, infiltration rate, root penetration and reducing runoff and soil erosion (USDA, 2001).

Free (1960) pointed out that the type of soil being struck is extremely important in determining the magnitude of soil movement by splash. He found that splash loss varied as $E^{0.9}$ for silt loam and $E^{1.46}$ for sandy soil, where E is the kinetic energy.Antecedent soil moisture between storms may also influence rainsplash as Truman and Bradford (1990) found that rewetting the soil greatly reduced the amount of soil splash by increasing soil shear strength.

3.2.3 Topography

Topography is the geometry of the land surface. Slope is a factor that affects not only the soil temperature, but also the erodibility of the soil. The greater the degree of slope, other conditions remaining constant, the greater the erosion due to increased velocity of water flow. Also, the more water is likely to run off. Theoretically, a doubling of the velocity enables water to move particles 64 times larger, allows it to carry 32 times more material in suspension, and makes the erosive power in total four times greater (Pirsson, 1929). The length of the slope is of prime importance since the greater the extension of the inclined area, the greater is the concentration of the flooding water (Brady and Buckman, 1974). Soil with a relatively low erodibility factor may have serious sign of erosion if it occurs on a long steep slope (Wischmeier and Smith, 1978).

Slope angle influences the amount splash transport (Savat, 1981; Reeve, 1982). The steeper the slope becomes, the greater the kinetic energy and the overland flow capacity and the more the soil stability and slope stability decrease. Therefore, splashing erosion is likely to increase and the possibility of the soil displacement downhill is likely to occur (Zachar, 1982).

3.2.4 Land Use and Land Cover

Land use refers to general land use and the management practice applied to that land use. Plant cover protects the soil from raindrop impact and splash. It provides protection from raindrop impact and surface runoff. Vegetation cover tends to slow down the movement of surface runoff and allows excess surface water to infiltrate into the subsoil. The decrease of vegetation cover increases soil erosion potential. Vegetation and residue both cover the soil and intercept falling raindrops at and close to the soil surface. The residues and residual root are also important as they provide channels that facilitate surface water to move into the soil.

3.3 Types of Soil Erosion

The study of water erosion is centered on water flows and its paths (Toy et al., 2002). Water flows in two forms of conduits, open channels and pipes (Figure 3-2).An open channel is exposed to atmospheric pressure whereas pipes flow under hydraulic pressures (Chow, 1959). Pipe flow occurs through the soil macropores in saturated soil. Overland erosion , the other hand is non-channelized erosion, such as sheet erosion and rill-interrill erosion.

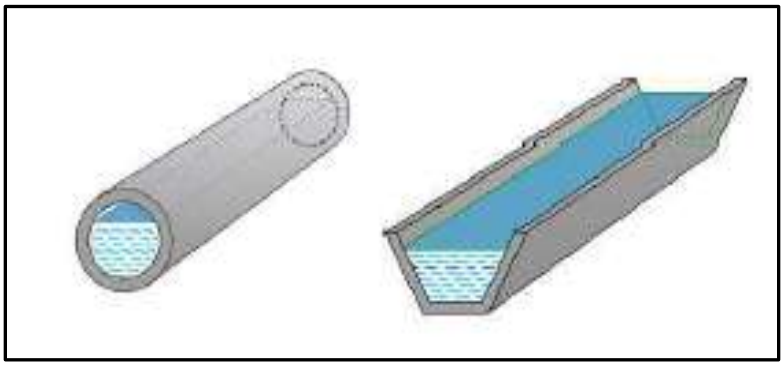

Figure 3-2. Open channel flow and part filled pipe flow (http://www.pipeflow.co.uk/public/control.php?_path=/497/595).

3.3.1 Sheet Erosion

Sheet erosion occurs when runoff removes relatively thin layers of soil from the land (Batie, 1983). It occurs on areas that have overland-flow and deposition may occur in the furrows if the slope along the furrow is relatively flat when interrill erosion is high. Rill and sheet erosion classification is based on the level of severity. Sheet erosion rate is generally low and it is a uniform removal of soil from the surface, and it is assumed to be the first phase of the erosion process.

3.3.2 Rill-interrill Erosion

Any erosion by runoff occurring in these areas is referred to as rill erosion. The interrill areas are the areas between the rill areas and erosion occurring in these areas is defined interrill erosion. The rill and interrill areas together create overland-flow of landscapes. Rill plus interrill erosion is the total water erosion that takes place on the overland flow areas of the landscapes (Troeh et al., 1991). In fact, interrill erosion is similar sheet erosion as it is uniform over the interrill area. It occurs when rainwater or snowmelt water, along with dislodged soil particles, accumulates in the waterway (Batie, 1983). Soil loss for this type of erosion is closely related to runoff velocity. As the velocity increases, the amount of soil carried by water also increases. Rill erosion can be explained as a function of the flow's ability to detach sediment, of the sediment transport capacity, and of the existing sediment load in the flow (Toy et al., 2002).

3.3.3 Gully Erosion

Gully erosion is a severe form of rill erosion occurring generally within field-sized areas where farming and other similar land disturbing operations takes place (Toy et al., 2002). Gully erosion creates large channels rather than rills and these channels carry water during and immediately after the rainstorm events. Unlike rill erosion, gully erosion cannot be eliminated by ordinary tillage operations (Schwab et al., 1996). A number of forms may appear in gully erosion as a large amount of water gradually accumulates and deepens the rills. It occurs as a result of rain water or water from snowmelt movement in the rill (Batie, 1983). The amount of sediment produced by this kind of erosion may be equal to the amount of sediment caused by rill and interrill erosion in the same field (Foster, 1986; Thomas et al., 1986).

3.3.4 Stream Channel Erosion

Stream channel erosion refers to both stream bed and stream bank erosion, which are controlled by fluvial processes. Stream bed erosion occurs when flows cut into the bottom of the channel and makes it deeper. Stream bank erosion occurs when the channel deepens due to the stream bed erosion, the sides of the channel become unstable and slough off and the more hydraulic shear occurring along the wet bank may lead to lateral migration (Howard, 1984). Stream channel erosion is naturally occurring, however, human activities on upland areas and the activities within the channels themselves can greatly influence stream channel erosion (Toy et al., 2002).

Channel features, including grade and meander form, adjust to accommodate the flow and sediment delivery from the upland (Schumm, 1977). Thus, changes in land use, such as urban development, that cause significant increase in frequency and duration of runoff, and sediment load delivery may cause stream channel erosion. Stream channel erosion usually occurs on the outside of the meander bends where the channel can retreat several meters during severe storms (Toy et al., 2002). This is because of the high velocity flow (the water does not flow at the same speed at all points across the cross-sectional flow pattern) as the friction near the stream bank/bed causes a core region away from the channel perimeter of higher than average velocity.

Stream channel erosion can be controlled and reduced by the reduction of runoff rates with impoundments, construction of enlarged channel cross section, installation of grade-control structures in the channel, bank protection operation such as maintaining adequate vegetation, and placement of in-stream vanes in order to divert flow away from channel banks (Shields et al., 1995).

3.4 Water Erosion Processes

Erosion is variable because of the spatial variability of precipitation, wind storms, topography, soils, and land use. Also, the erosion process is not uniform due to physics, though affecting factors are uniform (Toy et al., 2002). The different stages of the erosion process are: detachment, entrainment, transport, and deposition and sedimentation.

3.4.1 Detachment

The erosion process starts with the detachment of particles by breaking their cohesion bonds. The bonds that hold the particles together exhibit different levels of particle cohesion and some of the strongest ones exist between the particles found within igneous rocks. The weaker bonds are found in sedimentary rocks due to the cementing effect of some compounds such as iron oxides, silica or calcium. In a study of rill erosion mechanisms, Meyer and Monke (1965) suggested that the rate of soil detachment is inversely related to the magnitude of the sediment load at a given time and location.

The bonds in soil particles are even weaker than those in the sedimentary rock due to cohesion effects of water and the electro-chemical bonds found in clay and particles of organic matter (Lambe and Whitman, 1969). The detachment rate is a fraction of detachment capacity, which depends on the fraction of the transport and capacity filled by the sediment load (Toy et al., 2002). A detachment-limiting condition occurs when soil resists erosion and sediment load is correspondingly low due to low supply of sediment for transport though the flow transport capacity is bigger than the sediment load (Toy et al., 2002).

3.4.2 Entrainment

Entrainment is the process by which the detached particles get entrained by the flow's capacity. Once the particles are already detached, the sediment load is limited by the ability of the flow to entrain and transport particles (Toy et al., 2002). In most cases, it is difficult to distinguish between entrainment and detachment. Frictional force, among other forces, is the most important force providing particles with a resistance to this process (Foster et al., 1989). Factors increasing frictional resistance are gravity, particle mass, particle slope angle relative to the flow direction of eroding medium, and surface roughness (Blackburn, 1975; Scoging, 1989).

Entrainment takes place when overland flow is occurring and some particles are entrained downslope with the flowing water before settling down (Linsley et al., 1958). A thin film layer of water flowing across the land at low velocity moves in laminar flow. Fast flowing fluids move in random oscillation in direction and both horizontal and vertical velocity varies. This type of motion is called turbulence (Troeh et al., 1980). However, laminar flow can only move loose soil particles on the soil surface and particles from a soil mass cannot be detached by this type of flow (Linsley et al., 1958). The turbulence creates vertical lift that pushes the particles upward. When the particle is already lifted, the only force against its transport is gravitational force as the other forces such as friction, slope angle, and cohesion no longer exist.

Fluid drag between flow and materials in the flow is the main force responsible for entrainment (Nichols, 1999).It is the reduction in the flow velocity due frictional effects and it varies depending on the mass of water flow and its velocity. It causes the particles to move as a result of the horizontal force and vertical lift as shown in Figure 3-3. Horizontal force occurs from the push of water flow against the particles and the vertical lift occurs due to the *Bernoulli Effect*(Nichols, 1999). The Bernoulli Effect can be demonstrated as when a fluid flows in a tube

that one end is narrower than the other end. Therefore the cross sectional area at one end is larger than at the other one, yet in order to maintain the transport of fluid that goes in and out, the fluid must move at higher velocity through the narrow end. As a result, pressure energy is reduced and kinetic energy increases, meaning that there is a reduction in pressure at the narrow end of the tube.

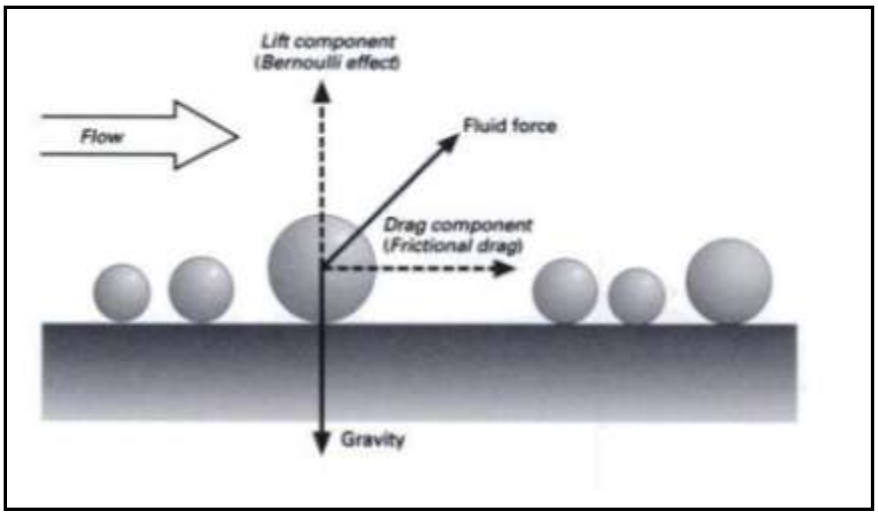

Figure 3-3. Forces acting on a grain in a flow (After Middleton and Southard, 1978; Collinson and Thompson, 1982).

When this push outweighs friction and the resistance of cohesive bonds, it causes the particles to move horizontally. Substances such as kaolinite, montmorillonite, biotite help increase cohesion force between soil particles and therefore decrease the erodibility of soil (Patra, 2001).

The velocity required to entrain a particle into the moving medium of air or water is a function of particle sizes, density, and shape. The relationship of stream flow velocity and particle size, particle erosion, transport and deposition is shown in Figure 3-4. The curve indicates that particles below a certain size are just as resistant to entrainment as particles with larger sizes and masses. Fine silt and clay particle tend to resist entrainment due to the strong

cohesive bonds between particles. The “erosion velocity” on Figure 3-4 suggests the velocity required to entrain particles from the stream’s bed and banks. The graph also indicates that the transport of particles requires lower flow velocities than erosion. The settling velocity represents the velocity at which particular sized particles are deposited (Nichols, 1999http://www.phsycalgeography.net/).

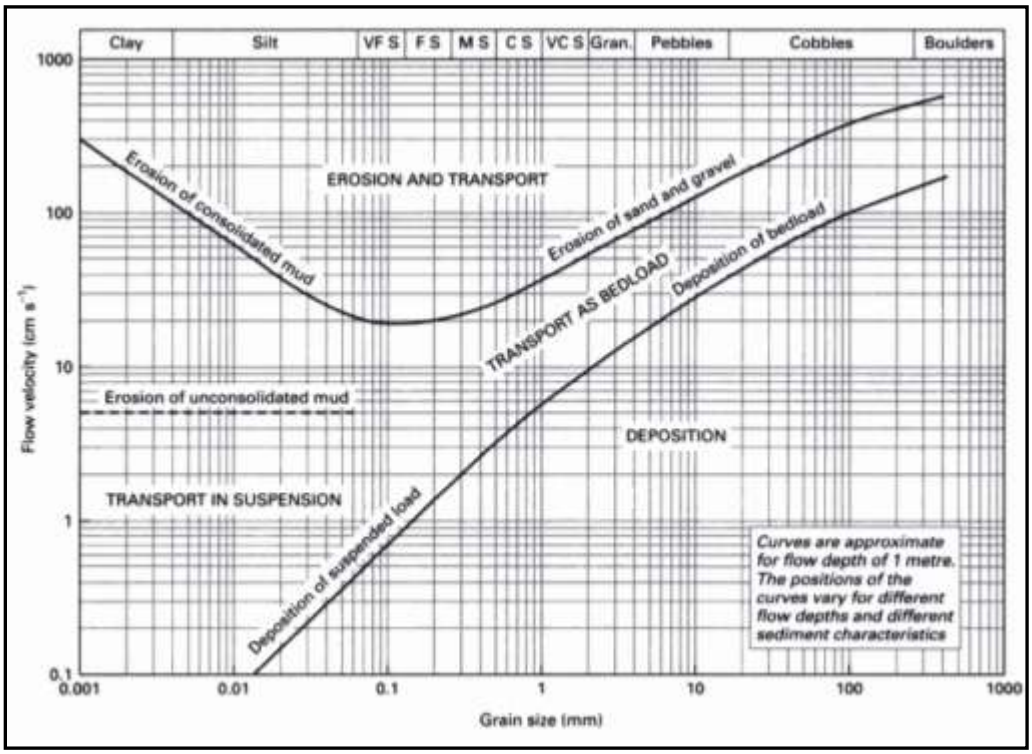

Figure 3-4. The Hjulström diagram, demonstrating the relationship between stream flow velocity and particle size, transport, and deposition (Nichols, 1999).

3.4.3 Transport

Sediment transport is a direct function of water movement. Once entrainment takes place, a particle may be transported in different ways, such as suspension, saltation, traction, or solution depending on the particle size, weight, shape, and surface configuration. Soil grains that jump along the bed of the stream may be 2.65 times as dense as the clear water, assuming density of

quartz. Therefore, they carry about 2.65 times as much energy as an equal volume of water (Troeh et al., 1980).

The capacity of flow's transport is a function of the flow's erosivity and the transportability of the sediment as determined by the size and density of the sediment particles (Toy et al., 2002). The relationship of sediment transport capacity and supply is shown in Figure 3-5.

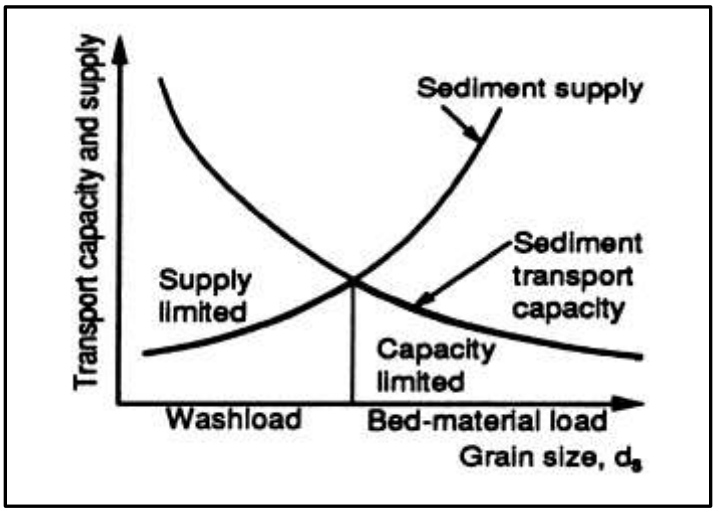

Figure 3-5. Sediment transport capacity and supply curves (Julien, 1995).

3.4.4 Deposition and Sedimentation

Deposition occurs when the water flows into the lake or river reservoir and the flow velocity and load capacity decrease and therefore the sediment is deposited (Brune, 1953).

Transport capacity is controlled by flow velocity, as a reduction of flow velocity, or an increase in resistance of the particles may cause deposition. Deposition rate is proportional to the difference between the transport capacity and the sediment load, velocity, height within the flow that sediment is transported, and the speed with which a sediment particle of a given size and density falls through a column of water (Toy et al., 2002). Sediment load decreases with the distance downstream as deposition takes place and eventually it reaches an equilibrium condition

(Mutchler et al., 1994). The deposited sediment may be re-eroded by raindrop impact and this process is called ‘rainfall re-detachment’. The rate of re-detachment of previously detached and deposited sediment, under the same rainfall rate, is higher than the detachment rate of the original soil if that soil is cohesive (Hairsine et al., 1981).

The fragment of earth material eroded, transported and deposited elsewhere is defined as sedimentation, therefore the loss of material in one area is balanced by the building up of material elsewhere (Troeh et al.,1980). Sediment deposits in lakes, reservoirs, and moving waterways such as stream channels. The deposited sediment often changes the ecological condition of aquatic organisms. Sedimentation raises streambeds and decreases stream depth and capacity of the channels, which may also lead to flooding and navigation issues (Troeh et al., 1980).

3.4.4.1 Suspended Sediment Transport and Flocculation

In the environment particles usually bond together to form flocs as they move (Droppo et al., 1997; Phillips and Walling, 1999). Flocculation is an important process when particles in the water column bond together and settle down to the bottom of the stream, lake or ocean. Usually flocs have low density, large pore size, and reactive surfaces absorbing contaminants from the water column (Droppo et al., 2001). The kinetics of flocculation have been mathematically described since 1917 (Lawler, 1993). During the flocculation process, floc growth occurs in several phases and the process that cohesive sediments settle and deposit influence the transport of suspended particles (Krishnappan, 2000; Lick et al., 1993). Micro floc (small particle clusters) forms at the initial phase of flocculation formation through random collisions in turbulent flow. The micro flocs combine together to form larger flocs at higher sheer stress (Klimpel et al., 1986,

Stone and Krishnappan 2003). An elongation of flocs occurs as they grow, which causes the collision frequency to increase and floc strength to decrease (Li et al., 1997).

Stone and Krishnappan (2003) suggested that turbulence has dual role in the flocculation process. Flocs formed at lower sheer stress may be broken up by high turbulence and there is an optimum shear stress for both formation and stability of flocs. Stone and Krishnappan(2003) stated that micro flocs are the building blocks of larger flocs.

Suspended sediment is transported in flowing water as a bed load, which slides along the bottom of the stream channel and saltation is the process when the particle bounces along the bed (Linsley et al., 1982). The settling velocity of suspended sediment in still water is calculated by Stokes's Law, where particles are solid spheres.

$$v_s = \frac{2(\rho_g - \rho)gr^2}{9\mu} \qquad \text{(eq. 3.4.4.1-1)}$$

Where

$\rho_g$and ρ- densities of the particles and the liquid respectively

r-the radius of the particle, generally diameter of particle ranges from 0.0002 to 0.2mm

μ- the absolute viscosity of the water

In turbulent flowing water, gravitational settling of particles is influenced by upward transport by turbulent eddies (Linsley et al., 1982). The upward moving eddies carry more sediment than the downward moving eddies as the concentration of sediment is the greatest near the bottom of the channel. At the equilibrium state, the gravity movement and turbulence transport are in balance and the amount of suspended sediment remains constant (Linsley et al., 1982).

Sediment transport and settling velocity is influenced by the hydrodynamic characteristics of sediment such as size, density and porosity of flocs. Droppo et al. (2000) studied the influence

of floc size, density and porosity on the sediment and contaminant transport using a 2.5L settling chamber interfaced with a stereoscopic microscope, CCD camera, SVHS and VCR and a computer image analysis. The result shows transport of sediment and contaminants is a function of the relationship between floc structure and settling velocity. An increase in floc size augmented settling velocity. Large flocs do not always settle within Stokes' region of Reynolds number. Flocs less than 100μm settle within Stoke'region (Re<0.2) (Droppo et al., 1999). The prediction of settling velocity of flocs by Stokes' formula is poorly estimated due to the variation in floc morphology such as shape and porosity, and floc composition such organic, inorganic and water content (Nicholas and Walling, 1996; Droppo et al., 2000). Strokes' formula demonstrates that the settling velocity of flocs is proportional to the diameter squared while Droppo et al. (2000) suggested that the settling velocity is proportional to just the diameter of the particle.

The primary factors that control density of floc are floc size, floc porosity, and floc composition such as organic and inorganic proportion, extracellular polymeric substances and water content (Droppo et al., 2000). Floc size and floc density are inversely related (Droppo et al., 2000). Floc porosity plays an important role in the physical, chemical and biological behavior of the floc as it controls water content, density and the movement of water within the floc (Li and Ganczarczyk., 1987, 1988; Droppo et al., 2000). The relationship between floc porosity and settling velocity as described by Droppo et al. (2000) is that floc porosity increases as floc size increases.

3.4.4.2 Bed Load Transport

Bed material transport can be approximated based on the classical equation of du Boys (du Boys, 1879):

$$G_i = \gamma \frac{\tau_0}{w}(\tau_0 - \tau_c)$$

(eq. 3.4.4.2-1)

Where

G_i- rate of bed load transport per unit width of stream (m^3/sec.m)

γ- an empirical coefficient depending on the size and shape of the sediment

w- the specific weight of water (N/m^3)

τ_o- the shear at the streambed (kg/m^2)

τ_c- the magnitude of shear at which transport begins.

A number of variations on the original du Boys equation have been proposed using the concept of a critical tractive force to initiate motion (Graf,1971). However this approach ignores turbulence and boundary layer as they affect entrainment of bed sediment (Linsley et al., 1982). Successful application of du Boys equation (eq. 3.4.4.2-1) can be derived through the proper selection of coefficient ϒ and values, given by Straub (1935) based on studies with small flumes, as listed in Table 3-1.

Table 3-1. Factors for eq. 4.4.4.2-1 for bed load movement (Straub, 1935).

Particle diameter,	γ		τ_c	
	Ft^6/lb^2. S	m^6/kg^2.s	lb/ft^2	kg/m^2
1/8	0.81	0.0032	0.016	0.078
¼	0.48	0.0019	0.017	0.083
½	0.29	0.0011	0.022	0.107
1	0.17	0.0007	0.032	0.156
2	0.10	0.0004	0.051	0.249
4	0.06	0.0002	0.090	0.439

3.5 Factors Causing Erosion

3.5.1 Human Factors

Agriculture and construction are two primary ways that humans cause erosion. Aside from that, agriculture and deforestation are also the substantial causes of erosion as they make the ground surface bare and extremely prone to erosion by natural force. In the 19th and early in the

20th centuries, the development of agriculture in some parts of United States resulted in increased rates of rill, interrill, and gully erosion on newly cleared and cultivated lands (Toy et al.,2002; Trimble, 1977). Therefore, large amounts of sediment were produced and delivered to valley streams, where much deposition and aggradation occurred.

3.5.2 Natural Factors

Wind and water are the two main natural agents of erosion though there are other factors such as climate, topography, soil structure and land cover that influences these two types of erosion.

3.5.2.1 Wind Erosion

Wind refers to the movement of air. Like moving water, moving air causes erosion, transportation and deposition of materials (Skidmore, 1994). Moving air is considered as a fluid and it works similarly to water erosion. However, the velocity of wind is generally lower than water. Wind erosion has been an issue in the United States and cannot be dismissed as the problem of the American Dust Bowl during the 1930's (Figure 3-6). The most famous episodes of wind erosion in the United States were the great "black blizzards" of the 1930's. They blew soil and dust hundreds of miles across the land.

Figure 3-6. Dust Bowl 1930's (Source: NOAA, http://www.nasa.gov/centers/goddard/news/topstory/2004/0319dustbowl.html).

Wind erosion continues to be a problem in many parts of the arid and semiarid world, which includes much of North America and the Near East, parts of the eastern, central and southern Asia, Australia, northwestern China, southern South America, the Siberian Plains, and North Africa (Wind Erosion Research Unit, 2001). Soil problems associated with wind erosion are the changes in soil texture as fine particles are removed; decreasing soil depth and fertility, and decreasing land productivity. Wind erosion also causes sedimentation in ditches and on roadways, reduces visibility on the roadways and impacts water quality. In addition, wind erosion causes abrasion of plants, automobiles and houses (Toy et al., 2002). The global distribution of vulnerability to wind erosion was mapped by the U.S. Department of Agriculture (USDA) and Natural Resources Conservation Service (NRCS) (Figure 3-7). The mapping is based on a reclassification of the global soil climate map and global soil map.

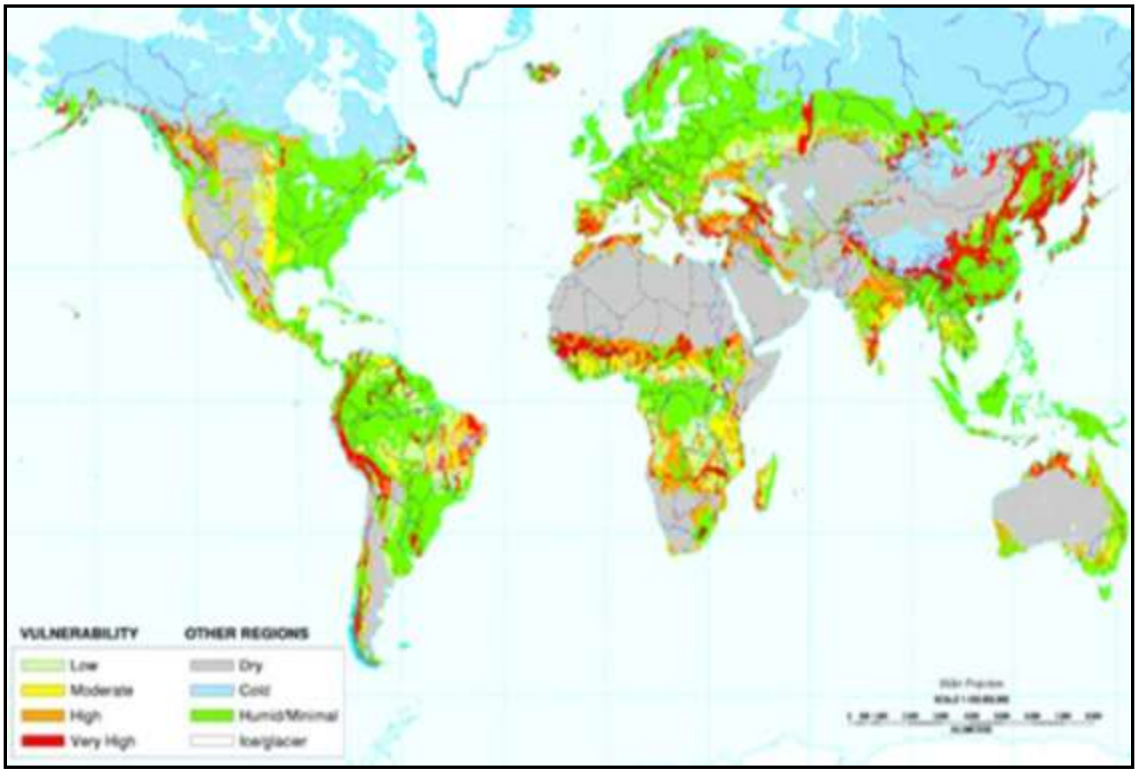

Figure 3-7. Wind Erosion Vulnerability map (Source: NRCS, http://soils.usda.gov/use/worldsoils/mapindex/eroswind.html).

3.5.2.2 Water Erosion

Water-induced erosion is the process by which hydraulic action moves materials through the exertion of pressure and shearing force (Nearing et al., 1994). Water erosion and sedimentation includes the process of detachment, entrainment, transport, and deposition of soil particles (Toy et al. 2002). The driving forces associated with water-induced erosion are shear stresses generated by raindrops and surface runoff and overland flow (Toy et al., 2002). A water erosion vulnerability map is shown in Figure 3-8.

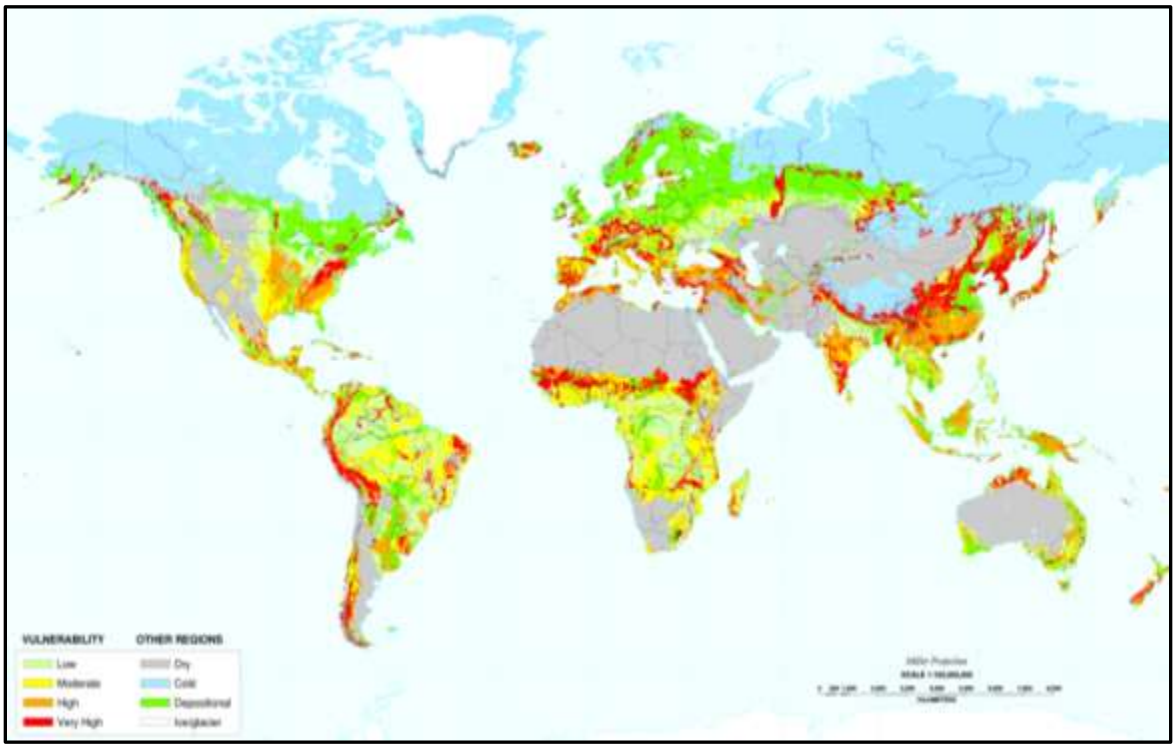

Figure 3-8. Water Erosion Vulnerability map (Source: NRCS,http://soils.usda.gov/use/worldsoils/mapindex/erosh2o.html).

3.6 Erosion Prediction

Erosion rates are a basic function of the four factors, climate, soil, topography, and land use. A simple erosion model is represented as below:

$$SL = CF.\ SF.\ TF.\ LUF \quad \text{(eq. 3.6-1)}$$

Where

SL- average annual soil loss;

CF- climate factor;

SF- soil factor;

TF- topography factor;

LUF- land use factor.

3.6.1 Sediment Yield

Sediment yield refers to the amount of sediment delivered at the outlet of a watershed whereas soil loss is expressed as a quantity per unit area and time (Foster et al., 1988). Sediment yield is the sum of the sediment produced by all erosional sources such as overland flow, gully, and stream channel erosion. The main factor controlling sediment yield for most situations is the transport capacity of runoff (Mutchler et al., 1988). The soil loss by water can be approximately computed by the "Universal Soil-Loss Equation" developed by Wischmeier and Smith (1965, revised 1978). Only A, R, L and K have dimensions:

$$A = R\ K\ L\ S\ C\ P \quad \text{(eq. 3.6.1-1)}$$

Where

A-the computed soil loss per unit area (t/ha/year);

R- Rainfall factor (hundreds of foot-ton inches per acre-hour year); or SI [MJ.mm/(ha.h.y)];

K- Soil Erodibility (ton-acre-hours per hundreds of toot-ton-inch-acres),or SI [t.ha.h/(ha.MJ.mm)];

L- Slope length (m);

S- Slope gradient;

C- Crop management or vegetation cover- depending on whether soil is vegetated, mulched, or bare;

P- Erosion-control practice- linking the soil loss with the given management practices to the loss that would occur with up-and-down slope cultivation.

More recently the USLE has been revised and it is known as the modified USLE (MUSLE) (Williams, 1995). The older USLE predicts average annual gross erosion as a function of rainfall energy. The MUSLE, replaces the rainfall energy factor with a runoff factor. This improves the sediment yield prediction, eliminates the need for delivery ratios, and allows the equation to be applied to individual storm events. Sediment yield prediction is improved because runoff is a function of antecedent moisture condition as well as rainfall energy. Runoff often decreases its transport capacity as it flows through a catchment with changes in topography, soil characteristics, and vegetation covers (Mutchler et al., 1988). Delivery ratios (the sediment yield at any point along the channel divided by the source erosion above that point) are required by the USLE because the rainfall factor represents energy used in detachment only. Delivery ratios are not needed with the MUSLE because the runoff factor represents energy used in detaching and transporting sediment (SWAT User's Manual,Version 2000).

Below is the MUSLE equation (Williams, 1995):

$$\text{Sed} = 11.8.(Q_{\text{surf}} .q_{\text{peak}} . \text{area}_{\text{hru}})^{0.56} K_{usle} .C_{usle} .P_{usle} .SL_{usle} .CFRG \quad \text{(eq. 3.6.1-2)}$$

Where

Sed- the sediment yield on a given day (metric tons);

Q_{surf}- the surface runoff volume (mm H_2O/ha);

q_{peak}- the peak runoff rate (m^3/s);

$Area_{hru}$- the area of the hydrologic response unit HRU (ha);

K_{usle} - USLE soil erodibility factor (0.013 metric ton m^2 hr/(m^3-metric ton cm)),

C_{usle} - the USLE cover and management factor;

P_{usle} - the USLE support practice factor;

LS_{usle} - the USLE topographic factor;

CFRG- the coarse fragment factor = exp (-0.053. *rock*), where *rock* is the percent rock in the first soil layer (%).

3.6.1.1 Surface Runoff

Surface runoff volume (Q_{surf}) is estimated using daily rainfall amounts. SWAT computes surface runoff volume and peak runoff rates for each HRU using a modification of the SCS curve number method (USDA Soil Conservation Service, 1972) or the Green & Ampt infiltration method (Green and Ampt, 1911). In the curve number approach, the curve number varies non-linearly with the soil moisture content and it drops as the soil reaches the wilting point and increases at the soil moisture content approaches saturation. Under the Green & Ampt approach, the infiltration is simulated as a function of the wetting front matric potential and effective hydraulic conductivity. The portion of water that does not infiltrate is the surface runoff.

The SCS method became commonly used in the 1950's. The SCS curve number equation is (SCS, 1972):

$$Q_{surf} = \frac{(R_{day} - I_a)^2}{(R_{day} - I_a + S)} \qquad \text{(eq. 3.6.1.1-1)}$$

Where

Q_{surf}– the accumulated runoff or rainfall excess (mm H_2O);

R_{day} – the rainfall depth for the day (mm H_2O);

I_a – the initial abstraction which includes surface storage, interception, infiltration prior to runoff (mm H_2O);

S – the retention parameter (mm H_2O), varies spatially upon the changes of soils, land use practices and soil moisture content. It may be defined as following:

$$s = 25.4\left(\frac{1000}{CN} - 10\right)$$

(eq. 3.6.1.1-2)

Where *CN*– the curve number for the day.

The initial abstraction, I_a, is commonly defined as $0.2S$, therefore the eq. 3.6.1-3 becomes:

$$Q_{surf} = \frac{(R_{day} - 0.2S)^2}{(R_{day} + 0.8\,S)}$$

(eq. 3.6.1.1-3)

Runoff occurs when the rainfall depth for the day (R_{day}) is higher than the initial abstraction (I_a). A graphical solution of eq. 3.6.1-5 for different curve number values is shown in Figure 3-9.

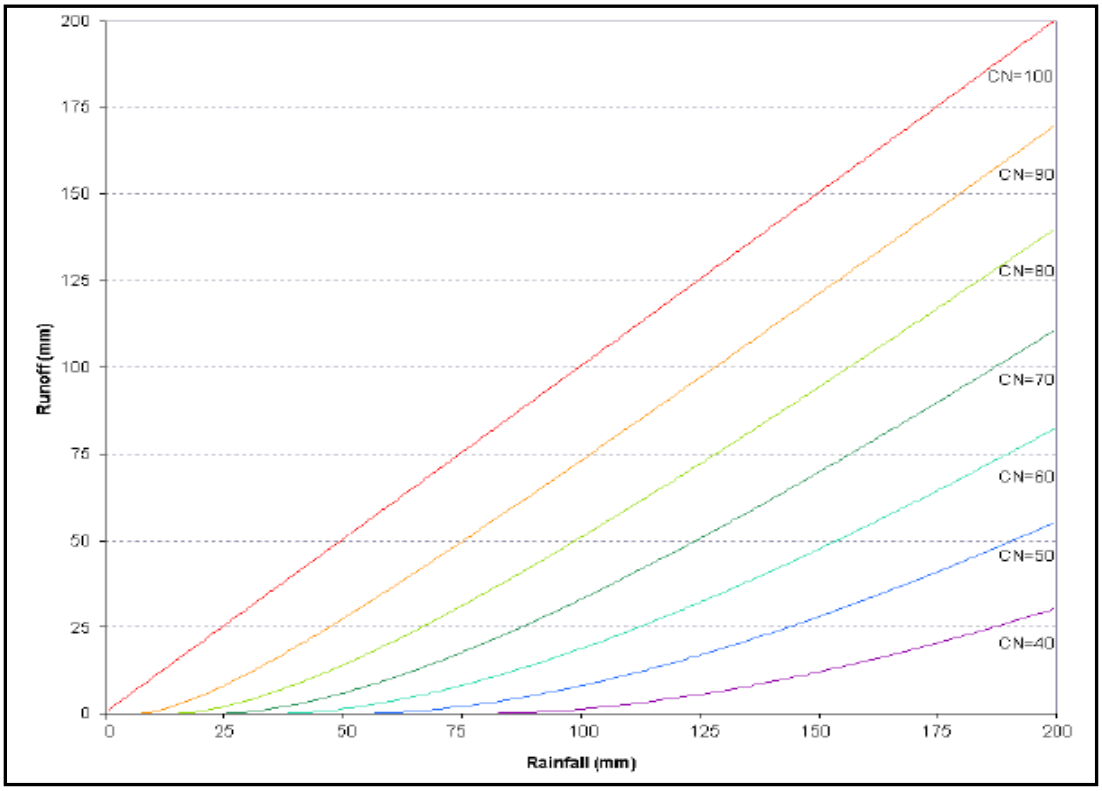

Figure 3-9. Relationship of runoff to rainfall SCS curve number method.

3.6.1.1.1 SCS Curve Number

The CN curve number is an approach used to determine the the approximate amount of runoff from a rainfall event. It is a function of soil permeability, land use and antecedent soil water conditions (SCS Engineering Division, 1986). The typical curve numbers used for cultivated agricultrural lands and urban use are presented in Table 3-2 and Table 3-3.

Table 3-2. Runoff curve number for cultivated agricultural lands, (SCS Engineering Division, 1986).

Land Use	Treatment or Practice	Hydrologic condition	Hydrologic Soil Group			
			A	B	C	D
Fallow	Bare soil		77	86	91	94
	Crop residue cover cover	Poor	76	85	90	93
		Good	74	83	88	90
Raw crops	Straight row	Poor	72	81	88	91
		Good	67	78	85	89
	Straight row w/ residue	Poor	71	80	87	90
		Good	64	75	82	85
	Contoured	Poor	70	79	84	88
		Good	65	75	82	86
	Contoured w/ residue	Poor	69	78	83	87
		Good	64	74	81	85
	Contoured & terraced	Poor	66	74	80	82
		Good	62	71	78	81
	Contoured & terraced w/ residue	Poor	65	73	79	81
		Good	61	70	77	80
Small grain	Straight row	Poor	65	76	84	88
		Good	63	75	83	87
	Straight row w/ residue	Poor	64	75	83	86
		Good	60	72	80	84
	Contoured	Poor	63	74	82	85
		Good	61	73	81	84
	Contoured w/ residue	Poor	62	73	81	84
		Good	60	72	80	83
	Contoured & terraced	Poor	61	72	79	82
		Good	59	70	78	81
	Contoured & terraced w/ residue	Poor	60	71	78	81
		Good	58	69	77	80
Close-seeded or broadcast legumes	Straight row	Poor	66	77	85	89

or rotation		Good	58	72	81	85
	Contoured	Poor	64	75	83	85
		Good	55	69	78	83
	Contoured & terraced	Poor	63	73	80	83
		Good	51	67	76	80
Pasture, grassland, or range-continuous forage for grazing[1]		Poor	68	79	86	89
		Fair	49	69	79	84
		Good	39	61	74	80
Meadow-continuous grass, protected from grazing and generally mowed for hay		---	30	58	71	78
Brush-brush-weed-grass mixture with brush the major element[2]		Poor	48	67	77	83
		Fair	35	56	70	77
		Good	30	48	65	73
Woods-grass combination (orchard or tree farm)		Poor	57	73	82	86
		Fair	43	65	76	82
		Good	32	58	72	79
Woods[3]		Poor	45	66	77	83
		Fair	36	60	73	79
		Good	30	55	70	77
Farmsteads-buildings, lanes, driveways, and surrounding lots.		----	59	74	82	86

Table 3-3. Runoff curve numbers for urban areas[4] (SCS Engineering Division, 1986).

Land Use/Cover Type	Hydrologic condition	Hydrologic Soil Group			
		A	B	C	D
Fully developed urban areas					
Open spaces (lawns, parks, golf courses, cemeteries, etc.) *Poor*: grass cover <50%; *Fair*: good grass cover 50-75%, *Good*: grass cover >75%	Poor	68	79	86	89
	Fair	49	69	79	84
	Good	39	61	74	80
Impervious areas:					
Paved parking lots, roofs, driveways, etc. (excl. right-of-way)	----	98	98	98	98
Paved streets and roads; open ditches (incl. right-of-way)	----	83	89	92	93
Gravel streets and roads (including right-of-way)	----	76	85	89	91
Dirt streets and roads (including right-of way)	----	72	82	87	89
Urban districts:					
Commercial and business	85%	89	92	94	95
Industrial	72%	81	88	91	93
Residential Districts by average lot size:					

[1] *Poor*:<50% ground cover or heavily grazed with no mulch; *Fair*: 50-75%, *Good*: >75%

[2] *Poor*:<50% ground cover; *Fair*: 50-75%, *Good*: >75%

[3] *Poor*: Forest litter, small trees, and brush are destroyed by heavy grazing or regular burning; *Fair*: Woods are grazed but not burned, and some forest litter covers the soil; *Good*: Woods are protected from grazing, and litter and brush adequately cover the soil

[4] SWAT will automatically adjust curve numbers for impervious areas when IUBAN and URBLU are calculated in the .hru file.

1/8 acre (0.05 ha) or less (town houses)	65%	77	85	90	92
1/4 acre (0.10 ha)	38%	61	75	83	87
1/3 acre (0.13 ha)	30%	57	72	81	86
1/2 acre (0.20 ha)	25%	54	70	80	85
1 acre (0.40 ha)	20%	51	68	79	84
2 acres (0.81 ha)	12%	46	65	77	82
Developing urban areas:					
Newly graded areas (pervious areas only. No vegetation)		77	86	91	94

Hydrologic Soil Groups are classified by the U.S Natural Resource Conservation Service (NRCS) based on infiltratioin characteristics of the soils. The hydrologic groups are defined as:

A- Low runoff potential due to the hight infiltration rate even though it is thoroughly wetted. This group contains deep, well drained to excessively drained sands or gravels. They have a high rate of water transmission.

B- This group of soils has a moderate infiltration rate when thoroughtly wetted. It consists of moderately deep to deep, moderately well drained to well drained soils that have moderately fine to moderately coarse textures. The rate of water transmission for these soil is moderate.

C- This group has a slow infiltration rate, therefore it results in high runoff potential and the rate of water transmission is low. They vary from moderately fine to fine texture.

D- The infiltration rate for this group of soil is very low. Hence the runoff potential is high and the water transmission rate is very slow.

3.6.1.2 Peak Runoff Rate

Peak runoff rate (q_{peak}) is calculated by modifying the rational method. The rational method has been applied in the design of ditches, channels and storm water control systems. The concept of the rational method is to observe the relationship of rainfall intensity and rainfall duration. For example if the rainfall of intensity 'τ' begins instantaneously and continues

indefinitely, runoff rate will increase until the time of concentration 't_c' when all the subbasins are contributing to flow at the outlet. Under the modification of the rational method, the peak of runoff rate is a function of the proportion of daily rainfall that occurs during the subbasin 't_c', the daily surface runoff volume, and the subbasin time of concentration. The proportion of rainfall that falls during the subbasin t_c is calculated as a function of total daily rainfall using a stochastic technique. Overland and channel flow are included in the Manning's formula used to estimate the subbasin time of concentration. The rational equation is:

$$q_{peak} = \frac{c.i.Area}{3.6} \qquad \text{(eq. 3.6.1.2-1)}$$

Where

Qpeak – the peak of runoff rate (m^3s^{-1});

C – runoff coefficient;

i– the rainfall intensity (mm/hr);

Area– the subbasin area (km^2).

3.6.1.3 Soil Erodibility Factor

Soils erode at different rates due to the properties of soil itself. According to Wischmeier and Smith (1978), the soil erodibility factor is defined as the soil loss rate per erosion index unit for a specified soil as measured on a unit plot. A unit plot is 72.6ft (22.1 m) long, with a uniform length-wise slope of 9-percent, in continuous fallow, tilled up and down the slope. Land that has been tilled and kept free of vegetation for more than two years is defined as continuous fallow, (for detailed method for defining K refer to the SWAT 2000 manual). A soil type usually becomes less erodible when the silt fraction decreases, regardless of whether the corresponding increase is in the sand fraction or clay fraction (Wischmeier and Smith, 1978).

To document direct measurement of the erodibility factor is time consuming and costly. Wischmeier et al. (1971) developed a general equation to calculate the soil erodibility factor when the silt and very fine sand content makes up less than 70% of the soil particle size distribution.

$$K_{usle} = \frac{0.00021.M^{1.14}.(12 - OM) + 3.25.(c_{soilstr} - 2) + 2.5.(c_{perm} - 3)}{100}$$

(eq. 3.6.2-1)

Where

K_{usle}- *the soil erodibility factor;*

M- the particle-size parameter;

OM- the percent organic matter (%);

$c_{soilstr}$- the soil structure code used in soil classification; and

c_{perm}-is the profile permeability class.

The particle-size parameter, *M*, is calculated as:

$$M = (M_{silt} + m_{vfs}).(100 - m_c)$$

(eq. 4.6.2-2)

Where

m_{silt}-the percent silt content (0.002-0.05 mm diameter particles);

Mvfs- the percent very fine sand content (0.05-0.10 mm diameter particles);

mc- the percent clay content (< 0.002 mm diameter particles).

The percent organic matter content, *OM*, of a layer can be calculated as:

$$OM = 1.72.orgC$$

(eq. 4.6.3-3)

Where *orgC* is the percent organic carbon content of the layer (%).

Downstream sediment yield data may be used to provide meaningful information about upstream erosion rate and soil loss within a watershed area, however, there are several major problems associated with this approach (Walling, 1988). The first problem is the process of sediment delivery in between on-site erosion and downstream sediment yields. Only a fraction of the soil eroded within a drainage basin reaches the basin outlet and is represented in the sediment yield. Plus, there may be some deposition and temporary storage along the slopes, especially where gradients decline. The magnitude of this loss tends to increase with increasing basin size (Hadley and Shown, 1976). In response, the concept of a sediment delivery ratio (SDR) has been introduced in order to quantify these effects. The second issue relates to the temporal discontinuity involved with the sediment delivery process. Sediment eroded at one site may be temporarily stored and subsequently remobilized several times prior to reaching the watershed outlet. A third major problem in relating downstream sediment yield to the upstream erosion rate is that sediment delivered by a river contains the materials from a variety sources other than upland soil erosion. These sources may be channel and gulley erosion and mass movements reaching the channel network.

3.6.1.4 Cover and Management Factor

Cover management factor (C_{usle}) is the ratio of soil loss from land cropped under specified conditions to the corresponding soil loss from clean-tilled, continuous fallow (Wischmeier and Smith, 1978). The plant canopy has an effect on soil erosion as it may reduce rainfall energy of intercepted raindrops. The velocity of water drops falling off the canopy is smaller than the terminal velocity of the free-falling raindrops. Since the plant cover changes over the growth

cycle of the plant, SWAT updates the cover and management factor using the following equation:

$$c_{USLE} = \exp(\left[\ln(0.8) - \ln\left(c_{USLE,mn}\right)\right].\exp\left[-0.00115.rsd_{surf}\right] + \ln\left[c_{USLE,NM}\right])$$

(eq. 3.6.1.4-1)

Where

$C_{USLE,mn}$– the minimum value for the cover and management factor for the land cover;

rsd_{surf} - the amount of residue on the soil surface (kg/ha).

$$c_{USLE} = 1.463\ln\left[C_{USLE,aa}\right] + 0.1034$$

(eq. 3.6.1.4-2)

Where $C_{USLE,mn}$– the minimum C factor for the land cover and $C_{USLE,aa}$ is the average annual C factor for the land cover.

3.6.1.5 Support Practice Factor

The support practices (P_{usle}) include contour tillage, stripcropping on the contour, and terrace system. It is defined as a ratio of soil loss with a specific support practice to the corresponding loss with up-and-down slope culture. Values for support practice factor and slope-length limits for contour support practices are listed on the Table 3-4.

Table 3-4. P factor values and slope length limits for contouring (Wischmeier and Smith,1978).

Land Slope (%)	PUSLE	Maximum lenth (m)
1 to 2	0.60	122
3 to 5	0.50	91
6 to 8	0.50	61
9 to 12	0.60	37
13 to 16	0.70	24
17 to 20	0.80	18
21 to 25	0.90	15

3.6.1.6 Topographic Factor

Topographic factor is defined the ratio of soil loss per unit area from a field slope to that from a 22.1-m length of uniform 9 percent slope under identical conditions. Topographic factor is calculated in the equation below:

$$LS_{USLE} = \left(\frac{L_{hill}}{22.1}\right)^{m} . (65.41. sin^2(\alpha_{hill}) + 4.56. sin\alpha_{hill} + 0.065) \quad \text{(eq. 3.6.1.6-1)}$$

Where

L_{hill} – the slope length (m);

α_{hill}– the angle of the slope;

m – the exponential term, is calculated: $m = 0.6 . (1-\exp[-35.835. slp])$.

Where *slp* is the slope of the HRU expressed as rise over run (m/m) and the relationship between α_{hill} and *slp* is $slp = \tan \alpha_{hill}$.

3.7 Modeling Soil Erosion

Initially soil erosion models were developed parallel to hydrologic models. Soil erosion models were first developed in the collaboration between agronomists and hydrologists. This is because most of the early models were purely empirical and did not require the input data from hydrological models. Plus, soil erosion issues were originally considered as a problem related to agricultural production. However, in the 1970's conceptual soil erosion models were merged with hydrological models when it became understood that erosion and sediment transport is a major factor that impacts water quality (Lorup and Styczen, 1996).

The most common method of estimating soil erosion from a catchment is still the 'Universal Soil Loss Equation (USLE)' (Wischmeier and Smith, 1965), an empirical equation

originally developed from hand calculations. A number of physically-based soil erosion models have been developed. Distributed physically-based models give a detailed and potentially more correct description of the hydrological processes in the catchment than do the other model types such as lumped or empirical models (Refsgaard, 1996). Lorup and Styczen (1996) stated that the good relationship of simulated and observed amounts of soil loss/sediment yield does not represent model-predictive credibility, however, a similar good relationship between simulated and observed discharge hydrographs will corroborate erosion estimates. There are distinct differences between rill and interill erosion processes, however, they are spatially linked and the rill-interrill concept has proven to be useful in the development erosion prediction models (Toy et al., 2002).

3.7.1 Development of Soil Erosion Models

Lorup and Styczen (1996) stated that the first soil erosion models were empirically-based models. Later on physically- based models were developed to depict the soil erosion processes and interactions.

A number of soil erosion models have been developed in the aim of obtaining a good tool for evaluation of soil erosion related issues. The models are expected to be applied in the following fields:

- Assessment of the extent of soil and nutrient losses and sediment transport in various environments.
- Land use planning, predicting the effects of land use changes and implementation of different soil conservation measures on soil losses and sediment yields.
- A better understanding of the erosion processes; the dynamic and relative processes that they interact with.

3.7.2 Classification of Soil Erosion Models

Soil erosion modeling has developed from empirical-based and mathematically-based models such as the Universal Soil Loss Equation, USLE (Wischmeier and Smith, 1965), to physically-based and mathematically more complicated models such as European Soil Erosion Models, EURISEN (Morgan et al.,1995). Lorupand Styczen (1996) classified soil erosion models into three categories: (a) empirical, (b) conceptual or partly empirical/mixed, and (c) physically-based models.

3.7.2.1 Empirical Soil Erosion Models

This type of model is based on data from field observations; mostly standard runoff curves on uniform slopes, and is usually statistical in nature. The USLE (see eq. 4.6.1-1, Wischmeier and Smith, 1965) was the first empirical model developed to predict soil erosion. This model is the most well known and widely used of the empirical models. Despite many criticisms, this model is still used and has been revised a number of times. RUSLE, revised USLE (Wischmeier and Smith, 1978), is used to model the annual soil loss from small area on a slope, and it maintains the basic structure of the USLE.

$$\boldsymbol{A = R\ K\ L\ S\ CP} \qquad \text{(eq. 4.7.2.1-1)}$$

Where

A- the computed soil loss;
R- rainfall-runoff erosivity factor;
K- soil erodibility factor;
L-slope length factor;
S-slope steepness factor;
C-cover management factor;
P- supporting practices factor.

RUSLE was done to incorporate recent research data, particularly for rangeland and conservation tillage, into the equation. Another reason to revise USLE was to expand the applicability of USLE to account for land use and climatic conditions beyond the original source of USLE (Foster et al., 1988). RUSLE provides better prediction of soil loss and sediment delivery as it has improved the effects of soil roughness and the effects of local weather (Renard et al., 1997). The difference between USLE and RUSLE are:

- New rainfall-runoff erosivity factor (R) in the western United States based on more than 1,200 gauge locations.
- Some revisions and additions for the eastern United States, including the adjustments of flat slope areas for splash erosion associated with raindrop falling on ponded water.
- Development of subfactor approach for determining cover management factor (C).
- Development of a seasonally variable soil erodibility factor (K).
- New slope length and steepness (LS) algorithms that reflects rill to interrill erosion ratio.
- New conservation practice (P) for rangelands, stripcrop rotations, contour factor values, and subsurface drainage.

The main limitation of empirical models in general is the limited applicability outside the range of conditions for which they are developed. Adaptation of an empirical model to a new environment requires a big investment in resources and time to build the database required to run the models (Nearing et al., 1994). The empirical model only provides insight to the relative importance of various variables and their sensitivities in different environments. Also, the estimate of annual soil loss is reasonable for the field, but for the catchment scale the estimate is still limited. For instance the models do not account for the deposition at the lower parts of the hillslope, which is relevant in relation to sediment and pollution transport toward rivers and reservoirs. Despite the capability of estimating the annual soil loss, the model cannot be used to

examine the temporal dynamics of erosion. In the USLE, rainfall and soil factors cannot be multiplied as the subtractive effect of soil infiltration capacity in generating erosive runoff from a given rainfall. This creates a conceptual defect affecting the USLE model (Kirkby, 1980).

A modified version of USLE is the MUSLE which was developed by Williams (1975). The aim of the MUSLE is to overcome the limitations of the USLE mentioned above by substituting a rainfall factor with an empirical runoff energy factor, and the model is able to predict the sediment yield from single storms. Elwell (1977) developed a similar model, the Soil Loss Estimation Model for Southern Africa, SLEMSA. It is primarily based on field plot erosion studies in Zimbabwe.

3.7.2.2 Conceptual Models

The development of conceptual models occurred because of the limitations of the empirical models. Conceptual models include CREAMS (USDA, 1980), ANSWERS (Beasley et al., 1980), modified ANSWERS, MODANSW (Park et al., 1982). The introduction of laws of conservation of mass and energy, for example, and the continuity equation and the grouping of the areas of concern into a number of elements/grid in order to describe the spatial variations in erosion and deposition was the main step forward in the development of conceptual models. These models are somewhat in between the empirically-based and physically-based models. The detachment and transport of sediment from each grid for example may follow the model proposed by Meyer and Wischmeier (1969). These models resemble the physically-based models because the outflux of sediment from a given grid is determined by the influx of sediment plus the net detachment of sediment by runoff and rainfall within the element, and the limit that the outflux never exceeds the total transport capacity (Lorupand Styczen, 1996).

The main limitations of conceptual models are the poor physical description of the processes and distortion of parameter values determined by the calibration (Elliot et al., 1994). Conceptual models are faster to calibrate and easier to understand than the more complicated physical hydrological models.

3.7.2.3 Physically-Based Models

The main objective of a physically-based soil erosion model is to describe the various processes and their interactions in the natural system. It is intended to represent the essential mechanisms that control the erosion process. Therefore it is necessary that a model is coupled with a hydrological model that fulfills the same purposes; for instance a model that provides a detailed description of the spatial and temporal changes in the flow of water. Physically-based models include most of the factors affecting erosion and their spatial and temporal variability, as well as the description of the subprocesses and their complex interactions (Lorup and Styczen, 1996). The basic concepts of erosion models are quite similar, but the ways they are coupled with hydrologic models and the use of equations to predict the individual processes vary (Lorup and Styczen, 1996). The equations used to model rill and interrill erosions are different as the detachment and transport in those two types of area are modelled in different ways.

The most important basis of physically-based models is an adequately distributed simulation of the driving variables in the soil erosion and transport processes, the overland flow. This is particularly important for a more precise description of rill initiation and development (Lorup and Styczen, 1996).

There are number of physically-based soil erosion models such as: WEPP (USDA Water Erosion Prediction Project), EURSEM (European Soil Erosion Model) that is based on soil erosion research in Europe (Morgan, et al., 1999), and the soil model developed by an Australian

group (Rose et al., 1983a,b). In the physically-based models, factors that are accounted for are the soil erosion by raindrop impact (splash erosion), infiltration condition and generation of overland flow, soil surface conditions and runoff processes, and soil detachment and transport by overland flow.

There are some advantages as compared to the empirical and conceptual models. Due to the description of the processes, scientists can identify the factors or erosion processes that are most important to the overall erosion processes. Due to the calculation of the spatial and temporal distribution of sediment concentrations, soil erosion rate can be extrapolated from plot to catchment scale. Distributed modelling shows the differences between different parts of the watershed and their dependencies.

3.7.3 Modeling Soil Erosion Using Hydrologic Models

Modeling the quantity of erosion delivered from an upland area to the outlet through runoff requires a close understanding of the relationships between the sediment detachment, transport, and deposition processes. Because these relationships are complex and not always well understood, the best ways of evaluating sediment yield is to use a hydrologic model (Young et al., 1987). The way that the model works is to estimate the outflow, sediment, and chemical load from a segment of the landscape or watershed.

A number of hydrologic models are available for use in studying hydrologic responses on a watershed based on the purposes, time base, spatial scale, and conceptual basis of the projects (Young et al., 1987). However, hydrologic models are divided into two main categories: stochastic and deterministic (Young et al., 1987).

Stochastic models are statistically based and operate on the premise of chance or probability of an event happening. For instance, for a watershed having sufficient historical data,

and if it is not encountering any changes in management, this model can be used to predict what might happen if a parameter such as rainfall varies (Young et al., 1987). The limitation of this type of model relates to its performance of being a function of the watershed characteristics, thus, it cannot be applied directly to another watershed.

Unlike stochastic models, deterministic models are based on a sequential approach. They consist of several components describing physical processes occurring within the catchment. Each of the components is associated with one or more watershed characteristic that can be measured. Deterministic models are very suitable for use on ungaged watersheds as in theory, flow records are not necessarily required for model development (Young et al., 1987). There are two types of models that fall into deterministic categories: theoretically-based model and empirically-based model. Most of the overland processes are empirical due to the availability of the data, while channel processes are physically-based. The classification of hydrologic models based on the description of process is shown in the Figure3-10.

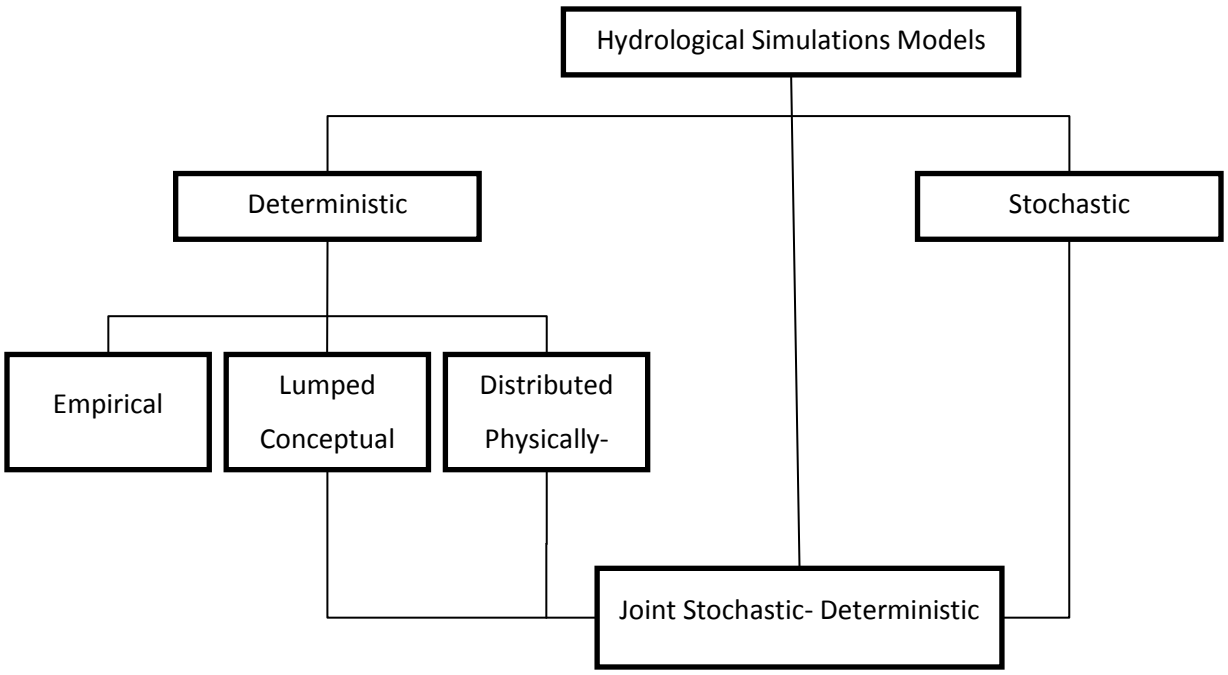

Figure 3-10. Classification of hydrologic models according to process description (Refsgaard, 1996).

3.8 BASINS Watershed Modeling

BASINS stands for Better Assessment Science Integrating point and Nonpoint Sources. It was developed by the Environmental Protection Agency's Office of Water and is a multipurpose tool used to analyze the environmental system by regional, state, and local agencies and universities. BASINS serves mainly three objectives: (1) to facilitate examination of environmental information, (2) to support analysis of environmental systems, (3) to provide a framework for examining management alternatives. BASINS components consist of hydrology, weather, sedimentation, crop growth model, nutrients, and pesticide.

There are three geographical-based analytical tools in the BASINS GIS environment in order to perform regional and site specific analysis. Those tools are *TARGET*, *ASSESS*, and *Data Mining*.

(1) TARGET permits a broad based analysis of water quality and point source loading data on a project area.

(2) ASSESS is a simple assessment tool that operates on a single watershed or a limited number of watersheds. It allows the assessment of water quality and point source discharge on a single watershed or multiple watersheds. It provides a comparative view of water quality at each monitored station separately. The magnitude of loading discharge at each Permit Compliance System (PCS) station and the corresponding data can be used to assess the point source discharge.

(3) Data Mining lets BASINS users more fully access the water quality and point source databases from water quality stations and parameter data, permitted facility locations and pollutant loading discharge data, and bacteria stations.

The three geographically based analytical tools are fully developed to operate on the water quality and point source data layers. BASINS operates on hydrologic units or watersheds as defined by the United States Geological Survey delineations referred to as “cataloging units”. Watershed modeling in BASINS can be performed on a single delineated watershed or multiple watersheds using the BASINS Hydrological and Simulation Program-Fortran (HSPF) or Soil and Water Assessment Tool (SWAT) model.

The watershed delineation tool in BASINS is used to define watershed boundaries at a level smaller than the 8-digit Cataloging Unit Boundary level. BASINS includes both manual and automatic watershed delineation options in the *Delineate* menu.

BASINS reveals some limitation of unavailability of GIS data outside the United States. Another limitation of BASINS would be the reliability of users on the completeness and accuracy of the geographic data. The USGS (1998a) conducted the evaluation of the database

quality assurance and suggested that many of the data records did not comply with the content of the standard for digital geospatial data. SWAT also reveals some limitations of no connectivity between the HRUs, and it does not simulate groundwater flow and transport. DEM resolution also affects the watershed delineation, stream networks and the classification of sub-basins (Chaubey et al., 2005). A study conducted by Chaubey et al. (2005) suggested that the choice of DEM resolution is based on the watershed response of interest and in order to achieve less than 10% error in simulating flow, DEM data resolutions range from 100 to 200 m (Chaubey et al., 2005).

There are a few versions of BASINS available for download and the latest version is Update 8 that was released in November 2006 (refer to www.epa.gov/ost/basins).The BASINS 3.1 version was used in this research project. Like the previous versions of BASINS, it includes a data extractor, projector, project builder, GIS interface, a number of GIS tools, custom database and a series of models. The data are available through a web data extraction tool from a variety of sources. This data extraction tool is a significant enhancement in version 3.1. Plus, this version includes new features that can archive and restore BASINS projects, updated data holdings, and allows the update of BASINS software interactively. There are four models in BASINS: HSPF, PLOAD, SWAT, and AGWA and all the scripts were written with ArcView GIS.

3.8.1 PLOAD-Pollutant Loading Model

A simplified GIS-based model used to simulate non-point source of pollution loads. Pollutants are required to be specified on an average annual basis by using either the export coefficient or simple method approach. The simple method approach is an empirical method developed for estimating pollutant export from urban development sites in the Washington DC

area; however, this approach is limited to small drainage area of less than one square mile (CH2M HILL, 2001). This model can be used as a screening tool in a wide range of applications, such as stormwater permitting, watershed management, or reservoir protection projects. The input data required for PLOAD are: GIS land use data, GIS watershed data, GIS BMP (best management practice) site and area data (optional), pollutant loading rate data tables, impervious terrain factor data tables, pollutant reduction BMP data tables (optional), point source facility locations and loads (optional).

3.8.2 HSPF- Hydrological Simulation Program Fortran (Nonpoint Source Model)

HSPF is a watershed model used to simulate nonpoint source runoff and pollutant loadings for a watershed, and combines those with point source distributions to perform flows and water quality routing in stream reaches. One advantage of HSPF is that it accounts for both point source and nonpoint source loadings and provides good display and interpretation of output data. HSPF requires Watershed Data Management (input and output timeseries data) files in order to run and it can be run on a single watershed or multiple hydrologically connected subwatersheds. It can generate continuous simulation with fixed selected timesteps ranging from 1 minute to 1 day to predict loading in mixed land use settings.

Data input, such as land use data, reach data, meteorological data, and information on the pollutants of concern in the watershed and the reaches, required for HSPF can be extracted from BASINS utilities. The reach network is automatically developed based on the subwatershed delineations. Then, site specific input files can be adapted and modified via WinHSPF and supporting information provided by BASINS utilities.

3.8.3 AGWA- Automated Geospatial Watershed Assess

AGWA is a GIS-based modeling tool having a multipurpose hydrologic analysis system for performing watershed and basin scale studies. It provides the functionality to conduct all phases for a watershed assessment for two widely used watershed hydrologic models: KINEROS2 and SWAT. It obtains the coverage from interaction with BASINS utilities to provide the coverage needed by SWAT by facilitating the assessment of land use and climate change impacts on water quality and yield at multiple scales. KINEROS2 is for the more detailed assessment at the smaller scale of an assessed area. AGWA is best suited for identifying the most important areas for watershed restoration and preventative measures (www.epa.gov/OST/BASINS/).

3.8.4 Soil and Water Assessment Tool (SWAT) Model

The Soil and Water Assessment Tool (SWAT), developed by the USDA Agriculture Research Service (ARS), is a watershed scale model that was developed to predict the impacts of land management practices on water, sediment and agricultural chemical yields in large complex watersheds with varying soils, land uses and management conditions over long periods of time. It is executed through selection of *SWAT* from the Models interface for BASINS 3.1. This extension provides a set of tools for setting up and running the SWAT model. It requires Spatial Analyst Extension ver.1.1 or later in ArcView. The development of the SWAT extension in BASINS is done by Blackland Research Center (Texas Agricultural Experiment Station), Texas A&M University System for the U.S. Environmental Protection Agency (USEPA).

The SWAT model is a spatially distributed and physically based hydrological model, which can operate on both a daily time step and annual time step for a long term (up to 100 years) simulating purpose.

SWAT is designed for use on rural ungaged basins. SWAT combines the water, sediment, and agricultural chemical yields with point source contributions and simulates the flows and water quality routing in stream reaches. There are three different types of data input required. Input data can be simulated and modified to enable the calibration of the models based on site specific conditions and data sources. To ensure a successful simulation, land use, weather, groundwater, water use, management, soil chemistry, pond, and stream water quality data, and the simulation period must be designated. Spatially distributed information is required for evaluation of soil and land use data. The soil data that comes with the installation are available only for a few states such as Texas, Pennsylvania, and Wisconsin. For other states, data can be installed separately as follows:

a) At ftp://ftp.brc.tamus.edu/pub/swat/pc/soilav/ download the soils data zipped by state.
b) In the directory drive:/Avs2000/AvSwatDB/AllUs/statsgo create a directory for each state of interest using the 2-letter alpha code for the state (e.g. NY for New York, etc.).
c) From the data obtained from the web site or CD, copy the zip file containing the soils data for the NY State to the directory created in previous steps.

Like HSPF, SWAT can run on a single watershed or multiple hydrologically connected subwatersheds, which may be divided from a watershed using the watershed delineation tool. Subwatersheds are then divided into hydrologic response units (HRUs) using the HRUs distribution tool. The concept of HRU is to create one or more unique land use/soil combinations for each subbasin in order to assess the varying hydrologic condition between sub-watersheds.

3.9 Modeling Soil Erosion/Sediment Yield Using SWAT

3.9.1 Erosion

SWAT, a physical-based model, uses the Modified Universal Soil Loss Equation, (MUSLE, as described in section 3.6.1) (Williams, 1975), to simulate erosion and sediment yield. However, SWAT generates the result of sediment yield calculated using USLE as well for comparison purposes.

The erosive power of rainfall and runoff is weaker when snow cover is present. When snow is present in the subbasin, SWAT modifies the sediment yield as follows:

$$sed = \frac{Sed'}{\exp\left[\frac{3.sno}{25.4}\right]} \qquad \text{(eq. 3.9.1-1)}$$

Where

sed- is the sediment yield on a given day (metric tons);

sed'- is the sediment yield calculated with MUSLE (metric tons);

SNO- is the water content of the snow cover, during the winter months (mmH_2O).

3.9.2 Sediment Lag in Surface Runoff

Time of concentration varies upon the size of subbasin, for instance in large subbasins, time of concentration can be greater than one day and only a portion of surface runoff reaches the main channel on the day it is generated. Therefore, SWAT combines a surface runoff storage feature to lag a portion of surface runoff that releases to the main channel. The lag of surface runoff results in the lag of sediment as well. Thus, once the sediment load in surface runoff is calculated, the sediment load released to the main channel is calculated as following:

$$sed = \left(sed' + sed_{stor,i-1}\right).\left(1 - exp\left[\frac{surlag}{t_{conc}}\right]\right)$$

(eq. 3.9.2-1)

Where

sed- the amount of sediment discharged to the main channel on a given day (metric tons);

sed'- the amount of sediment load generated in the subbasin on a given day (metric tons);

$sed_{stor,i-1}$- sediment stored or lagged from the previous day (metric tons);

sur_{lag}- the surface runoff lag coefficient;

t_{conc}- the time of concentration for the subbasin (hrs);

$1\text{-}exp[-sur_{lag}/t_{conc}]$ - represents the fraction of the total available sediment that will be allowed to enter the reach on any one day.

The relationship between time of concentration and the fraction of surface runoff storage reaching the stream is shown in Figure 3-11. For a given time of concentration, as sur_{lag} decreases in value, more sediment is held in the storage.

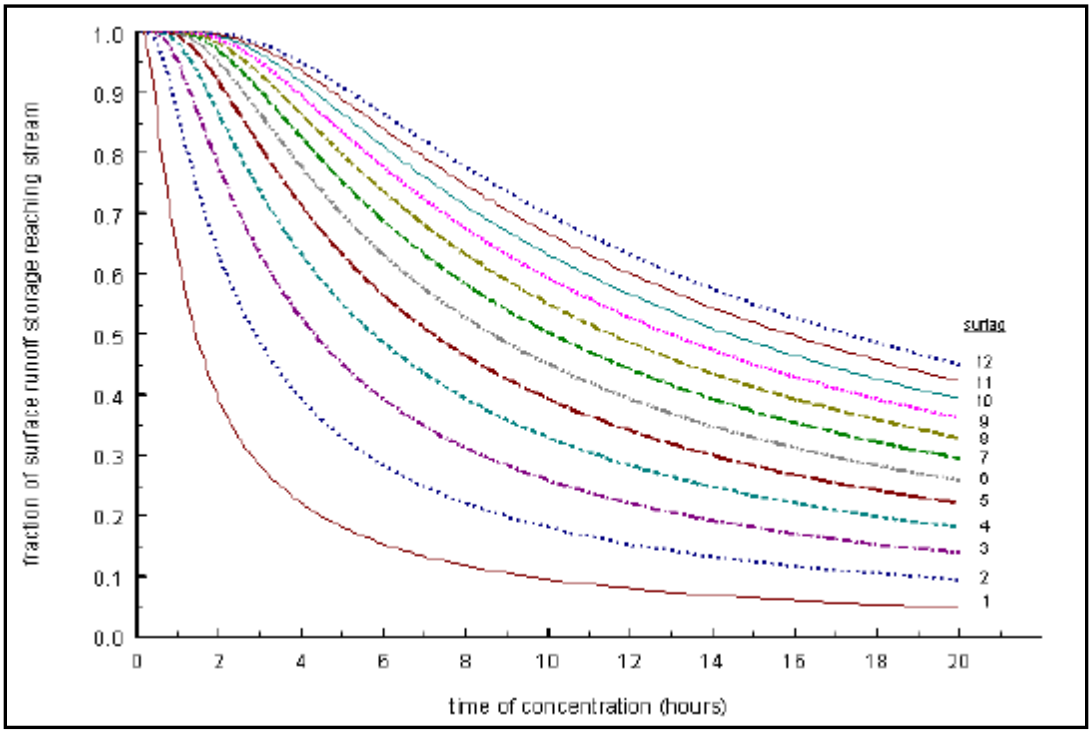

Figure 3-11. Influence of *surlag* and t_{conc} on fraction of surface runoff and sediment released.

SWAT also incorporates sediment in lateral and groundwater flow. The amount of sediment contributed by lateral and groundwater flow is calculated as show in the equation below:

$$Sed_{lat} = \frac{(Q_{lat} + Q_{gw}).area_{hru}.conce_{sed}}{1000}$$

(eq. 3.9.2-2)

Where

Sed_{lat} – the sediment loading in lateral and groundwater flow (metric tons);

Q_{lat}- lateral flow of a given day (mm H_2O);

Q_{gw}- the groundwater flow for a given day (mm H_2O);

$Area_{hru}$- area of the subbasin (km^2);

$Conc_{sed}$- the concentration of sediment in lateral and groundwater flow (mg/L).

3.9.3 Sediment Yield

3.9.3.1 Sediment Channel Routing

Once the soil particles are detached and entrained, they reach the stream channel through the transportation process from the subbasins. Sediment transport is a function of two processes: deposition and degradation. Deposition and degradation are computed in SWAT using the same channel dimension for the entire simulation. However, SWAT may simulate downcutting and widening of the stream channel and update the channel dimension throughout the simulation since the change in channel dimension due to downcutting and widening is an optional process in the main channel process.

Williams (1980) determined degradation as a function of channel slope and velocity using Bagnold's (1977) definition of stream power. The equation for calculating the maximum amount

of sediment that can be transported from a reach segment is a function of the peak channel velocity. The peak channel velocity is calculated as following:

$$v_{ch,pk} = \frac{q_{ch,pk}}{Ach} \quad \text{(eq. 3.9.3.1-1)}$$

Where

$V_{ch,pk}$- peak channel velocity (m/s);

$Q_{ch\text{-}pk}$- peak flow rate (m^3/s);

Ach- is the cross-sectional area of flow in the channel (m^2).

The maximum amount of sediment that can be transported from a reach segment:

$$conc_{sed,ch,mx} = c_{sp} . v_{ch,pk}{}^{spexp} \quad \text{(eq. 3.9.3.1-2)}$$

Where

$Conc_{sed,ch,mx}$- maximum concentration of sediment that can be transported by water (ton/m^3 or kg/L);

c_{sp}- coefficient defined by the user;

$v_{ch,pk}$- peak channel velocity (m/s);

spexp- an exponent (*spexp* varies between 1.0 and 2.0 and was set at 1.5 in the original Bagnold stream power equation (Arnold et al., 1995)).

The maximum concentration of sediment transported from a reach segment ($Conc_{sed,ch,mx}$) is then compared to the concentration of sediment in the reach at the beginning of the time step ($Conc_{sed,ch,i}$) in order to define if deposition and degradation take place.

- If ($Conc_{sed,ch,mx}$)>($Conc_{sed,ch,i}$), degradation is the dominant process in the reach segment.
- If ($Conc_{sed,ch,mx}$)<($Conc_{sed,ch,i}$), deposition is the dominant process.
    (a) ($Conc_{sed,ch,mx}$)>($Conc_{sed,ch,i}$), the amount of sediment reentrained is calculated:

$$sed_{deg} = (conc_{sed,ch,mx} - conc_{sed,ch,i}).V_{ch}.K_{CH}.C_{CH} \quad \text{(eq. 3.9.3.1-3)}$$

(b) ($Conc_{sed,ch,mx}$)<($Conc_{sed,ch,i}$), the amount of sediment deposited is calculated:

$$sed_{dep} = (conc_{sed,ch,i} - conc_{sed,ch,mx}).V_{ch} \quad \text{(eq. 3.9.3.1-4)}$$

Where

Sed_{deg}- amount of sediment reentrained in the reach segment (metric tons);

Sed_{dep}- amount of sediment deposited in the reach segment (metric tons);

$Conc_{sed,ch,mx}$- maximum concentration of sediment transported from a reach segment (kg/L or ton/m^3);

$Conc_{sed,ch,i}$- concentration of sediment in the reach at the beginning of the time step(kg/L or ton/m^3);

V_{ch}- volume of water in the reach segment (m^3H_2O);

C_{CH}- channel cover factor; is the ratio of degradation from a channel with specific vegetative cover to the corresponding degradation of a channel with no vegetative cover;

K_{CH}- channel erodibility factor (cm/hr/Pa).

Important parameters for determining channel erodibility factor (K_{CH}) are the volume of water in the reach segment. The channel erodibility factor is a function of properties of the bed channel or bank materials and it can be derived in situ via the jet index (Neitsch et al., 2002a). The K_{ch} value usually ranges from 0.10-0.45 (US customary units), soil having high clay and sand has lower K value than high silt content soil (Renard et al., 1994). A device, called a submerged vertical jet device, is used to measure channel erodibility. Hanson (1991) defined a jet index, J_i, to link erodibility and scour created by the submerged jet. The jet index is a function of the depth of scour beneath the jet per unit time and the jet velocity. For further details on the

method of determining the erodibility coefficient using submerged vertical jet device refer to Hanson (1991).

Once the jet index is calculated, the channel erodibility factor is defined:

$$K_{Ch} = 0.003.\exp[385.J_i]$$

(eq. 3.9.3.1-5)

K_{CH} is the channel erodibility coefficient (cm/hr/Pa), $J_i$is the jet index.

Once the amount of deposition and degradation has been calculated, the final amount of sediment remaining in the reach is determined:

$$sed_{ch} = sed_{ch,i} - sed_{dep} + sed_{deg}$$

(eq. 3.9.3.1-6)

Where

sed_{ch}- amount of suspended sediment in the reach (metric tons)

$sed_{ch,i}$- amount of suspended sediment in the reach at beginning of the time period (metric tons)

sed_{dep}- amount of sediment deposited in the reach segment (metric tons)

sed_{deg}- amount of sediment reentrained in the reach segment (metric tons)

The amount of sediment transported out of the reach is determined:

$$sed_{out} = sed_{ch}.\frac{V_{out}}{V_{ch}}$$

(eq. 3.9.3.1-7)

Where

sed_{out}- amount of sediment transported out of the reach (metric tons);

sed_{ch}- amount of suspended sediment in the reach (metric tons);

V_{out}- volume of outflow during the time step (m^3H_2O);

V_{ch}- volume of water in the reach segment (m^3H_2O).

CHAPTER 4

4 WATER QUALITY ASSESSMENT

4.1 Introduction

Two Hydrolab Datasonde 4a's were installed at two sites, upstream and downstream, in order to assess the water quality of Cayuga Creek. The downstream site is between Walmore Road and Niagara Falls Boulevard and the upstream site is located near Lockport Road. The downstream site was chosen as the upstream limit of flow impacts from the Niagara River and was previously used as a sample site by the Niagara County Soil and Water Conservation District office. A sample site map is shown in Figure 4-1.Grab samples were collected weekly in order to analyze total suspended solids concentration. Water samples were collected weekly at the two sample sites through a ten-week sampling period in the summer of 2007.

Based on field observation, at the upstream site (located near Lockport Road approximately 3.2 km north of Niagara Falls Boulevard), the reach looked undisturbed with a large amount of overhanging vegetation and the banks were in good condition with vegetation cover. The water at the upstream site was clear and fishes and some other macrobenthic organisms could be observed. The water appearance at the downstream site was cloudy and muddy most of the time. The banks were actively eroding and there was waste from construction such as concrete in the bed of the creek. There was some overhanging vegetation at the top of bare banks. Pools and riffles were present at both sites.

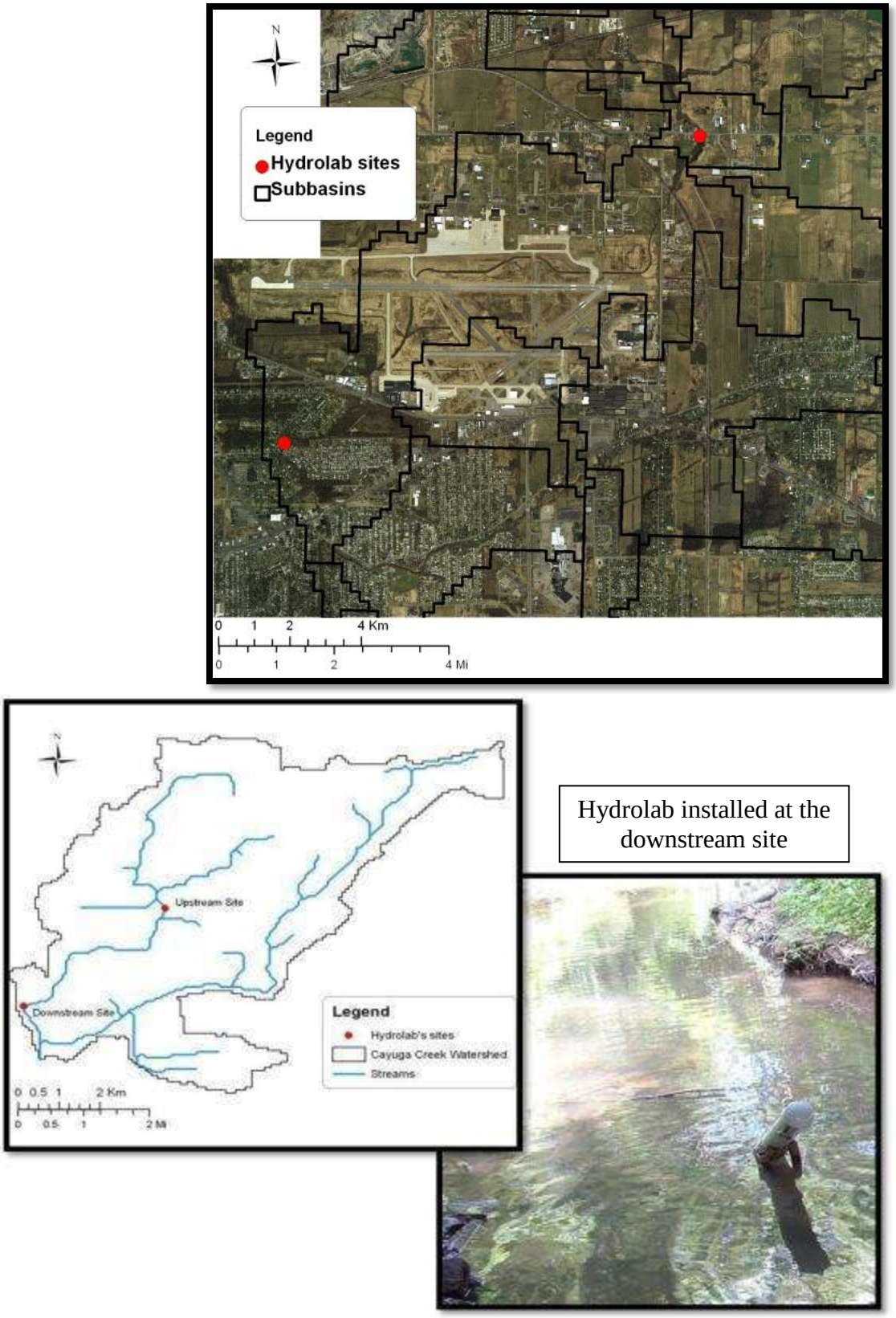

Figure 4-1. Hydrolab site locations.

4.2 Data and Methods

4.2.1 Continuous Water Quality Monitoring Using Hydrolab Datasonde 4a

Hydrolab Datasonde 4a's were used to assess water quality parameters. The datasondes contain multiple sensors for measuring different parameters. The parameters set in the Hydrolab for this study were: temperature, dissolved oxygen (DO), conductivity, pH, and turbidity. The time interval of measurement was set to 15 minute timesteps. The sensors of the Hydrolab are shown in detail in Figures 4-2 to 4-5. The water quality data were downloaded weekly from the Hydrolab Datasonde 4a's for the period of 10 weeks, starting from May 14th, 2007 to July 13th, 2007.

Figure 4-2. Hydrolab Datasonde 4a connected to a laptop.

Figure 4-3. Dissolved Oxygen Sensors.

DO sensors use field-proven Clark Cell technology, provides a continuous steady-state reading, with low maintenance. Range 0 to 50 mg/L, accuracy ±0.2 mg/L for 20 mg/L or less ±0.6 mg/L for over 20 mg/L, resolution 0.01 mg/L.

Figure 4-4. Circulator.

The circulator helps to provide fast, accurate, steady-state dissolved oxygen measurement by creating flow of water past the sensors and providing sufficient sample flow across the membrane surface; reducing response time that is important to detect moving contaminant plumes or movement within water column; sweeping away inert debris and biological growth that cause sensor fouling; and allowing deployment in any environment, even in poorly mixed areas.

Figure 4-5. Self-cleaning turbidity sensor.

A self-cleaning turbidity sensor was included with the Hydrolab being used at the upstream site. It measures the intensity of light scattered by particles in water at a 90 degree angle from an infrared light source.

4.2.1.1 Calibration Preparation and Procedure

The dissolved oxygen (DO) calibration was done weekly and the pH calibration was conducted monthly. The following is a general outline of the steps required to calibrate all the sensors (except DO).

- Select a calibration standard whose value is near the field samples.
- Clean and prepare the sensors.
- To ensure accuracy of calibration, discard used calibration standards appropriately.

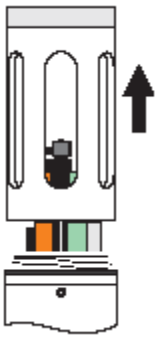

1. Remove the sensor guard.

2. Attach the calibration cup

3. Unscrew and remove the cap from the calibration cup.

4. Fill the calibration cup half full with standard.

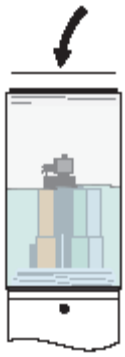

5. Place the cap on the calibration cup.

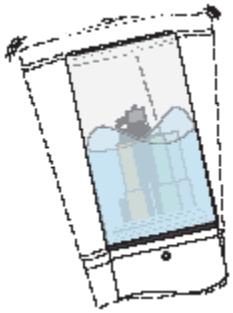

6. Shake the Sonde well to make sure that each sensor is free from the contaminants that might alter the standards. Repeat the process several times and rinse the sensors twice with the standard solution.

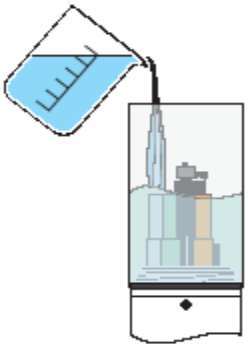

7. Complete the calibration.

4.2.1.2 Dissolved Oxygen Calibration

DO was calibrated at each site using Hydras 3LT software following the 100% air saturation method. The calibration procedure for calibrating DO is as follows:

- Assemble the data cable and the Sonde and attach the 9-pin connector to a laptop. Run Hydras 3 LT (as shown in Figure 4-6) and wait for the software to scan for connected Sonde.

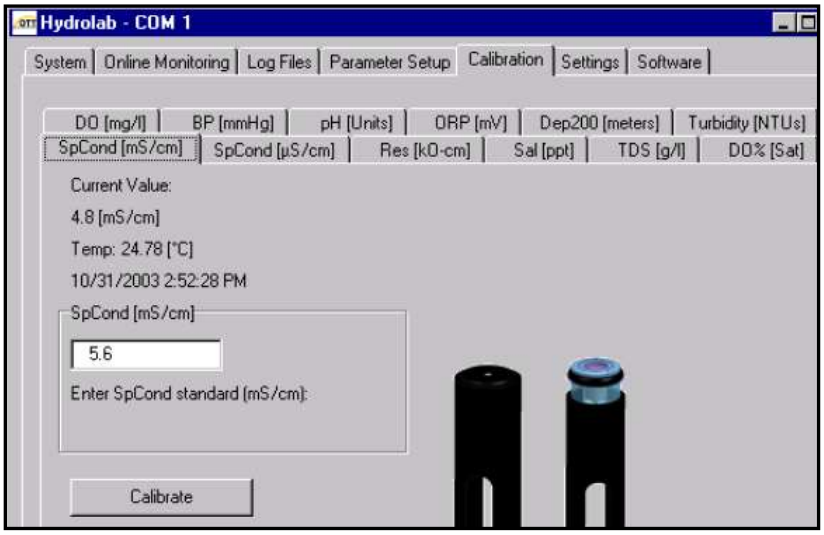

Figure 4-6. Hydras 3LT dialog box.

- Fill the calibration cup with distilled water until the water is just below the membrane.
- Remove all the droplets of water from the membrane using cleaning tissue.
- Connect the cup filled with water to the Sonde. Leave the water to equilibrate, and enter the pressure value to 760 mmHg, and click *Calibrate* button.

4.2.2 Total Suspended Solids Assessment

Total suspended solids are defined as those solids which are retained by a glass fiber filter and dried to constant weight at 103-105 °C. Total suspended solids is usually abbreviated TSS.

Grab samples were collected weekly, within ten weeks starting from May 14th, 2007 to July 13th, 2007; and 500ml of water sample was collected at each site for total suspended solids

analysis. The gravimetric method was used to analyze the total suspended solid and the analysis was performed in the watershed laboratory at Buffalo State College. To limit the inaccuracy, all filters were placed in a desiccator at least an hour prior to being used. The disposable aluminum dishes were dried up in the oven prior to usage and water sample bottles were left at room temperature prior to being weighed. It was assumed that the water sample density equal to one.

The samples were collected from the creek as close to the bottom as possible and the particulates such as leaves, sticks, fish, algae, lumps, should not be in the sampling bottle with the water sample. The samples were preserved in the refrigerator to 4°C to minimize the microbiological decomposition of solids; and the analysis was performed as soon as possible after sample collection.

4.2.2.1 Laboratory Methods

The filtration process was conducted by filtering a well-mixed sample through a weighed standard glass-fiber filter and the residue retained on the filter was dried to constant weight at 103 to 105°C, for approximately one and half hours. The increase in weight of the filter indicates the total suspended solids. The interferences for total suspended solids analysis can be large floating particles or submerged agglomerates of nonhomogeneous materials from the sample if it is determined that their inclusion is not desired in the final result. The variables that have been noted as the factors affecting the results are: filtration apparatus, filter material, pre-washing, post-washing, and drying temperature. For most of the downstream site samples, the duration for the water sample to pass across the filter was prolonged due to the excessive amount of sediment at the site.

4.2.2.2 Apparatus Required

The apparatus required for analysis of TSS concentration is demonstrated in Figure 4-7.

- Disposable aluminum dishes
- Flask funnel, 1000ml
- Fritted glass support base
- Anodized aluminum clamp
- Glass funnel
- Vacuum pump
- Drying oven
- Desiccator
- Forceps
- Analytical balance
- Filter cup
- Tubing
- Glass Fiber Filter (GFF).

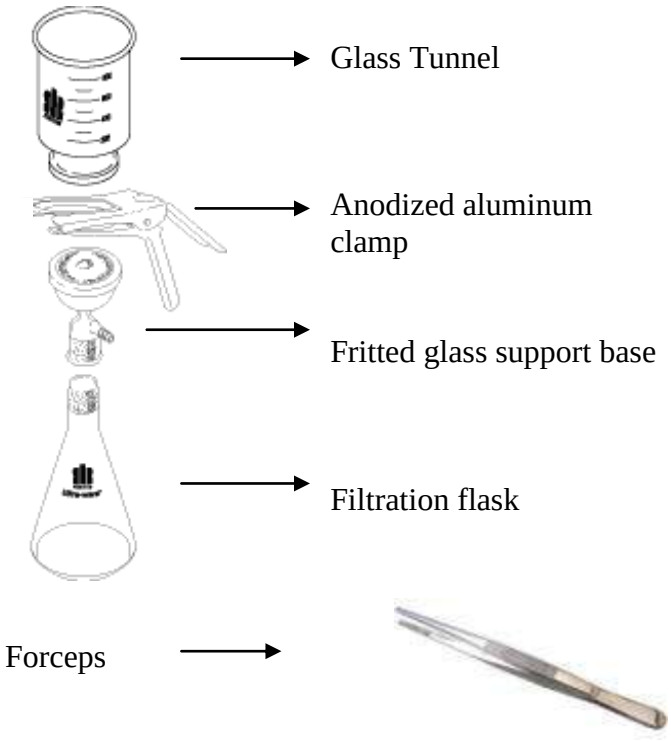

Figure 4-7. Filtration apparatus.

4.2.2.3 Procedure for Suspended Solid Analysis

Once the filtration took place, the sediment was transferred onto the filter. Sample duplicates were run at a rate of 10% of all samples.

a. Leave the water sample in order for it to get to the air temperature before weighing.
b. Leave the filter in the desiccator for at least an hour to dry off all the water that has been attached to the filter.
c. Measure the weight of the bottle with the water sample. Record the reading (A).
d. Place the clean filter in the aluminum dish and record the combined weight as (b)
e. Assemble the fritted glass support base and the filtration flask, which has been connected to the vacuum pump.
f. Place the filter paper on the fritted glass support base.
g. Connect flask funnel to the support base, which the filter is placed on, using the aluminum clamp.
h. Wet the filter with a small volume of distilled water to seal the filter against the base.
i. Shake the sample bottle thoroughly so that all the sediment gets in suspension and then pour the sample in the flask funnel. Turn on the vacuum to begin suction.
j. Weigh the empty bottle. Record the reading as (B).
k. Rinse the sample bottle by distilled water to maximize the transfer of sediment to glass funnel.
l. Use the tap water to remove the sediment that attaches to the glass funnel.
m. Once the water sample percolated out of the filter flask, carefully unscrew the glass funnel and lift the filter paper with the sediment with forceps. Quickly place the filter in the aluminum dish.
n. The aluminum dish with filter is then placed in the drying oven set at 105 °C; leave it dry for approximately one and half hours.
o. Remove the aluminum dish that has the filter with dried residue on; cool in a desiccator to balance temperature and weigh it and record the reading as (a).
p. Desiccate the aluminum dish, reweigh until a constant weight is obtained.

q. Input the records in the spread sheet and compute the suspended sediment concentrations.

4.2.2.4 Calculation

Milligram of Total Suspended Solid:

$$\frac{(a-b)\times 1000}{(A-B),ml} \qquad \text{(eq. 5.2.24-1)}$$

Where

a - Weight of (filter + dish + dried residue), mg

b- Weight of (filter + dish), mg

A- Weight of (water + bottle), mg (assuming that water density = 1)

B- Weight of (empty bottle), mg

4.3 Results and Discussions

Water quality parameters measured by the Hydrolabs included dissolved oxygen, pH, turbidity, temperature, and conductivity. The sampling period was 10 weeks in total, starting from May 14th, 2007 to July 13th, 2007 (Table 4.1).

Table 4-1. Hydrolab sampling dates.

Week	Date
Week1	4 May 2007 – 11 May 2007
Week2	11 May 2007 – 18 May 2007
Week3	18 May 2007 – 25 May 2007
Week4	25 May 2007 – 1 June 2007
Week5	1 June 2007 – 8 June 2007
Week6	8 June 2007 – 15 June 2007
Week7	15 June 2007 – 22 June 2007
Week8	22 June 2007 – 29 June 2007
Week9	29 June 2007 – 6 July 2007
Week10	6 June 2007 – 13 July 2007

4.3.1 Temperature

The weekly mean temperature pattern for the two sites are consistent, however, the water at the upstream site was consistently colder than the downstream site (Figure 4-8). This may be because the upstream site is located close to the base flow and groundwater spring inputs and as the water flows downstream it received more discharge from the urban environment. Furthermore, the overhanging vegetation along the creek at the upstream site may be one of the reasons why the water temperature at the upstream site was obviously low. The greater amount of total suspended solids at the downstream site may cause an increase of water temperature as the light suspended particles may absorb the heat from the sunlight. The maximum values of weekly mean temperature were approximately 15 °C and 22 °C and the minimum values were approximately 13°C and 15°C at the upstream site and downstream sites respectively.

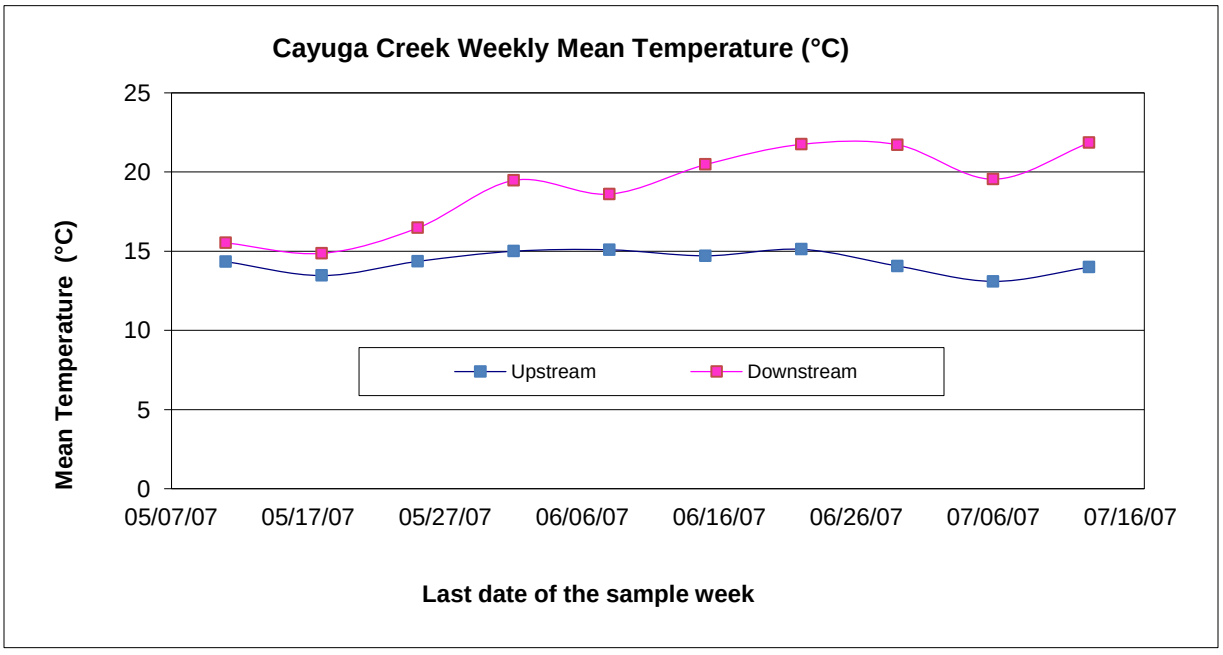

Figure 4-8. Weekly mean temperature data at the upstream and downstream sites.

Daily temperature ranged from 9 °C to 21 °C at the upstream site and 11 °C to 25 °C at the downstream site and the 15 minute time step data showed a characteristic diurnal pattern (Figure 4-9).

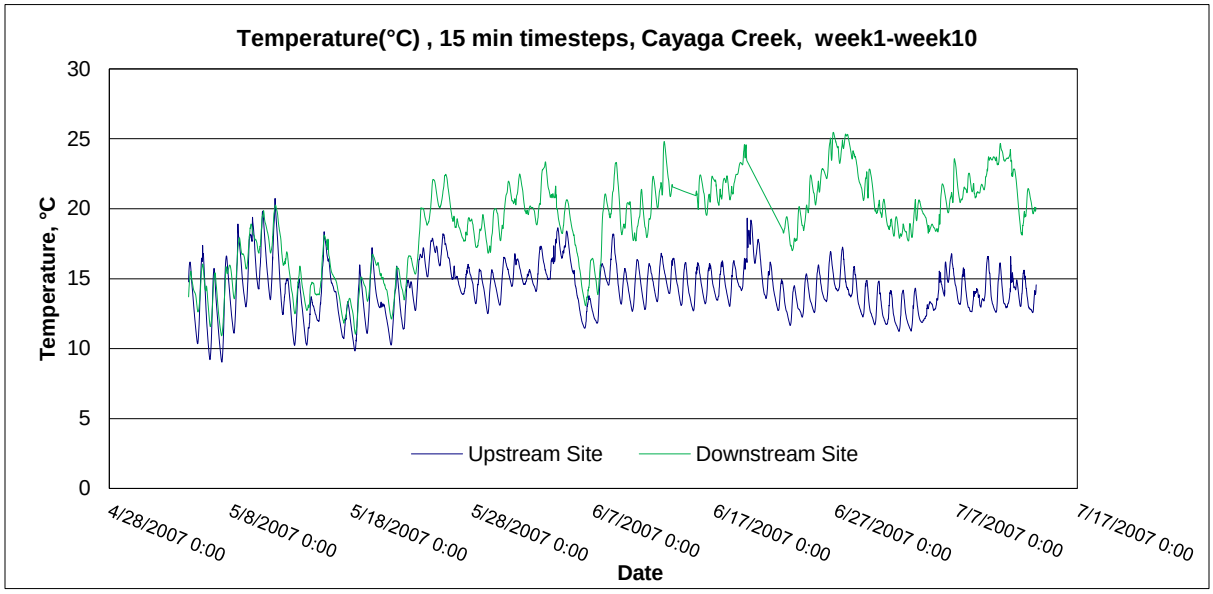

Figure 4-9. Temperature measured at 15 min. timesteps.

4.3.2 Dissolved Oxygen (DO)

Dissolved oxygen is necessary in aquatic systems for the survival and growth of aquatic organisms. Dissolved oxygen is used as the indicator of the health of the surface waterbody. Dissolved oxygen (DO) is affected by many factors such as atmospheric pressure, ambient temperature and ion activity. The DO data are important for documenting the change of DO due to human activity and natural phenomena. Anthropogenic activities such as sewage discharge or urban runoff can cause a decrease in DO as high BOD in sewage discharge or runoff from the urban areas consume the available oxygen in the water. The concentration of dissolved oxygen has a close relationship with the water temperature and these data are important for aquatic

habitat and ecological assessment of the Cayuga Creek. The sources of dissolved oxygen in surface water include atmospheric aeration and photosynthesis activities of aquatic plants.

The weekly mean DO patterns of the two sites tended to correspond. During week 1, the DO concentrations appeared to be at their maximum of 9.6 mg/L and 6.5mg/L for the upstream and downstream sites respectively (Figure 4-10). They dropped to their minimum values at week 4. These results were consistent with the temperature of the water in early May which was still cold. Water temperature can be a main factor controlling the amount of DO in the water as the colder the water is, the greater the DO the water contains. The DO levels tended to be stable from week 4 to week 10 at both sites. Although weekly mean DO appeared similar at both sites (6.05 mg/L at the upstream site and 6.0 mg/L at the downstream site), the upstream site had a higher degree of variability (standard deviation is 1.56) than the downstream site (standard deviation is 0.67). This greater variability also was reflected in the 15 minute data shown in Figure 4-11.

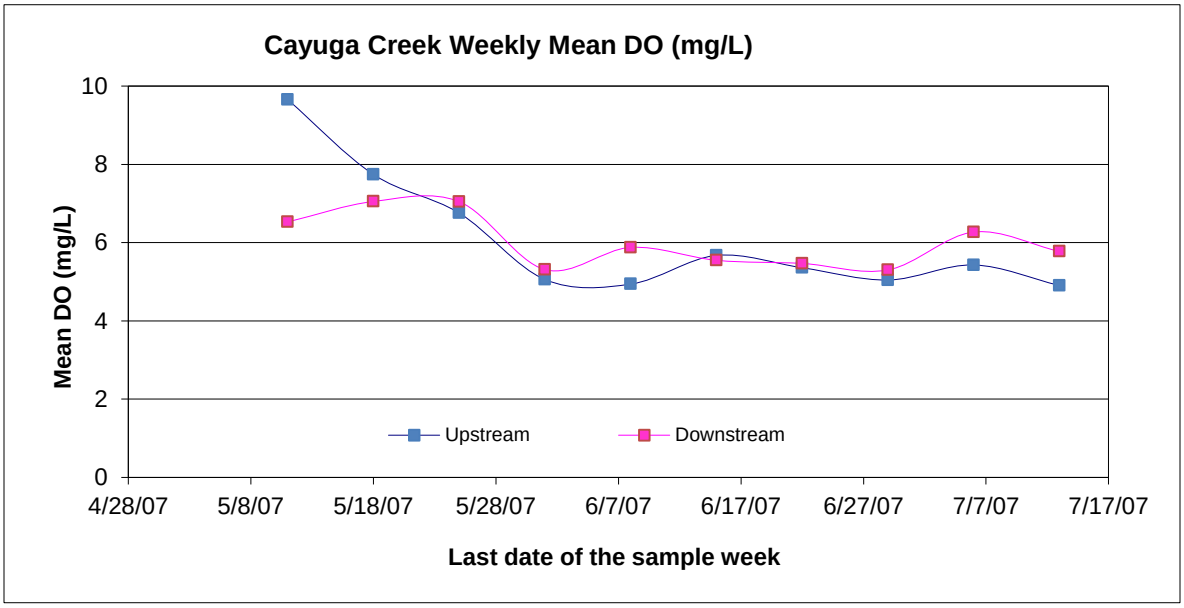

Figure 4-10. Weekly mean DO data at the upstream and downstream sites.

The daily maximum value of DO tended to occur between 13:00 to 18:00 due to the presence of light for photosynthesis by aquatic plants and phytoplankton and it decreased at night as respiration by plants and aquatic organisms occurred. The upstream site had a greater diurnal swing (Figure 4-11) than the downstream site due to the photosynthetic activity and the upstream site water was colder.

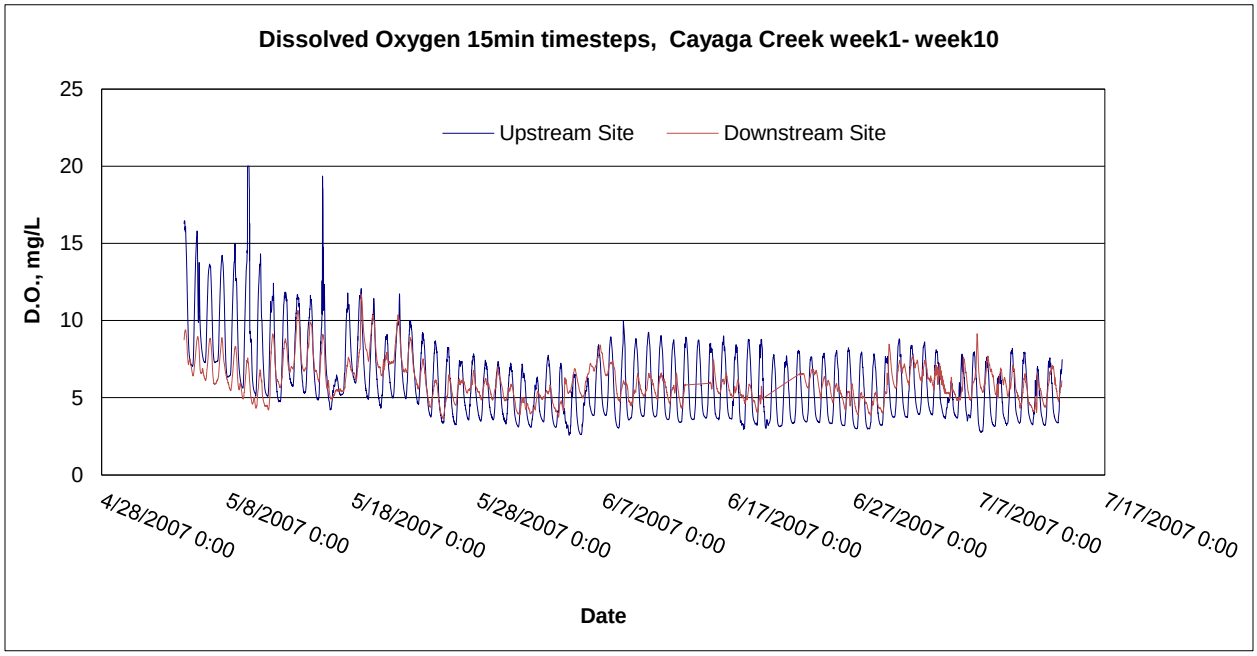

Figure 4-11. DO measured at 15 min. timesteps.

4.3.3 Conductivity

The weekly mean conductivity patterns at the upstream site looked very stable (0.8 mS/cm). At the downstream site, weekly mean conductivity shifted from 1.2 mS/cm at week 1 to about 1.7 mS/cm at week 7 to week 10. The change in conductivity at the downstream site could be an indicator of discharge or some other source of pollutants that had entered the creek. Results

of weekly mean conductivity obtained from the Hydrolabs at the upstream and downstream sites are presented in the Figure 4-12.

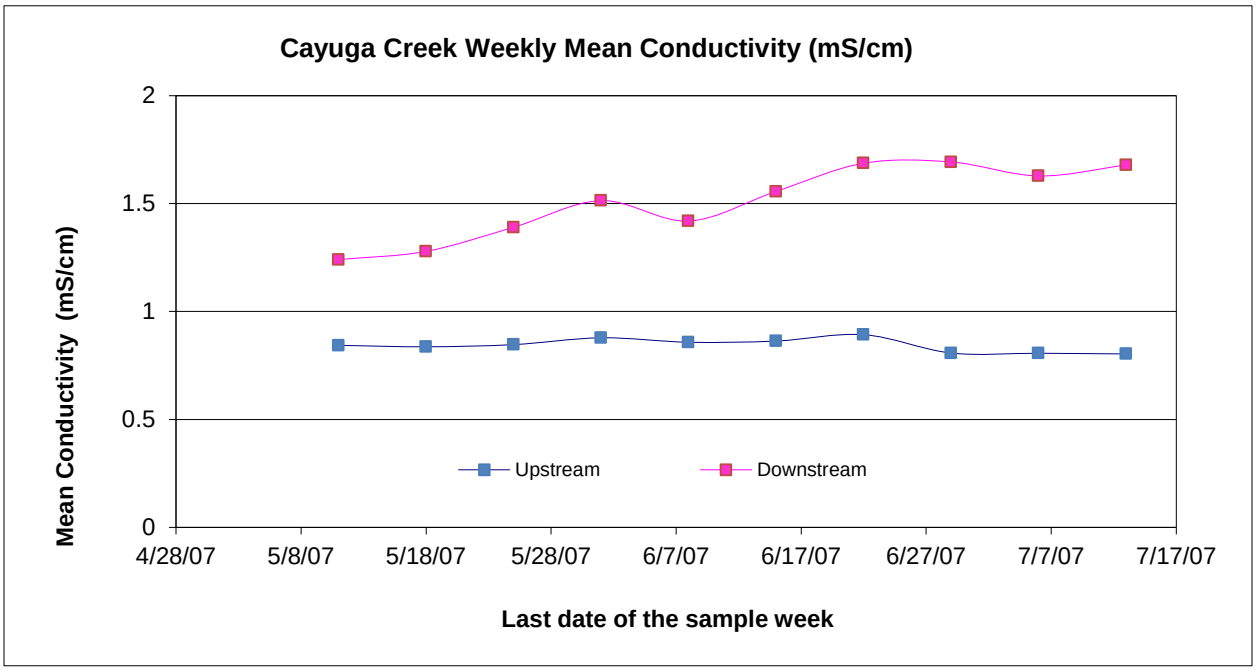

Figure 4-12. Weekly mean conductivity data at the upstream and downstream sites.

The daily diurnal pattern in conductivity was quite apparent at the upstream site, the value ranged from 0.2 – 2.2 mS/cm at the downstream site (except on 06/20/2007) and 0.5-2.9 mS/cm at the upstream site. The USEPA stated that the conductivity of rivers in the United States generally ranges from 0.05-1.50 mS/cm and streams that support good mixed fisheries have a conductivity range from 0.15 to 0.50 mS/cm (USEPA, Monitoring and Assessing Water Quality, http://www.epa.gov/volunteer/stream/vms59.html). Based on this statement, the conductivity of Cayuga Creek water tends to be higher than streams expected to support good mixed fisheries.

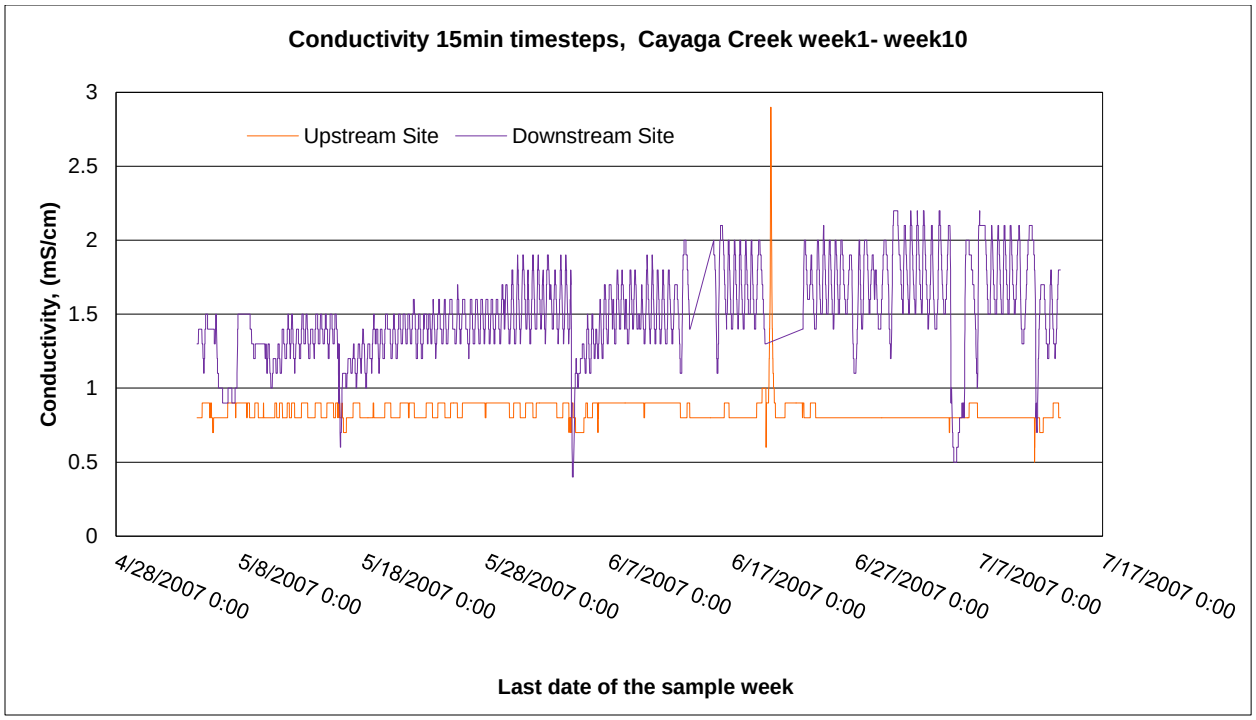

Figure 4-13. Conductivity measured at 15 min. timesteps.

4.3.4 pH

Weekly mean pH curve at the upstream site appeared to be good throughout the 10 weeks of assessment (Figure 4-14). At the downstream site, the weekly mean pH tended to be high. It started at about 9, and stayed stable for the first four weeks prior to a decline to the value of about 5 at week 5, week 6, and week 7.There was a swing from between week 4 and week 5 (Figure 4-14), the reason for this to occur is unclear. It is possible there was an illicit discharge to the creek during this time, although conductivity did not show a response over the same period. Daily mean pH curves are presented in the Figure 4-15. Daily pH ranges from 4.7 to 9.5 at the downstream site and from 6.8 to 8.3 at the upstream site (Figure 4-15).

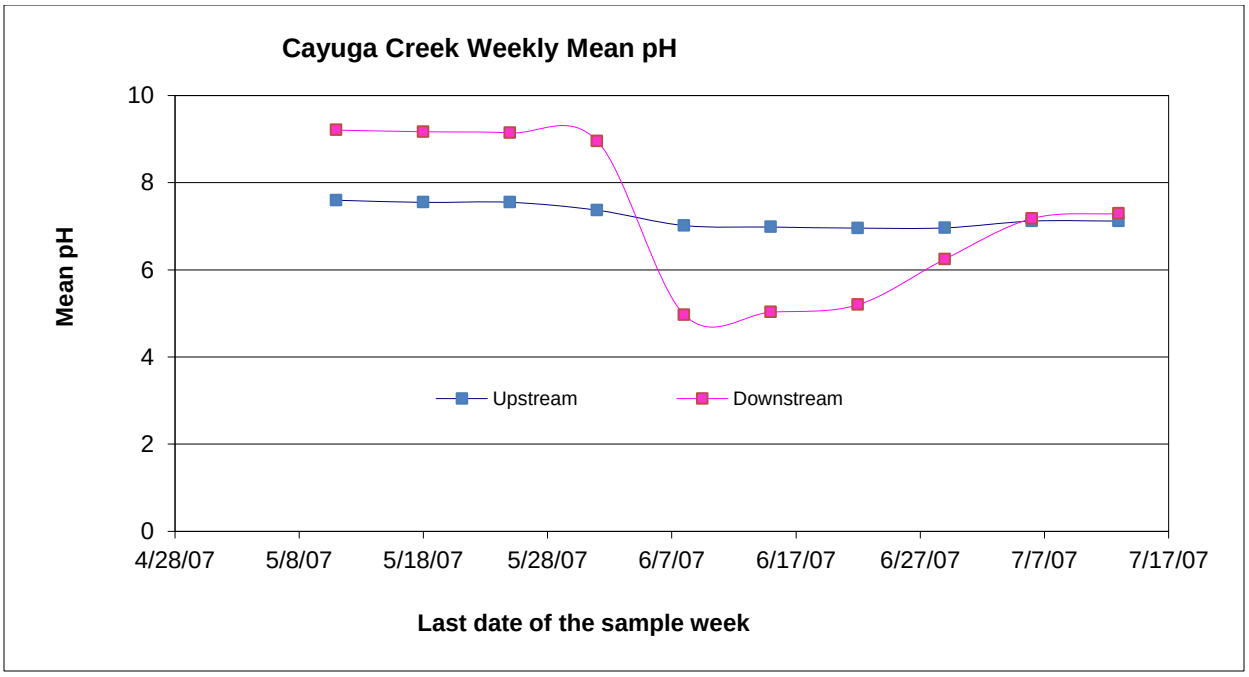

Figure 4-14. Weekly mean pH data at the upstream and downstream.

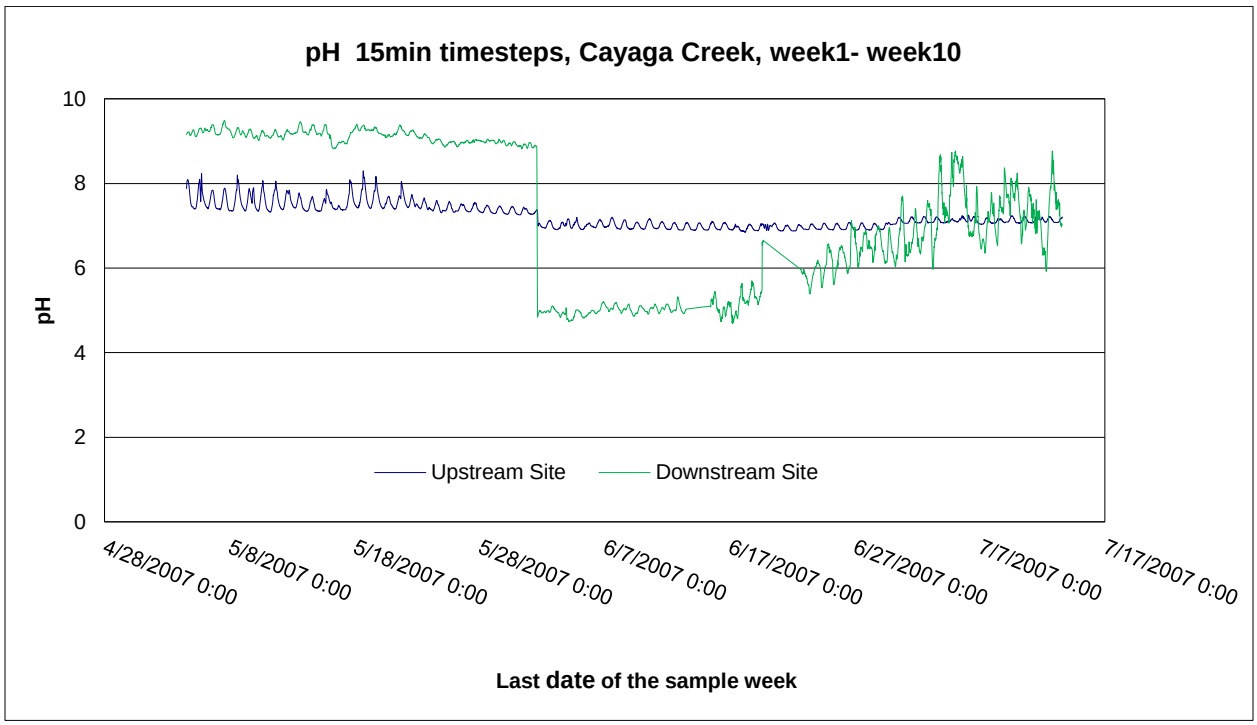

Figure 4-15. pH measured at 15 min. timesteps.

4.3.5 Turbidity

The results obtained from the Hydrolabs indicate that the amount of turbidity is very low at the upstream site, which is consistent with visual observation of water appearance during the field work. The data for week 5 at the upstream site are missing as during the routine calibration of the Hydrolab sensors on week 5, the recording unit for turbidity was mistakenly set to Volts instead of NTU. At the downstream site, the amount of sediment was very high and that required frequent cleaning operations at the site. Even after the frequent cleaning, the reading was still maximum. The data between 06/19/2007 and 06/22/2007 -22 June were missing as the sensor of the Hydrolab was broken due to operator error.

At the downstream site, the turbidity tended to be high. The weekly mean turbidity ranges from 280 NTU to about 880 NTU. There was a decreasing trend week 4, week 5 and week 6. Results of weekly mean turbidity in NTU is shown in the Figure 4-16. At the upstream site, the weekly mean turbidity ranged from 0.1 NTU to 14 NTU (Figure 4-16).

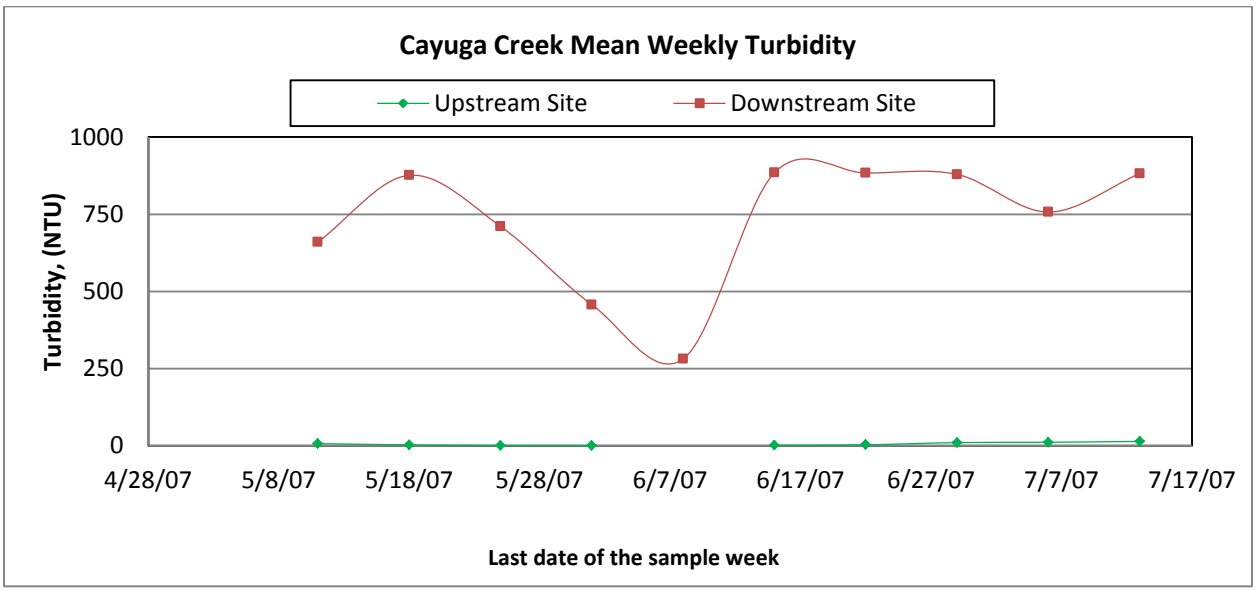

Figure 4-16. Weekly mean turbidity data at upstream and downstream site.

The daily 15 min. timesteps data indicated that the turbidity at the downstream site is quite high and often the measurement reached the maximum reading capacity of the sensor. The 15min timestep values ranged from 22 – 1000 NTU (Figure 4-17). Unlike the downstream site, the turbidity data measured at the upstream site were quite low. The 15min. timestep values ranged from 0 – 641NTU. Therefore, this high concentration of turbidity would reduce the transmission of light penetrating the water and it would increase the water temperature as the suspended particles absorb the heat from the sunlight. The increase in temperature will reduce the capacity of water to hold the amount of oxygen. As a result, the system will lose it capacity to support a diversity of aquatic organisms in the system as the photosynthesis decreases due to less light penetration. Turbidity can affect aquatic life by clogging fish gills, reducing growth rate, decreasing resistance to disease, and preventing egg and larval development (Chen et al., 1994).

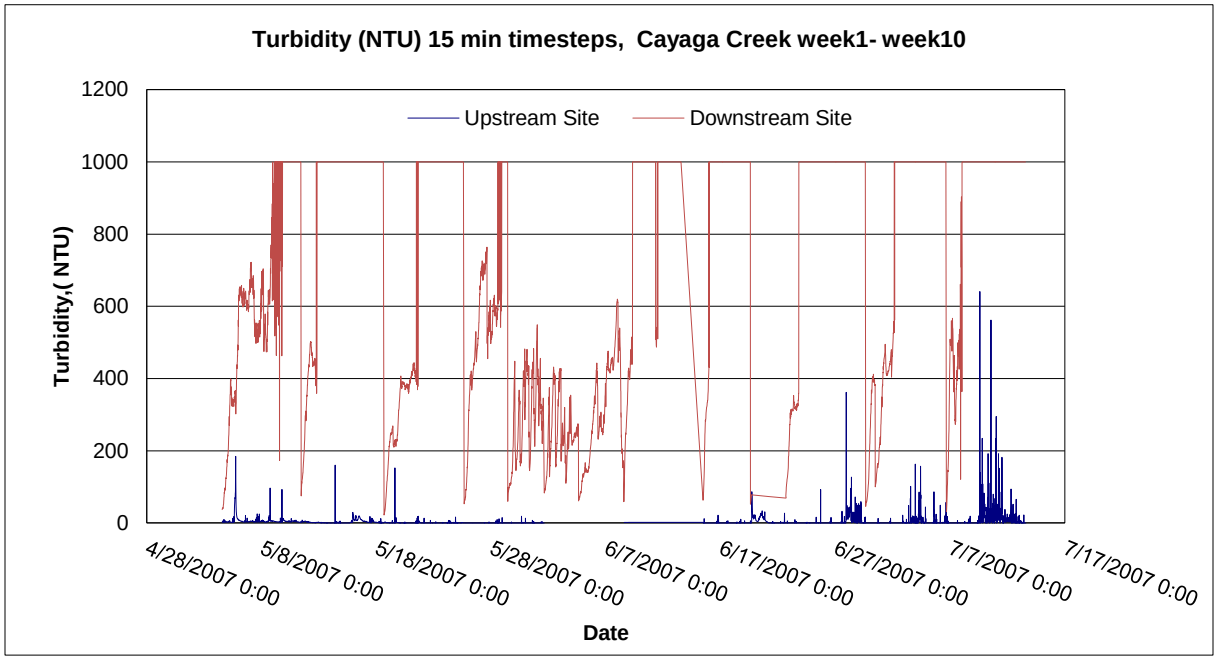

Figure 4-17. Turbidity measured at 15 min. timesteps.

4.3.6 Total Suspended Solids Results and Discussion

The results from the grab samples showed that TSS concentration at the upstream site were lower than the downstream site (Figure 4-18). Two samples on 05/08/07 and 05/11/07 at the upstream site were lost as the sampling bottles were broken due to the storage temperature. One sample on 05/04/07 at the downstream site was lost as the sample bottle broke. The TSS data are plotted in Figure 4-18.

The TSS concentration at the downstream site of Cayuga Creek ranged from 4.4 mg/L to 49.65 mg/L. The maximum TSS concentration at the downstream site was found on the 06/01/05 and the minimum value was found on 05/18/2007 (Figure 4-18). The TSS concentration varied at the upstream site from 0 mg/L to 4.41 mg/L. The high TSS concentration at the upstream site was found during the rainstorm events that occurred on 07/04/07 and 07/06/07 (Figure4-18).

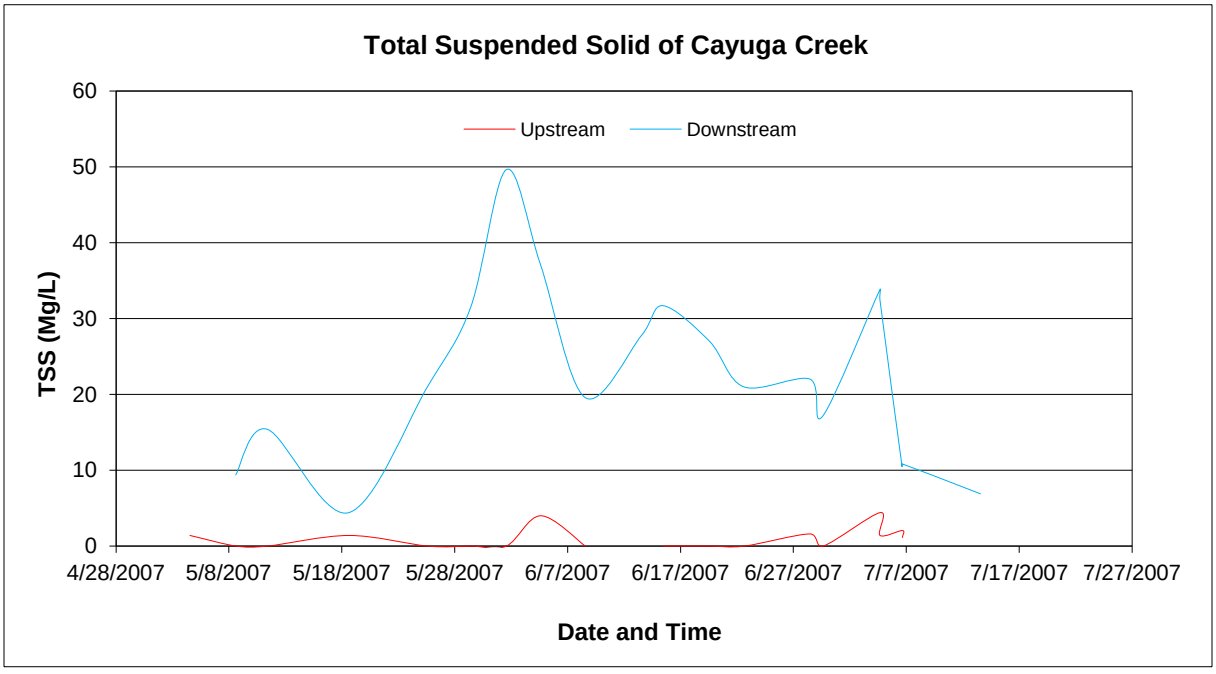

Figure 4-18. Total suspended solid concentrations at the upstream and downstream site.

Suspended sediment concentration is often predicted from different hydrologic variables using least squares regression due to the computational simplicity of the method. However there are some concerns about the poor accuracy of regression rating curves (Irvine and Drake, 1987). The seasonality often observed in suspended sediment concentrations has been related to hydrometeorologic controls, agriculture, and natural plant growth (Guy,1964; Ketcheson, et al., 1973; Temple and Sundborg, 1972).

4.3.7 Regression Analysis of Turbidity and TSS

The source and pathway of sediment input contribute to the nature and concentration of particulate matter in the aquatic system (Eisma, 1993; Webster et al. 1990). Turbidity is measured to calculate the amount of TSS, and the simple linear regression of TSS/turbidity is shown in Figures 4-19 and 4-20.

The results of these models indicate that turbidity measurement may be used to determine TSS at the upstream site. At the downstream site, more data should be collected in order to get a better coefficient of correlation used to derive the amount of TSS from turbidity measurement.

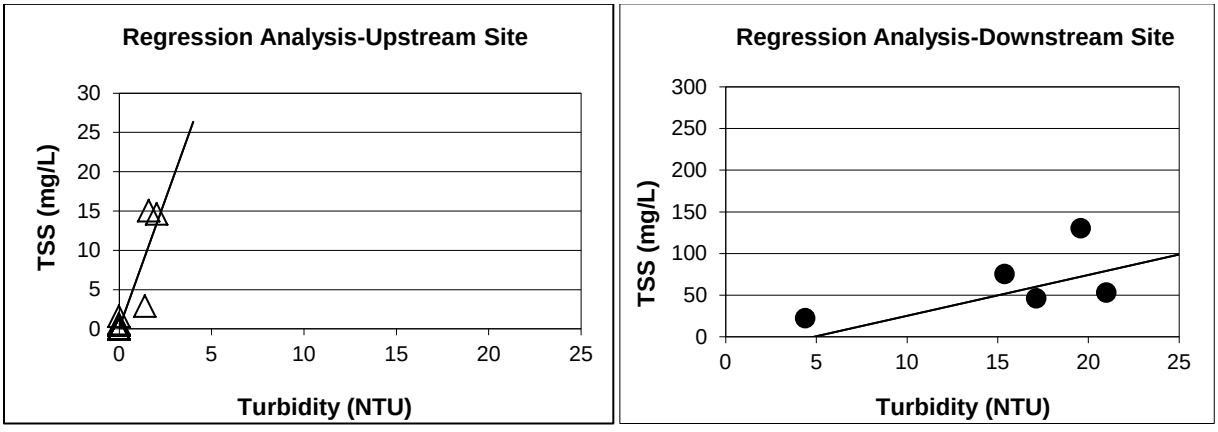

Figure 4-19. Regression TSS vs. turbidity at the upstream and downstream sites.

CHAPTER 5

5 WATERSHED DELINEATION

5.1 Introduction

BASINS Watershed Delineation tools can be used to define the entire land area contributing to the flow in the stream. Delineation of the boundary of the watershed is one of the BASINS features. It allows the subdivision of a watershed into several smaller hydrologically connected subwatersheds based on the watershed's drainage topography. The automatic watershed tool was applied in this study.

Watershed analysis can be performed on delineated watersheds using the BASINS Watershed Characterization Report Tools. The reports include land use distribution, point sources (PCS), water quality data, toxic chemical release (TRI), soil distribution (STATSGO), and elevation (DEM). The watershed boundary should not be delineated in Geographic Coordinates (Lat/Long) as the flow direction may be incorrectly derived (BASINS 3.1 Manual).

The BASINS tool consists of both Manual Watershed Delineation and Automatic Watershed Delineation. The manual watershed delineation tool allows the delineation of subwatersheds using a mouse for analysis and modeling. This tool operates on ArcView vector data and does not require the Spatial Analyst extension. Reach file, V1 or reach file V3 or NHD reach file can be used for this delineation depending on which data will be used for modeling.

5.2 Data and Methods

The Automatic Watershed Delineation tool can be used to delineate a watershed into smaller subwatersheds based on an automatic procedure using Digital Elevation Model (DEM) data. DEM data come with the BASINS software, but it can also be obtained from the USGS

website. In accordance with the DEM data, the ESRI Spatial Analyst extension is required for the Automatic Watershed Delineation process.

BASINS 3.1 includes a web-based Data Extractor allowing access to the data through the World Wide Web. In creating a new BASINS project, it is mandatory to run the data extraction prior to delineating the watershed. The *Data Extraction* tool in BASINS enables the extraction of the GIS data for New York State such as core data, Digital Elevation Model (DEM) grid and polygon data, soil data, Reach file Version 3 Alpha (Rf3), and meteorological data (WDMs). The *Data Extraction* tool allows the extraction of environmental data for a specific geographic area from the BASINS website and to define the projection. The BASINS GIS data from the BASINS website, which currently is organized by the U.S. Geological Survey (USGS) eight-digit hydrologic unit code (HUC), are available at: http://www.epa.gov/ost/basins. After the data for the study area have been extracted from the BASINS CD or website, the Project Builder is used to create an ArcView project file from the extracted data. The created project includes all BASINS GIS tools and utilities and also links to the geographic data that have been extracted. This new project contains a customized ArcView Graphical User Interface (GUI). All the environmental data layers are automatically included in the project file except Reach File Version 3 (RF3) and DEM data. When opening a new project, the display interface shows the 48 contiguous United States, the counties within those states, and the 8 digit hydrologic units or HUCs (Figure 5-1). From that interface, the hydrologic cataloging unit boundary of *Niagara, New York* (04120104) can be selected for data extraction as it is where Cayuga Creek is located. The projection properties for the BASINS data may be set before the processing of data extraction. The UTM NAD 1983_Zone17N is specified for the data that will be extracted. The extracted data are shown in Figure 5-2.

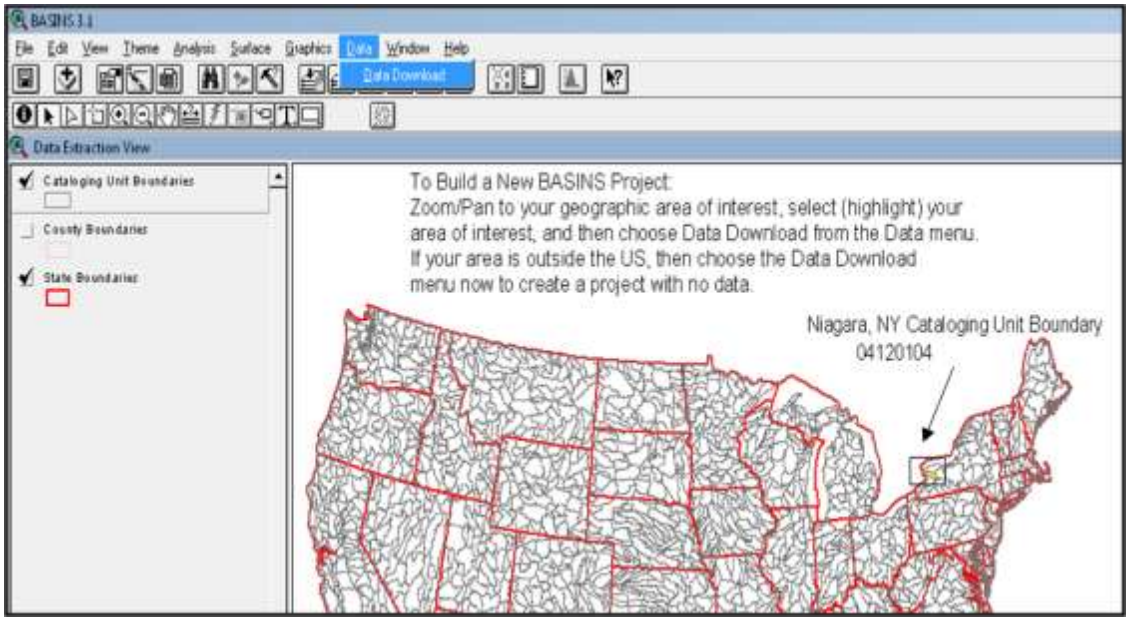

Figure 5-1. The BASINS 3.1 Data Extractor (selected Niagara, New York HUC).

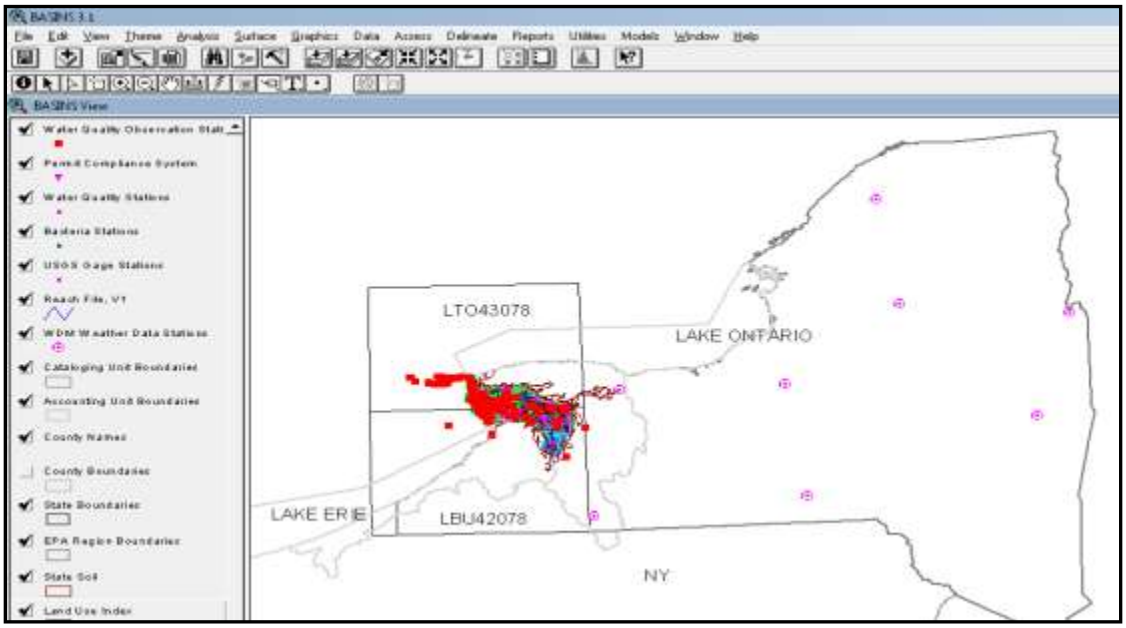

Figure 5-2. Results of data extraction for Niagara, New York HUC.

The extracted data are in decimal degrees and are based on the 1983 North American Datum (NAD 1983). The decimal degree system is a spherical coordinate system, which means unprojected. It is necessary to project the data in order to be used with certain features in

BASINS such as the distance calculation in ArcView. Therefore, the data were projected into the UTM zone 17 coordinate system in meter units. The standard core data include all environmental data for BASINS 3.1. The core data file is required to set up a BASINS project, whereas the RF3 and DEM files are optional. Once the core data set has been extracted for a new cataloging unit, BASINS project builder needs to be run in order to build a new project.

The required shape files for watershed delineation are obtained from the Data Extraction tool in BASINS. The required data for delineating are listed in the Table 5-1.

Table 5-1. Input data for watershed delineation.

Data	Data format	Data source
DEM	Grid (cell size 300m x 300)	Topographic map USEPA/Office of Water/OST Basins
Mask Grid	Grid, based on DEM	Manually drawn on BASINS interface
NHD	Vector map	Obtained from NHD Download tool

5.2.1 Automatic Delineation Procedure

The procedure for the automatic watershed delineation consists of the following steps: (1) activate the Cataloging Unit Boundary theme, and then (2) bring up the *Automatic Delineation* dialog from the *Delineate* menu in order to begin the delineation process. The delineation dialog consists of five sections: (a) Setup, (b) Stream Definition, (c) Outlet and Inlet Definition, (d) Main Watershed Outlet(s) Selection and Definition, and (e) Reservoirs (Figure5-3).The DEM grid has to be projected from State Plane 1983, NY West into UTM 1983 Zone 17.

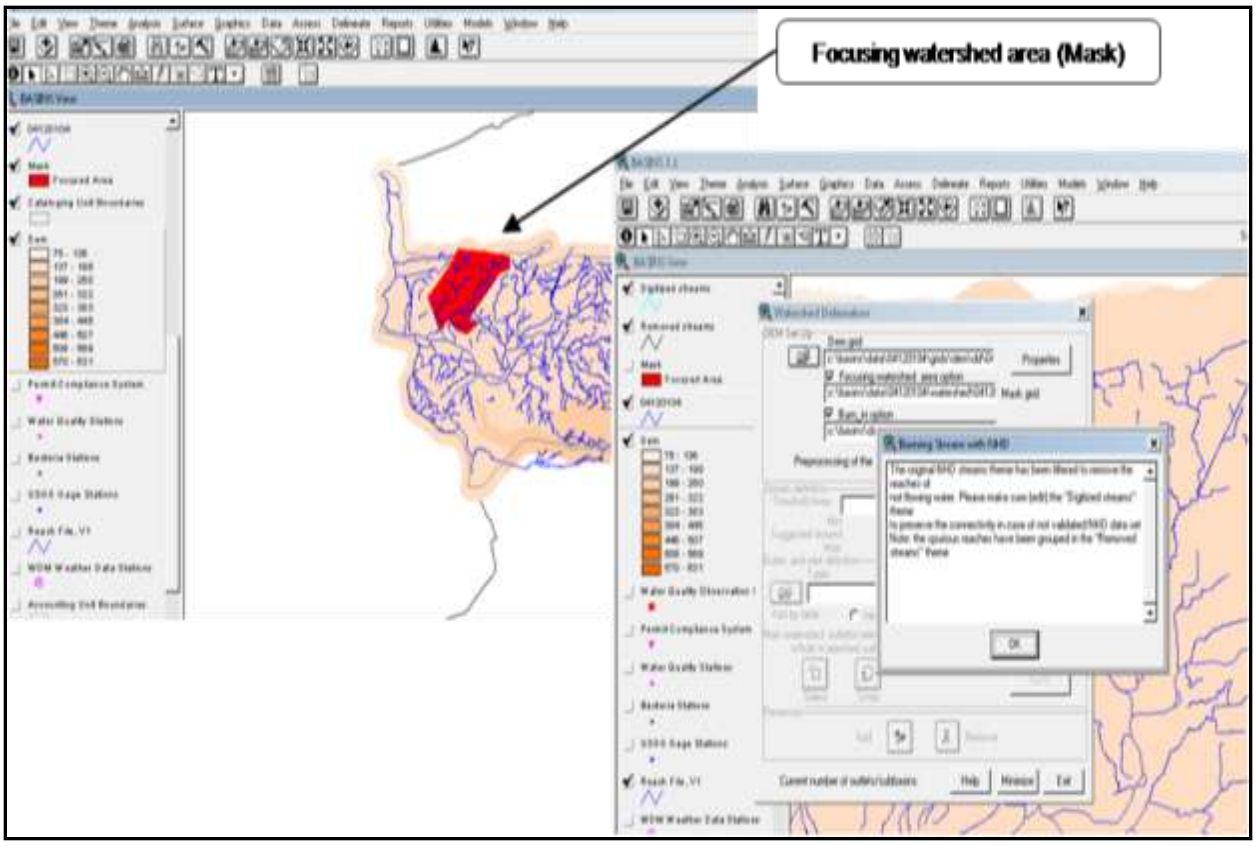

Figure 5-3. Cayuga Creek watershed delineation dialog box.

Filling DEM process will take place in order to remove the imperfection in the data by filling the "Sinks" in the DEM. The sinks are filled to a point where water will flow out of the cell and the pour point is the boundary of the cell with the lowest elevation for the contributing area of a sink. The function of the DEM is to define flow direction and flow accumulation based on elevation of which each cell will flow to the neighboring cell. Once the DEM file is loaded and filled, a focusing watershed area (Mask file) may be manually digitized or the existing file can be loaded from the disk. The focus watershed provides a boundary to which BASINS will delineate. This operation creates a grid map that masks out a part of the loaded DEM and it helps reduce the processing time of the GIS functions. For detailed operation refer to BASINS 3.1 Manual.

The stream network that is used in this process is the NHD vector map. The "stream burn-in" option defines the locations of stream networks by forcing flow directions. Furthermore, it helps correct problems associated with DEM data. The "stream definition" feature allows the change of minimum size of the subwatershed. This feature is also used to determine size and number of subwatersheds. The "Outlet and Inlet Definition" option is used to add, delete, or refine the drainage inlets and watershed outlets by importing the predefined table of inlets/outlets or manually editing.

5.3 Result of Watershed Delineation

The BASINS automatic watershed delineation output consists of the Cayuga Creek watershed boundary, subbasins, stream reaches and outlets. The area of the entire watershed is 5947ha (14,695 acres) acres. The Cayuga Creek watershed was divided into 31 subbasins, 31 stream reaches, and 31 added outlets to link between the stream reaches (Figure 5-4). The area of the subwatersheds ranged from 3 to 740ha (7.4 – 1,828 acres). Subbasin #13 was the smallest subwatershed and subbasin #3 was the largest subwatershed.

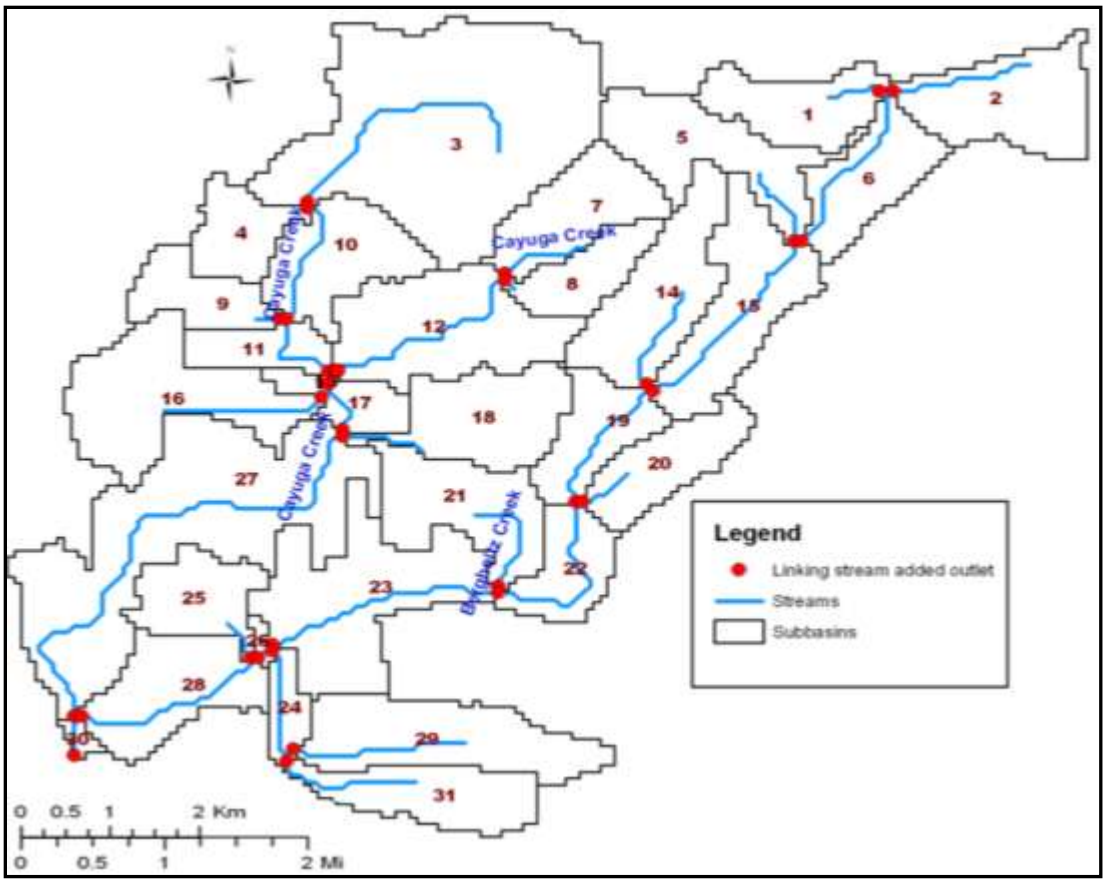

Figure 5-4. Automatic watershed delineation outputs: subwatersheds, stream reach within the subwatershed and linking stream outlets.

The stream reach length varied from 0.0737mi to 3.905mi (118.67m to 6291.68m) located within subbasin # 4 and # 27 respectively (Figure 5-4). The reaches of Bergholtz Creek are located in subbasin # 1, 5, 14, 21 and 24, reaches of Cayuga Creek are within subbasins # 7, 8, 10, 12, 27 and 28, and a small segment (451.5 m) of Niagara River is located within subbasin # 30 (Figure 5-4). The subbasin slope and stream reach slope in percentage, reach dimension, minimum and maximum elevation of stream reach, the subbasin area, and the hydrologic connection between subwatersheds are listed on the Table 5-2 and Table 5-3.

Table 5-2. Watershed delineation output field data description.

Field Name	Description
Sub R	Subbasin # receiving surface water from the subbasin
Area	Cumulated drainage area [hectares]
Len1	Stream reach (longest path within the subbasin) length [ft]
Len2	Stream reach length [ft]
R Wid	Stream reach width [ft]
R Dep	Stream reach depth [ft]
MinEl	Minimum elevation of the stream reach [ft]
MaxEl	Maximum elevation of the stream reach [ft]
Elev	Elevation of the subbasins centroid [ft]

Table 5-3. Watershed delineation output data.

Sub #	Sub R	Subbasin Area [ha]	Len1 [mile]	Len2 [mi]	R Wid [ft]	R Dep [ft]	Subb slope [%]	Reach Slope [%]	MinEl [ft]	MaxEl [ft]	Elev [ft]	Stream Name
1	6	148.3381	1.4842	0.4993	5.3619	0.4993	0.0066	0.0050	6.1680	6.30	6.17	Bergholtz Cr
2	6	215.9353	2.3378	1.1096	6.7169	0.5804	0.0034	0.0028	6.1352	6.30	6.27	
3	10	740.4389	2.0176	2.1285	14.0692	0.9501	0.0046	0.0006	6.2664	6.33	6.27	
4	10	104.5252	1.5327	0.0737	4.3461	0.4341	0.0036	0.1000	6.2664	6.27	6.30	
5	15	217.1871	3.3687	0.6959	6.7402	0.5817	0.0052	0.0027	6.1680	6.27	6.30	Bergholtz Cr
6	15	158.3525	1.1359	1.4242	5.5764	0.5125	0.0028	0.0017	6.1680	6.30	6.27	
7	12	170.2446	1.7395	0.7163	5.8238	0.5276	0.0077	0.0017	6.2664	6.33	6.40	Cayuga Cr
8	12	105.1511	1.3869	0.1534	4.3619	0.4350	0.0028	0.1000	6.2664	6.27	6.27	Cayuga Cr
9	11	106.4029	1.3181	0.2416	4.3927	0.4373	0.0056	0.0026	6.1352	6.17	6.27	
10	11	186.5180	1.9667	1.0070	6.1519	0.5472	0.0044	0.0025	6.1352	6.27	6.30	Cayuga Cr
11	13	83.2446	1.1629	0.7002	3.7913	0.3963	0.0062	0.0018	6.0367	6.10	6.14	
12	13	289.1655	0.1721	1.6580	8.0033	0.6522	0.0045	0.0022	6.0696	6.27	6.20	Cayuga Cr
13	17	3.1295	2.0404	0.0983	0.5295	0.1066	0.0061	0.1000	6.0696	6.07	6.07	
14	19	230.9569	2.5777	0.9045	6.9934	0.5961	0.0099	0.0007	5.9711	6.00	6.20	Bergholtz Cr
15	19	239.0935	2.0973	1.6243	7.1404	0.6043	0.0047	0.0019	5.9711	6.14	6.00	
16	17	284.7842	0.9087	1.2163	8.0446	0.6545	0.0063	0.1000	6.0039	6.00	6.04	
17	27	73.2302	2.1208	0.4459	3.5105	0.3766	0.0055	0.0028	5.9711	6.04	6.04	
18	27	198.4101	2.0513	0.6654	6.3842	0.5610	0.0074	0.1000	6.0039	6.00	6.07	
19	22	133.3166	1.2869	1.1580	5.0292	0.4783	0.0026	0.1000	5.9711	5.97	5.97	
20	22	142.0791	1.7514	0.4807	5.2251	0.4908	0.0006	0.1000	5.9711	5.97	5.97	
21	23	205.2950	1.9955	0.9621	6.5164	0.5686	0.0034	0.0013	5.9055	5.97	5.91	Bergholtz Cr
22	23	118.9209	1.6089	1.4614	4.6959	0.4570	0.0006	0.0009	5.9055	5.97	5.97	
23	26	342.9928	1.2816	1.7971	8.9921	0.7047	0.0055	0.0021	5.7743	5.97	5.94	
24	26	51.3237	0.3764	0.8764	2.8363	0.3268	0.0044	0.0007	5.7415	5.77	5.77	Bergholtz Cr
25	28	130.1871	2.5608	0.3908	4.9580	0.4741	0.0054	0.0016	5.7087	5.74	5.77	
26	28	10.0144	4.2943	0.1390	1.0640	0.1699	0.0050	0.1000	5.7415	5.74	5.74	
27	30	630.2806	0.3441	3.9095	12.7730	0.8907	0.0057	0.0016	5.6759	6.00	5.84	Cayuga Cr
28	30	197.7842	1.6988	1.4530	6.3720	0.5604	0.0015	0.0009	5.6759	5.74	5.68	Cayuga Cr
29	24	252.2374	1.1816	1.3350	7.3734	0.6175	0.0040	0.0023	5.8071	5.97	5.84	
30	0	13.7698	2.3835	0.2806	1.2881	0.1929	0.0000	0.1000	5.6759	5.68	5.68	NIAGARA R
31	24	163.9856	2.1293	1.0892	5.6946	0.5197	0.0052	0.0034	5.7743	5.97	5.97	

CHAPTER 6

6 LAND USE AND LAND COVER CHANGE

6.1 Introduction

Examining how the land use changes over time provides an essential description of how the landscape evolves. Evolution of land use and land cover can be due to both human activities and natural processes and this evolution causes impacts on human society, cultural and natural resources within the landscape. Therefore the interaction between human activities and land use and land cover has been a major concern in the modern world. In this research land use and land cover change between 1970's and 2005 is a key concept to examine how land use change impacts erosion in the Cayuga Creek watershed.

As described in the Chapter 2, the historical land use and land cover data of the Cayuga Creek watershed was documented by ENCRPB (1975) and NYPA (2006). The 1975 land use and land cover was described as agriculture at the upper part of the drainage area, some industrial and commercial and areas were located along the mouth of the creek, residential areas were found in the land along Lockport, Saunders Settlement, and Walmore Roads, and approximately 2,000 acres (8.1 km^2) was occupied by the air base complex (ENCRPB, 1975). NYPA (2006) described the 2002 land use as widely ranging from residential and agriculture to commercial and industrial.

6.2 Selecting Land Use Classification

The Anderson Level II Classification was used for the land use mapping in this study. This classification is for use with remotely sensed data. The classification system has been adopted by Federal and State agencies throughout the country for an up-to-date overview of land use and land cover. Land utilization pattern is the basic information needed for calibrating SWAT to

model the soil erosion yield. Table 6-1 describes the land use and land cover classification system to be used with remotely sensed data, and Table 6-2 lists the land use classification of Anderson Level II.

Table 6-1. Land use and land cover classification system for use with remote sensor data (Anderson, 1976).

Classification Level	**Typical data characteristics**
I	LANDSAT (formerly ERTS) type of data
II	High-altitude data at 40,000 ft (12,400 m) or above (less than l:80,000 scale)
III	Medium-altitude data taken between 10,000 and 40,000 ft (3,100 and 12,400 m) (1:20,000 to 1:80,000 scale)
IV	Low-altitude data taken below 10,000 ft (3,100 m) (more than 1:20,000 scale)

Table 6-2. Anderson Level II Classification (Anderson et al. 1976, U.S. Geological Survey Professional Paper 964).

Classes	**Explanation**
11.0 Urban/ Residential (Level1)	Areas of intensive use where much of the land is covered by structures.
11.1 Residential, high density	Highly populated areas. Includes apartment buildings and sub-divisions. Vegetation accounts for around 20% of the cover.
11.2 Residential, low density	Population densities lower than in high density residential areas.
11.3 Residential, rural	Very low density rural settlements, typically: ▪ 1-2 houses on large lots ▪ surrounded by agricultural fields or forest
11.4 Urban, Recreational	Grassy areas in urban settings used primarily for recreation. Examples include: playgrounds, parks, golf courses, cemeteries.
12.0 Urban/ Commercial and services	Areas used for the sale of goods and services.

13.0 Urban/ Industrial	Light manufacturing to heavy manufacturing plants.
14.0 Urban/ Transportation	Major transportation routes.
15.0 Urban/ Industrial & Commercial Complex	Areas where commercial and industrial activities occur in close proximity.
16.0 Urban/ Mixed, built-up	Areas where individual urban land uses cannot be separated.
17.0 Urban/ Other built-up	Urban areas which have an unidentified land use.
21.0 Agricultural/cropland and pasture	Fields that look like they are actively worked. Boundaries are relatively sharp ▪ Smooth texture, no brush.
21.1 Agricultural/Fallow	Fields that look like they were last worked 4-5 or more years ago: ▪ Boundaries somewhat blurred ▪ Texture is not as smooth as for active cropland; somewhat rough due to some brush, but not as pronounced as for the brush land (32.0).
24.0 Agricultural/ Other	Everything that is agricultural, but not 21.0 or 32.0. Includes, for example, horse jogging tracks, free farm, orchards, and nurseries.
32.0 Brush	Former agricultural fields or vegetation along streams: ▪ Rough texture, often on relatively smooth background (fields transitioning back to forest land).
41.0 Forest/ Deciduous	Forest areas where predominately covered by deciduous trees.
42.0 Forest/ Evergreen	Forest areas where predominately covered by evergreen trees.
43.0 Forest/ Mixed	Forest areas with mixed of deciduous and evergreen trees.
51.0 Water/ Stream and canals	Rivers, creeks, canals, and straight water bodies.
52.0 Lakes	Non-flowing, enclosed bodies of water.
53.0 Water/ Reservoirs	Artificial impoundments of water used for irrigation, flood control, and municipal water supply.
61.0 Wetland/ Forested	Wetlands dominated by woody vegetation.
62.0 Wetland Nonforested	Non-vegetated wetlands.
75.0 Barren/ Strip mines	Areas where mining and quarrying occur.
76.0 Barren/ Transitional areas	Areas where no activity is occurring or where transition is in progress, i.e. a housing subdivision is being built.

6.3 Land Use Change Methods

6.3.1 GIRAS USGS Land Use 1970's

The GIRAS 1970's land use classification was established by the USGS from the beginning of 1977 to the early 1980's to provide the historical land use and land cover data for the conterminous United States and Hawaii (Price et al., 2003).This classification was done using Anderson Level II classification. The data were then transformed to ArcInfo format by the USEPA and stored in EPA's Spatial Data Library for the assessment of land use patterns in relation to water quality analysis, growth management, and different varieties of environmental impact assessment. GIRAS land use and land cover data are currently being used in the water quality assessment model, BASINS (USEPA, Office of Water/Office of Science and Technology (OST), 1998).

Polygons of land use and land cover were delineated manually from aerial photography and mapped according to the Anderson et al. (1976) hierarchical classification system. GIRAS land use shapefiles can be downloaded through the Data Download tool in BASINS or they can be ordered through phone or mail at USEPA/Office of Water/OST, for the order instructions refer to http://www.epa.gov/waterscience/basins/.

The GIRAS land use shape file for the cataloging unit code (HUC) of the Niagara watershed (04120104) was downloaded for this study. In order to create the *GIRAS land use shapefile* for the entire Cayuga Creek watershed, the downloaded shapefile was clipped with the watershed boundary that was obtained from the automatic watershed delineation operation in BASINS. The clipping process was done in ArcGIS 9.1.

6.3.2 Digitizing 2005 Land Use

The state plane 2005 aerial photographs (1 ft resolution (0.3 m), natural color) were downloaded from the New York State digital orthoimagery for the entire watershed area. Then the GIRAS land use shapefile was overlaid with the orthoimagery prior to beginning the digitizing process. ArcGIS 9.1 was used to perform the digitizing of land use types. The *Edge, Vertex and Edge* in the *Snapping Environment* setting were activated and the *Snap Tolerance* value was set to 15 in order to minimize the errors while performing the editing process. The required data for digitizing land use are listed in Table 6-3.

Table 6-3. Sources and format of the data required for digitizing land use change.

Data	**Data format**	**Source**
Aerial photographs	1 ft resolution, natural color	NYS Department of State, Division of Coastal Resources, GIS Unit
GIRAS Land use shapefile	Shapefile	USGS/USEPA

As the digitizing of 2005 land use is based on the existing GIRAS historical land use, the digitizing process involved mainly creating new-polygons/adjacent polygons, editing polygon shared boundary, and merging neighboring polygons having the same land use type.

The attribute table of every new created polygon or edited polygon has to be edited and coded based on land use type in the Editor Tool in ArcGIS 9.1 (Figure 6-1).

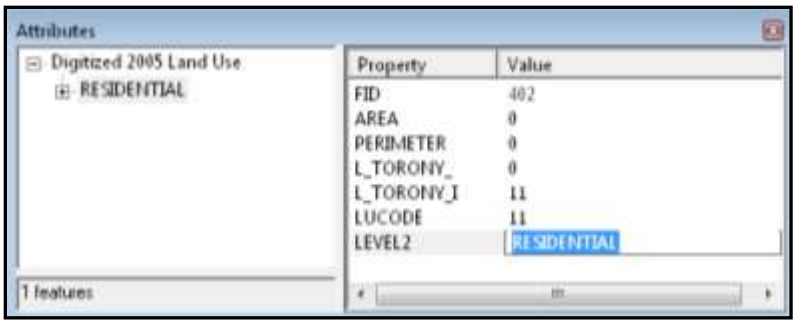

Figure 6-1. Attributes dialog box.

Tiny sliver polygons, overlapping or gaps often occur unavoidably in the editing process. Therefore, once the digitizing process was complete, the new shapefile containing new land use data for year 2005 was cleaned of slivers, gaps filled, and the geometry errors corrected. These cleaning and fixing functionalities were completed though the ArcGIS tool box. Polygons with the same land use code were dissolved together using the *Dissolve Tool* in the ArcInfo toolbox. The *Clip Tool* was used to clip overlaying polygons to make them coincident or adjacent by clipping out the overlapping portion. Select the polygon feature whose border you want to maintain. The other polygon will be clipped back to match it.

The *Integrate Geoprocessing* tool can compare features and makes any lines, points, or vertices within a certain distance range identical or coincident (Figure 6-2).

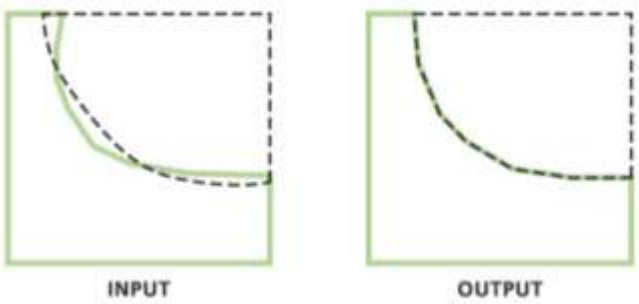

Figure 6-2. Input and output for *Integrate Geoprocessing* tool.

The area and the perimeter of the polygons were not automatically recalculated when editing a shapefile. Areas and perimeters of every single polygon were updated once the digitizing was done using the VBA script in ArcGIS (Figure6-3). The VBA script is used to process the data prior to calculating the area, length or perimeter fields (ArcGIS 9.2 Desktop Help).

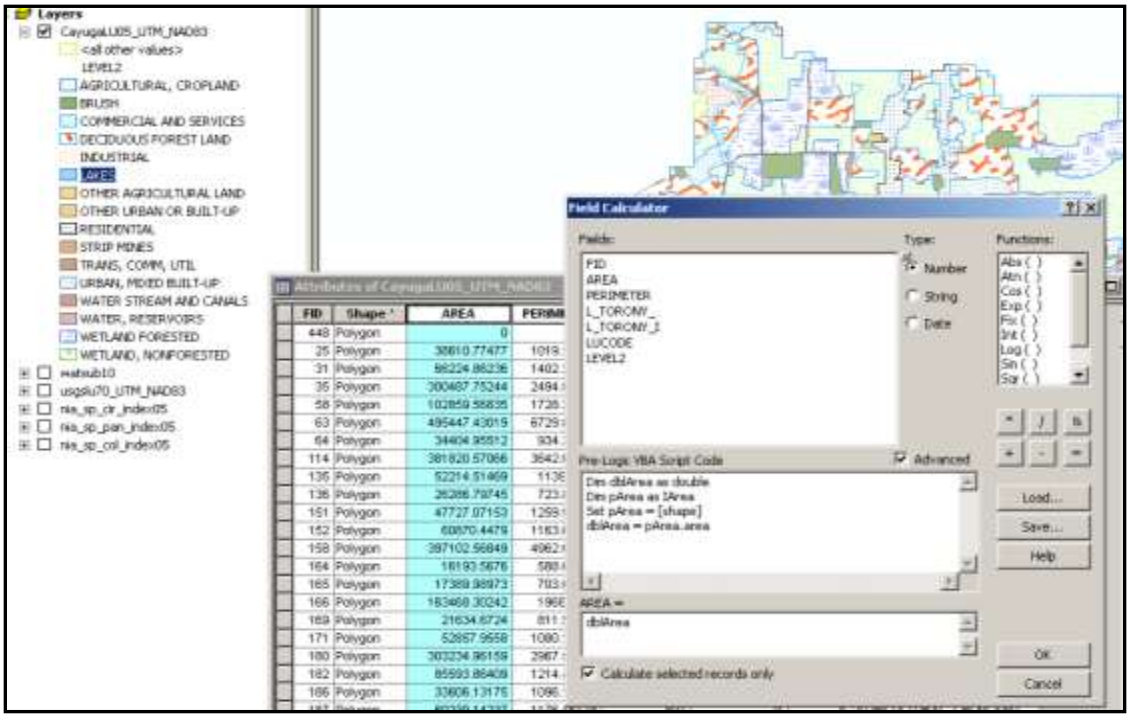

Figure 6-3. Updating area and perimeter of the digitized land use shape file in ArcGIS 9.1.

6.4 Land Use Change Results and Discussion

6.4.1 Results

The land use distributions in 1970's and 2005 based on the Anderson level II classification are detailed in Table 6-2. Figure 6-4 provides a comparison of land use changes at two different periods of time (GIRAS USGS 1970's and digitized land use in 2005). After clipping the GIRAS land use with the watershed boundary (area 5947 ha = 14695acres), the GIRAS land use within the watershed had the same area of 5947 ha (14695acres). The area of the digitized 2005 land

use, after running the cleaning process and updating the area and perimeter, also was 5947 ha (14695 acres).

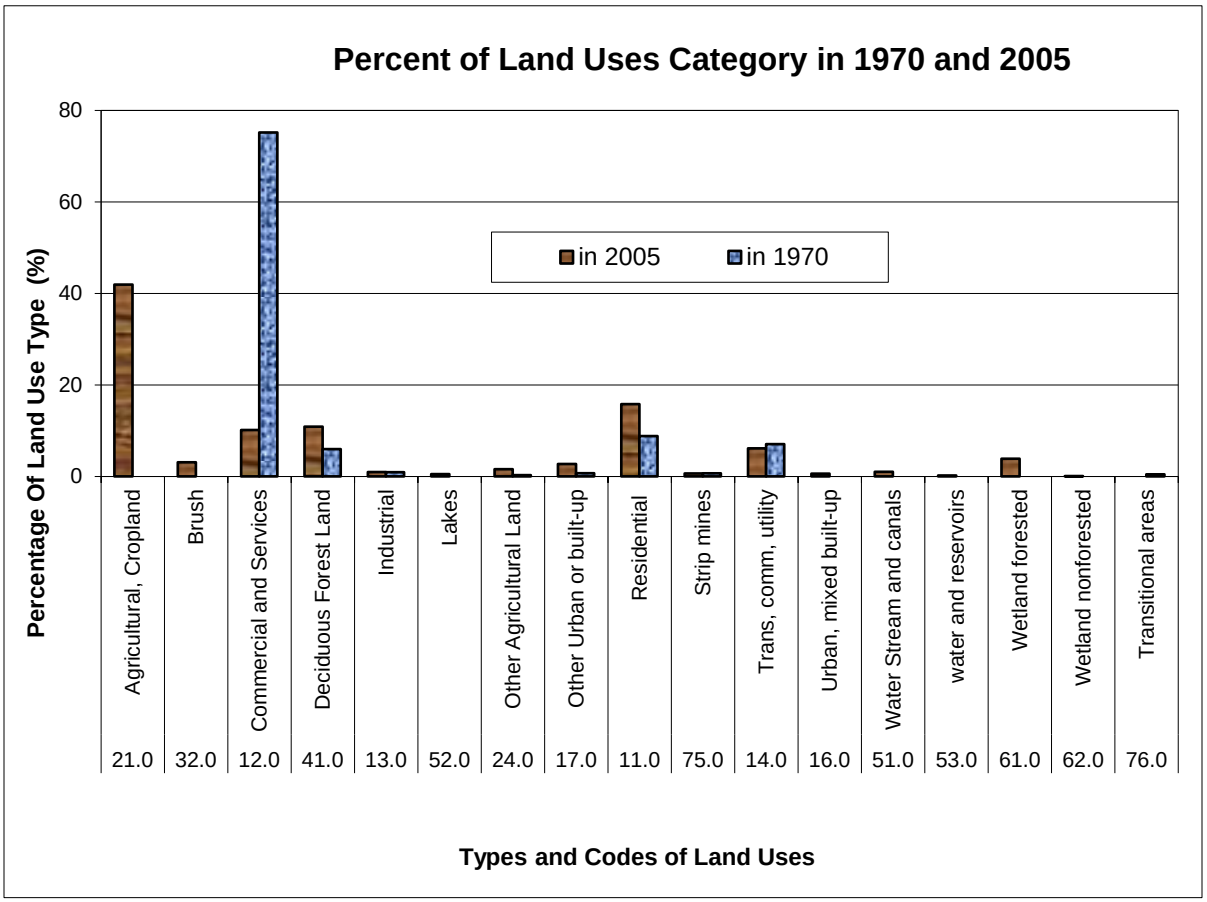

Figure 6-4. Comparison of percent of land use category within the watershed area 1970's and 2005, Cayuga Creek watershed, NY.

The 1970's land use in the Cayuga Creek watershed was mainly classified as commercial and services land use, which takes up about 75% (4471 ha = 11048 acres) of the total watershed area (Figure 6-4 and Figure 6-5). About 9% (523 ha = 1292 acres) of the land use was defined as residential and 7% (419 ha = 1035 acres) was listed as major transportation routes and utilities located in the southwest part of the watershed (Figures 6-4 and Figure 6-5). The other types of

land use were industrial (about 1% of the watershed area), strip mines (0.67 %), transitional areas (0.45%), and other agricultural land (0.27%). The detail of the GIRAS land use classification is listed on the Table 6-4 below.

The 2005 land use classification shows that the main type of land use was agricultural cropland type, approximately 42% of the watershed area (2493ha = 6160 acres). Most of this land use type was located in the upper part of the watershed. About 16% (939 ha = 2320 acres) of the watershed area was classified as residential land use (Figure 6-4). Commercial and services land use and deciduous forest land use had similar percentages of approximately 11% of the total watershed area. About 6% of the watershed area appeared as transportation routes and utilities, which is 1% off from the GIRAS land use classification (Table 6-4). Wetland forested and non-forested land covered approximately 4% of the watershed area. The Cayuga Creek watershed contained about 3% of brush land type and 1.7% of surface water type including lakes, water reservoirs and streams (Table 6-4, Figure 6-5). Industrial facilities tended to remain constant from the 1970's to 2005 (about 1%). About 2.7% of the watershed area was classified as other urban or built-up.

Other types of land use such as strip mines, urban/mixed built-up and other agricultural land appeared to be minor land use, which covered about 2.8% of the entire watershed area. The comparison of land use change between the GIRAS land use and the 2005 land used is shown in Figure 6-4 and Figure 6-5.

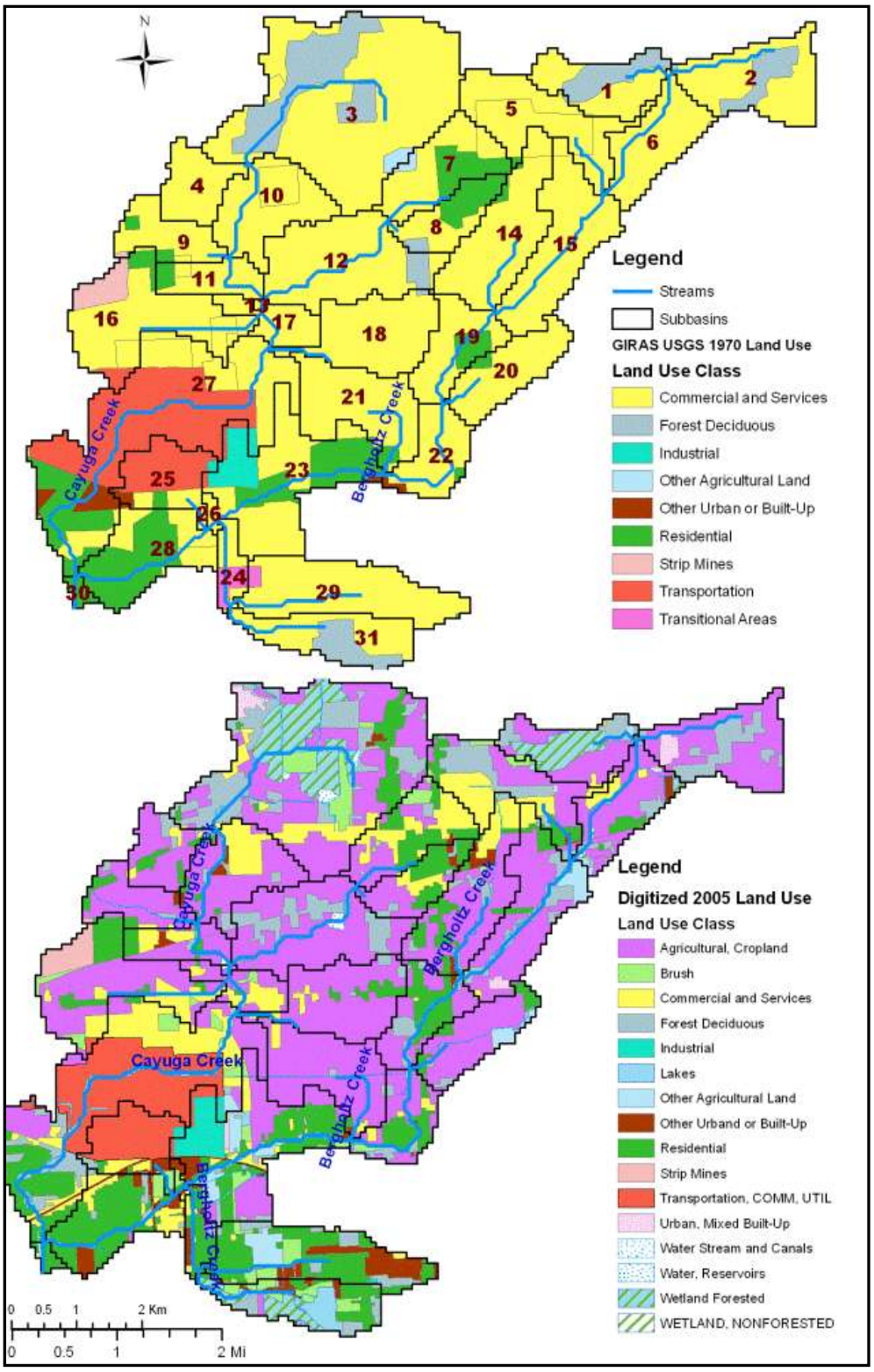

Figure 6-5. Land use map for Cayuga Creek in 1970's and 2005.

Table 6-4. Land use distributions and percentages of land use with the watershed area in 1970's and 2005.

LU Code	Description	Area (Hectares)		% of Watershed Area	
		in 1970's	in 2005	in 1970's	in 2005
21.0	Agricultural, Cropland	0	2493	0.00	41.93
32.0	Brush	0	183	0.00	3.08
12.0	Commercial and Services	4471	603	75.18	10.14
41.0	Deciduous Forest Land	354	646	5.96	10.87
13.0	Industrial	54	56	0.91	0.95
52.0	Lakes	0	29	0.00	0.50
24.0	Other Agricultural Land	16	93	0.27	1.57
17.0	Other Urban or built-up	41	161	0.69	2.71
11.0	Residential	523	939	8.81	15.80
75.0	Strip mines	39	37	0.67	0.64
14.0	Trans, comm, utility	419	364	7.05	6.13
16.0	Urban, mixed built-up	0	35	0.00	0.60
53.0	water and reservoirs	0	11	0.00	0.20
51.0	Water Stream and canals	0	59	0.00	1.00
61.0	Wetland forested	0	229	0.00	3.86
62.0	Wetland nonforested	0	2	0.00	0.04
76.0	Transitional areas	26	0	0.45	0.00
	Total	**5947**	**5947**	**100**	**100**

6.4.2 Discussion

The historical land use and land cover data (1970's) in the geographic information system (GIS) format were done by the U.S. Geological Survey (USGS) and the Environment Protection Agency (USEPA) (Price et al., 2003). The 1970's land use data were done by the USGS during the mid 1970's through the early 1980's. The data were then converted to ArcInfo format by the

USEPA. It appears that somehow the data contain some coding and topological errors. The 1970's land use data done by the USGS were poorly classified as the percentage of the commercial areas and services is 75% of the total watershed areas which appears unlikely (ENCRPB, 1975). A visual examination of the classification suggests that agricultural land may have been mis-coded as "commercial" land and this would account for the high percentage of commercial land. However, this speculation cannot be verified. As for the land use in 2005, only 41% was found to be agricultural and crop land.

CHAPTER 7

7 MODELING SEDIMENT

7.1 Introduction

Soil erosion can be simulated using a hydrologic model in conjunction with a Geographic Information System (GIS). For this research, the SWAT Model built in BASINS 3.1 was used to model sediment for the Cayuga Creek watershed. As described in Chapter 2, SWAT is a physically-based model that uses the Modified Universal Soil Loss Equation, (MUSLE, as described in section 3.6.1) (Williams, 1975), to simulate erosion and sediment yield. This section presents the methods of modeling sediment erosion in the Cayuga Creek watershed for two scenarios of land uses, 1970's and 2005 using SWAT.

7.2 Building a SWAT Project

The BASINS extension consists of AVSWAT, which is an ArcView extension developed for an earlier version of SWAT (Di Luzio et al., 1998). Once the data extraction and watershed delineation have been done, the SWAT project interface can be built in a new View object with the designed graphical user interface (GUI). The SWAT interface requires the designation of land use, soil, weather, groundwater, water use, management, soil chemistry, pond, water quality data and simulation period for the purpose of successful simulation (Luzio et al., 1998). SWAT can be run on a single watershed or multiple hydrologically connected subwatersheds. In the SWAT interface, the watershed is divided first into subwatersheds by running the *Watershed Delineation* extension in BASINS. The subwatersheds are then divided into Hydrologic Response Units (HRUs) defined by the land use and soil distributions. The required data for the SWAT model setup are listed in table 7-1.

Table 7-1. Required data for SWAT model setup.

Data	Data format	Data source
DEM	Grid (cell size 300m x 300)	Topographic map USEPA/Office of Water/OST Basins
Soil map	Shape file	BASIN built-in state soil layer (STATSGO)
Land use maps	Shape file	USGS http://nhd.usgs.gov and digitizing
Stream river network NHD,	Shape file	USGS http://nhd.usgs.gov
NY state soil	Shape file	BASIN built-in state soil layer (STATSGO)
Weather data stations	US database,	NYLOCKPORT2NE
Rainfall Data	Gridded rainfall data	National Weather Service, Advanced Hydrologic Prediction Service (NWS, AHPS), http://water.weather.gov/download.php

7.2.1 Methodology

Building the SWAT model consists of the following steps:

(a) Load the required software: *Dialog Designer* extension version 3.1 or later, *Spatial Analyst* extension version 1.1 or later.

(b) Data extraction and watershed delineation (see chapter 6).

(c) Define the HRUs (details of the procedure are found in BASINS manual section 9.1, and a summary is provided in section 7.2.1.1).

(d) Define weather data.

(e) Apply the default input files (edit is optional).

(f) Set up the specifications such as simulation period etc. and run SWAT.

7.2.1.1 Define Hydrologic Response Units

HRUs distribution is completed using *Land Use and Soil Overlay* and HRU *Distribution* extension. *Land Use and Soil Overlay* is useful for assessing land use and soil distribution in subwatersheds. Land use and soil themes (can be either shape or grid format) are loaded into built project and the land use soil class combination and distributions are determined for the

delineated watershed and the subwatersheds. Figure 7-1 represents the *Land Use and Soil Overlay* dialog box for SWAT model.

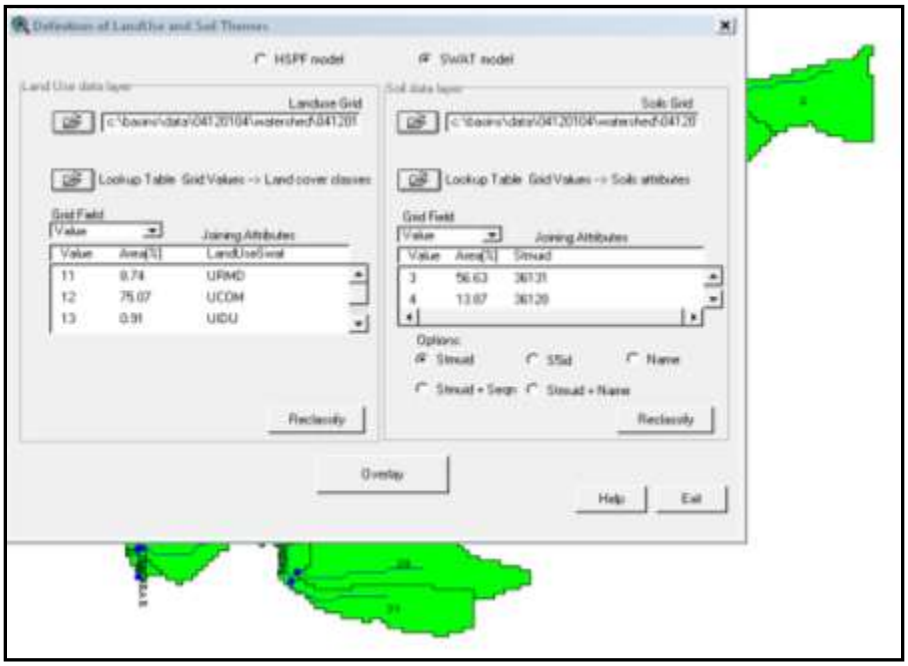

Figure 7-1. Land use and Soil Overlay dialog box.

There are two main sections: *Land Use data layer* and *Soil data layer*. Required shape files for running *Land Use and Soil Overlay* are: New York State Soil shape file and Land Use shapefile. These shapefiles are obtained from the *Data Extraction* tool. The land use data were obtained from the USGS Geographic Information Retrieval and Analysis System (GIRAS), which uses the Anderson Level II classification. Soil data were the STATSGO soils database (shape format) included in the BASINS database. The STATSGO database was developed by USDA-NRCS and incorporated by US EPA in the BASINS system. The STATSGO soil data theme contains the *Muid* field in the attribute table and the interface will look for it by default in order to convert the shape file to grid format. Once land use and soil layers have been clipped with the watershed boundary and reclassified, the *Overlay* process may be begun to obtain the detailed description of the distribution of the land use and soil classes in the watershed and

subwatersheds. Different urban land uses contain different imperviousness ranges. The range and average imperviousness for different land use types are listed in Table 7-2.

Table 7-2. Range and average imperviousness for different urban land use types.

Urban Land Type	Average total impervious	Range total impervious	Average directly connected impervious	Range directly connected impervious
Residential-High Density (> 8 unit/acre or unit/2.5 ha)	0.60	0.44 - 0.82	0.44	0.32 - 0.60
Residential-Medium Density (1-4 unit/acre or unit/2.5 ha)	0.38	0.23 - 0.46	0.30	0.18 - 0.36
Residential-Med/Low Density (> 0.5-1 unit/acre or unit/2.5ha)	0.20	0.14 - 0.26	0.17	0.12 - 0.22
Residential-Low Density (<0.5 unit/acre or unit/2.5 ha)	0.12	0.07 - 0.18	0.10	0.06 - 0.14
Commercial	0.67	0.48 - 0.99	0.62	0.44 - 0.92
Industrial	0.84	0.63 - 0.99	0.79	0.59 - 0.93
Transportation	0.98	0.88 - 1.00	0.95	0.85 - 1.00
Institutional	0.51	0.33 - 0.84	0.47	0.30 - 0.77

After completing the overlay of land use and soil distribution, the HRU distribution can be performed by subdividing the watershed into smaller areas having unique combinations of land use and soil prior to assessing the varying hydrologic conditions between subwatersheds. This enables SWAT to reflect differences in evapotranspiration and other hydrologic conditions for various crops and soils.

SWAT predicts runoff separately for each HRU and routes the runoff to obtain the total runoff for the entire watershed. Therefore, SWAT theoretically provides good accuracy on the physical description of the water balance for the watershed. A single HRU or multiple HRUs may be assigned to each subwatershed. If a single HRU per subbasin is set, the HRU is determined by dominant land use category and soil type within the watershed. The multiple HRUs option allows the setting of sensitivities for the land use and soil data that will be used to

determine the number of and type of HRUs in each watershed. With the multiple HRUs per subbasin option, land use and soil threshold levels may be set to eliminate the minor land use and soil in each subbasin as in the scale control in Figure 7- 2. There is no specific criterion for setting up the threshold value for land use and soil, but for most projects, the default threshold values are set as 20% for land use and 10% for soil (BASINS 3.1 Users Manual, Section9.1.2). Once the threshold values are set, the land uses and soil that cover a percentage of the subbasin area less than the threshold levels are eliminated. After the elimination process, the areas of the remaining land use and soil are reapportioned in order to maintain 100% of land area in the subbasin to be modeled. For this project, the single HRU was used to define the HRU distribution within the subwatersheds (i.e. the dominant land use and soil approach).

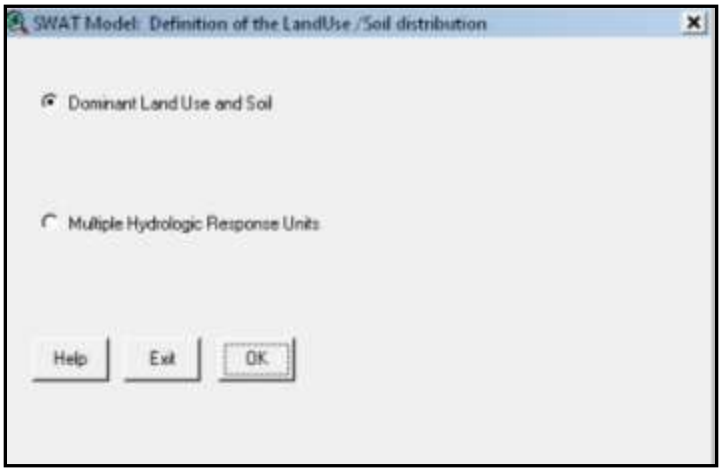

Figure 7-2. HRUs distribution dialog allowing the selection of *Dominant Land Useand Soil* or *Multiple Hydrologic Response Units* (threshold levels for land use and soil).

After determining the HRU distribution, a report is generated that provides a detailed description of the distribution of the HRUs, land use and soil classes in the watershed and subwatershed after threshold application. At the end of the HRUs distribution process, the SWAT interface is loaded in a new view (Figure 7-3). SWAT view is customized in a GUI in order to set up and run the SWAT model.

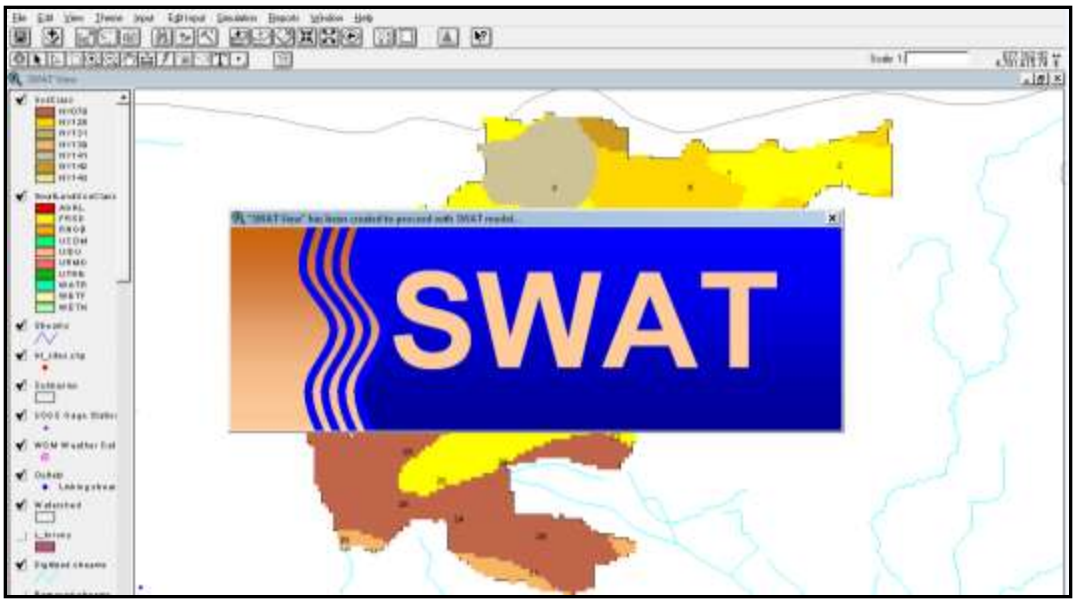

Figure 7-3. BASINS SWAT view is automatically loaded (*SWAT view*).

7.2.1.2 Input Files

7.2.1.2.1 Define weather data (Set up weather Database)

SWAT uses the Weather Generator program to generate weather data. Those data include daily precipitation, daily maximum and minimum temperatures and solar radiation, wind speed, snow cover, and soil temperature. These weather data used for watershed simulation are imported once the HRU distribution has been established (Di Luzio et al., 2002). The setting of these parameters can be assigned in the *Weather data definition* dialog box (Figure 7-4) that can be selected from the *Input* menu on the SWAT view.

There are six sections in the weather data dialog box: *Rainfall data*, *Temperature data*, *Solar Radiation data*, *Wind Speed data* and *Relative Humidity data*, and *Weather simulation data*.

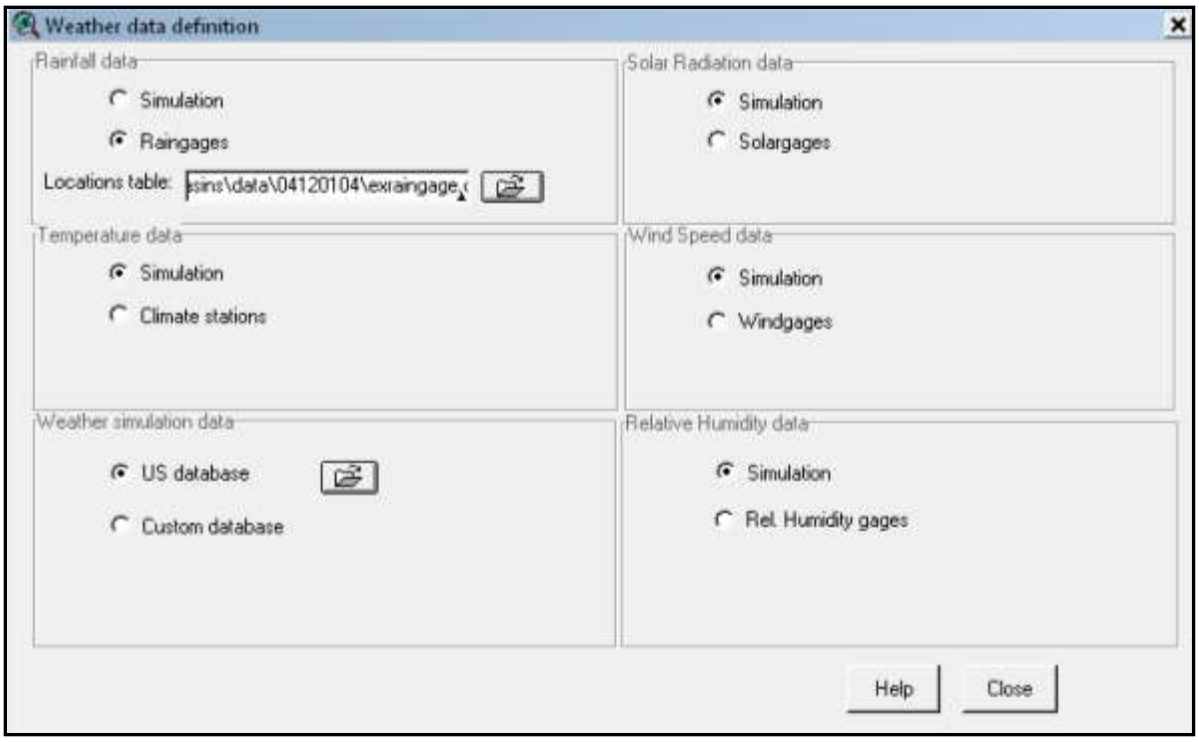

Figure 7-4. Weather data definition dialog box.

i. Weather Simulation Data

This option allows the selection of data to be used to generate each weather parameter for model simulation. This process will create a *.wgn* file for the dataset. There are two sources of Weather Station databases: (1) the *built-in US database* (consists of 1041 stations throughout the US), (2) the *User Weather Station Database*. For this project the built-in US database was selected. There is no weather station site located within the Cayuga Creek watershed. Therefore the nearest weather station, NYLOCKPORT2NE, was selected. NYLOCKPORT2NE station is located northeast of the Cayuga Creek watershed by approximately 14.3 miles (23km) from the upstream and 16.7 miles (27km) from the downstream site (Figure 7-5).

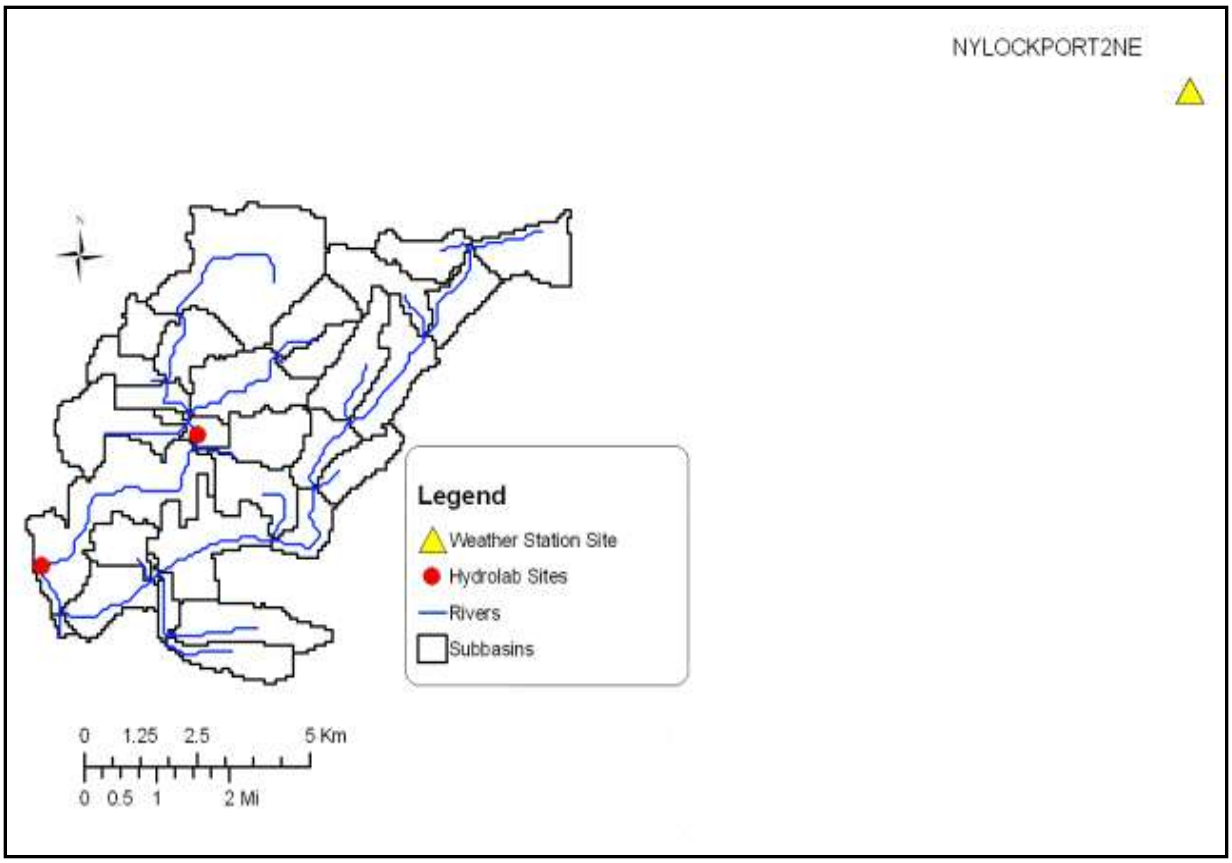

Figure 7-5. NYLOCKPORT2NE weather station site.

ii. Rainfall Data

Precipitation is classified as rainfall, freezing rain or snow using mean daily temperature. A raingage file was made in dBASE table format. Under the "***Name***" field, "***Cyrgage***" is the name of the raingage. Therefore a rainfall data table saved as "***Cyrgage"*** was created in either dBASE or Text table format to link daily rainfall data and the raingage that are used in the ***Weather Data Definition***.

Measured daily rainfall data used in the simulation are quality-controlled and multi-sensors (satellite and raingage) gridded rainfall data obtained from the National Weather Service (NWS), Hydrologic Advanced Prediction Service (AHPS). These data are represented in a form of grid bins (data derived from satellite and raingage) and the observed precipitation shapefile will be

shifted from the lower left corner to the center of each 4x4km grid cell. Three grid bins fall within the watershed area as shown in Figure 7-6. Thus the rainfall is obtained by averaging the values of the three grids. The measured daily rainfall data from November 2005 to 2006 is the average value of the three grid bins (Figure 7-7) and this was the rainfall used in this study.

The shapefile contains the following fields:

1) id - a unique value for each grid bin
2) hrapx - column number of the HRAP grid cell (higher numbers are further north)
3) hrapy - row number of the HRAP grid cell (higher numbers are further east)
4) latitude of the Hydrologic Rainfall Analysis Project(HRAP) grid point
5) longitude of the HRAP grid point
6) globvalue - 24-hour precipitation value in inches. "-2" values correspond to "Missing Data", e.g. an incomplete dataset.

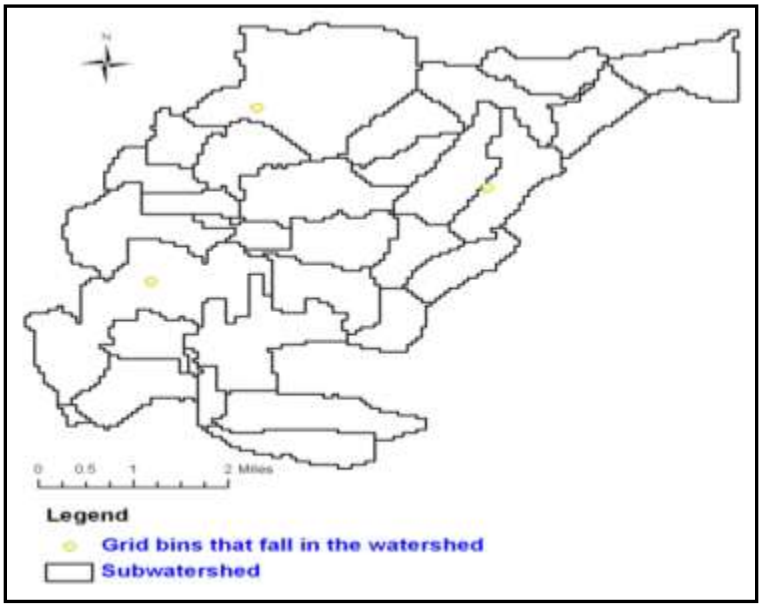

Figure 7-6. Grid bins for satellite rainfall data that fall within the watershed.

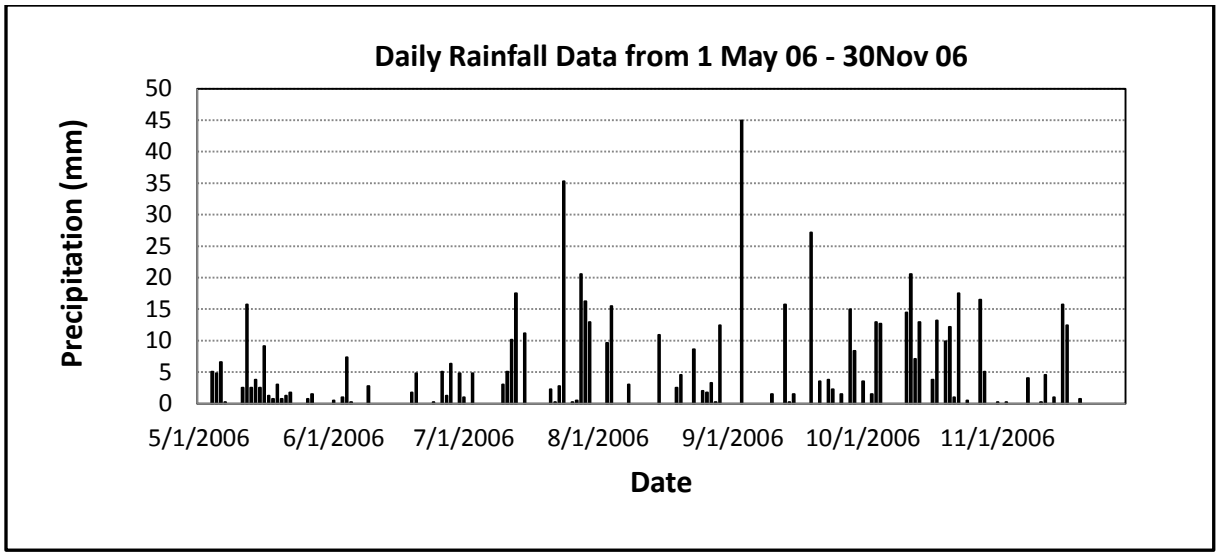

Figure 7-7. Daily rainfall data from May 2006 to November 2006 (Source NWS, AHPS).

iii. Other Weather Data

The rest of the weather data including temperature, solar radiation, wind speed, and relative humidity were set to simulation (Figure 7-4). These data were obtained from the built-in US database (NYLOCKPORT2NE station).

7.2.1.2.2 Write Input – Write All

Write All is to build initial watershed input values. This step is taken after the completion of *Weather Data Definition*. The values are built based on watershed delineation and land use-soil characterization. The input values include *Watershed Configuration File* (.fig), *Soil Input*(.sol), *Weather Generator Input* (.wgn), *Subbasins General Input* (.sub), *HRU General Input* (.hru), *Main Channel Input* (.rte), *Ground Water Input* (.gw), *Management Input* (.mgt), *Soil ChemicalInput* (.chm), *Pond Input* (.pnd), and *Stream Water Quality Input* (.swq). The Write All dialog box is shown in Figure 7.8.

Figure 7-8.*Write All* dialog box used to build initial watershed values.

7.2.1.3 Set up the Specifications and Run SWAT

This section covers the set up of the simulation period, precipitation time step, method of calculating runoff, routing time step, rainfall distribution, potential evapotranspiration (PET) method, crack flow, channel water routing, channel degradation, stream water quality process, lake water quality process, print out frequency, basin and water quality input files. The input control code file (.cod) is a watershed level file that specifies the length of the simulation, printing frequency, and selected option for various processes (Table 7-4). The details of parameter specifications are shown in Table 7-3 and Figure7-9. The CN curve numbers used are listed in Table 7-6.

Table 7-3. Parameter set up for running SWAT model.

Parameters	Set Up
Simulation Period	12/01/2005 to 11/30/2006
Rainfall/Runoff/Routing	Daily Rain/CN/Daily , CN- Curve number runoff
Rainfall Distribution	Skewed Normal
Potential ET Method	Penman-Monteith
Crack flow	Not Active
Channel water routing	Variable storage
Channel degradation	Not Active
Stream water and lake water quality Process	Not Active
Print out frequency	2 sets – Daily and Monthly
Basin and Water Quality Input File	Default

Table 7-4. Input control code file(.cod). (SWAT Manual 2000, Chapter 32.2).

	Description	
NBYR	Number of calendar years simulated. The number of years simulated in a SWAT run can vary from 1 to 9,999 years.	1
IYR	Beginning year of simulation (for example, 1980). The value entered for this variable is not important unless measured data is used in the run. When measured data is used, the model uses this variable to locate the beginning year within the data file.	2006
IDAF	Beginning julian day of simulation. With this variable, SWAT is able to begin a simulation at any time of the year. If the variable is left blank set to zero, the model starts the simulation on January 1st.	121
IDAL	Ending julian day of simulation. With this variable, SWAT will end the simulation on the date specified. If the variable is left blank or set to zero, the model ends the simulation on December 31st.	334
IPD	Print code. This variable governs the frequency that model results are printed to output files. There are three options: 0 monthly, 1 daily, 2 annually.	0,1
NYSKIP	Number of years to ***not*** print output. The options are 0 print output for all years of the simulation 1 print output after the first year of simulation 2 print output after the second year of simulation.	0
IPRN	Print code for input.std file. There are two options: 0 entire input.std file is printed 1 condensed version of input.std file is printed.	1
ILOG	Streamflow print code. This variable allows the user totake the log10 of the flow prior to printing streamflow values to the .rch file. There are two options: 0 print streamflow in .rch file 1 print log of streamflow in .rch file.	0
IPRP	Print code for .pso file. There are two options: 0 do not print pesticide output (.pso file will be empty) 1 print pesticide output.	1

IGN	Random generator seed code. A set of random numbers is needed by SWATto generate weather data. SWAT has a set of default random numbers embedded in the code. To use the default random numbers, the user should set IGN = 0. This is the default value for IGN.	0
PCPSIM	Rainfall input code. This variable identifies the method the model will use to process rainfall data. There are two options: 1 measured data read for each subbasin 2 rainfall generated for each subbasin.	0
IDT	Time step used to report measured rainfall data (minutes). Required if IEVENT = 2 or 3. One of the following should be chosen: 1 min, 2 min, 3 min, 4 min, 5 min, 6 min, 10 min, 12 min, 15 min, 20 min, 30 min.	30
IDIST	Rainfall distribution code. There are two options: 0 skewed distribution 1 mixed exponential distribution	0
REXP	REXP Value of exponent for mixed exponential rainfall distribution. A value for REXP must be entered if IDIST = 1. The model will set REXP = 1.3 if no value is entered.	1.30
TMPSIM	Temperature input code. This variable identifies the method the model will use to process temperature data. 1 measured date read for each subbasin 2 daily max/min generated for each subbasin	1
SLRSIM	Solar radiation input code. This variable identifies the method the model will use to process solar radiation data. 1 measured data read for each subbasin 2 solar radiation generated for each subbasin	2
RHSIM	Relative humidity input code. This variable identifies the method the model will use to process relative humidity data. 1 measured data read for each subbasin 2 relative humidity generated for each subbasin	2
WNDSIM	Wind speed input code. This variable identifies the method the model will use to process wind speed data. 1 measured data read for each subbasin 2 wind speed generated for each subbasin	2
IPET	Potential evapotranspiration method. There are four options for potential ET calculations: 0 Priestley-Taylor method 1 Penman/Monteith method 2 Hargreaves method 3 read in potential ET values	1
IEVENT	Rainfall/runoff/routing option: 0 daily rainfall/curve number runoff/daily routing 1 daily rainfall/Green & Ampt runoff/daily routing (sub-hourly rainfall required for Green & Ampt is generated from daily) *this option not yet operational* 2 sub-hourly rainfall/Green & Ampt runoff/daily routing 3 sub-hourly rainfall/Green & Ampt runoff/hourly routing Option 0 was the only active option in prior versions of the model and is the default.	0
ICRK	Crack flow code. There are two options: 0 do not model crack flow in soil 1 model crack flow in soil The default option is ICRK=0.	0
IRTE	Channel water routing method: 0 variable storage method	0

	1 Muskingum method	
IDEG	Channel degradation code. There are two options: 0 channel dimensions are not updated as a result of degradation (the dimensions remain constant for the entire simulation) 1 channel dimensions are updated as a result of degradation	0
IRESQ	Lake water quality code. The variable identifies whether or not lake water quality is simulated in the reservoirs. There are two options: 0 do not model lake water quality 1 model lake water quality	0
IWQ	In-stream water quality code. The variable identifies whether in-stream transformation of nutrients is allowed to occur. 0 do not model in-stream nutrient transformations 1 model in-stream nutrient transformations	0
ISPROJ	Special project flag. SWAT includes sections of code specific to particular projects. This variable flags the code used in the particular simulation. There are three options: 0 not a special project 1 HUMUS project 2 Missouri River climate change project	0

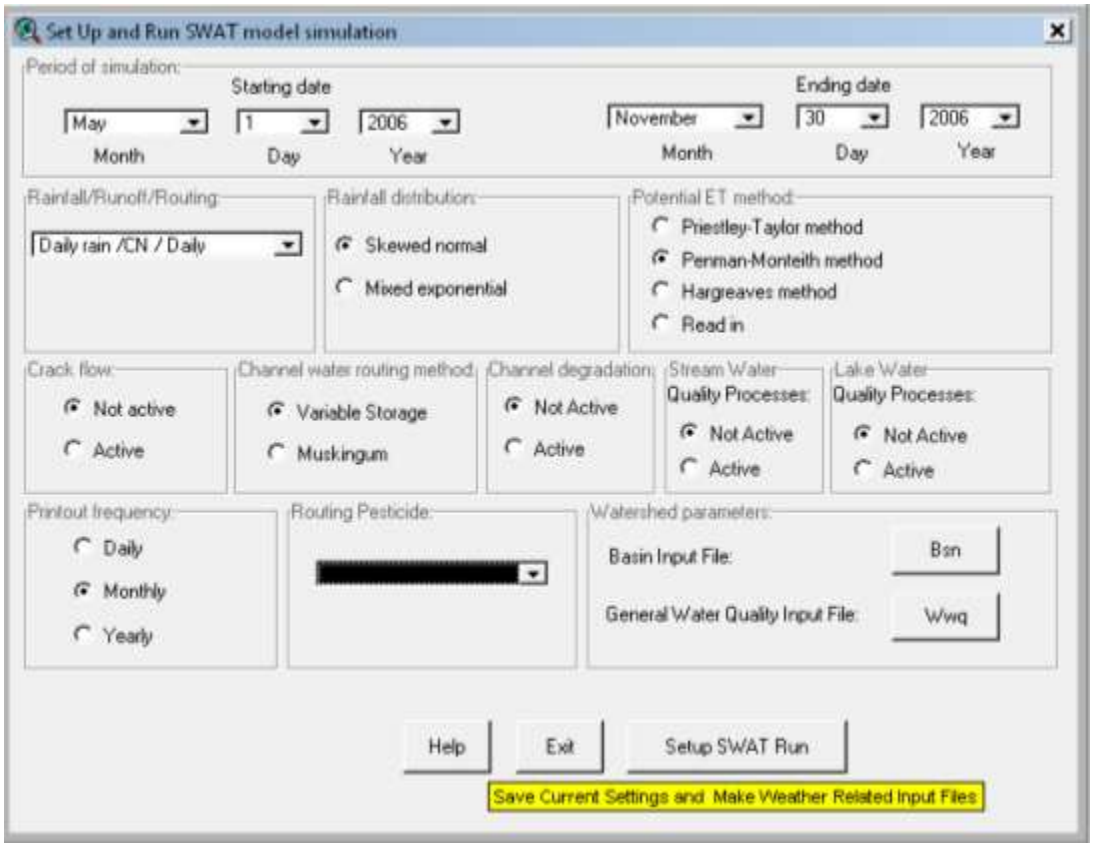

Figure 7-9. Set up parameters and Run SWAT model simulation dialog box.

7.2.1.4 Potential ET Method -Penman-Monteith Approach

The Penman-Monteith equation was used to estimate water evaporation from vegetated surfaces. To estimate potential evapotranspiration (PET), the Penman-Monteith equation considers the components of the energy balance, the strength of the mechanism required to move water vapor and aerodynamic and surface resistance (plant canopy) terms. The Penman-Monteith equation is:

$$\lambda E = \frac{\Delta.(H_{net} - G) + \rho_{air}.C_p\left|e_z^{\circ} - e_z\right|/r_a}{\Delta + \gamma.(1 + \frac{r_c}{r_a})}$$

(eq. 7.2.1.4)

Where

λE – the latent heat flux density (MJ m^{-2} d^{-1});

E – the depth rate evaporation (mm d^{-1});

Δ - the slope of the saturation vapor pressure-temperature curve *de/dT* (kPa $°C^{-1}$);

H_{net} – the net radiation (MJ m^{-2} d^{-1});

G – the heat flux density to the ground (MJ m^{-2} d^{-1});

ρ_{air} – the air density (kg m^{-3});

C_p – the specific heat at constant pressure (MJ kg^{-1} C^{-1});

$e°_z$ - the saturation vapor pressure of air at height z (kPa);

e_z – the vapor pressure of air at height z (kPa);

γ – the psychrometric constant (kPa $°C^{-1}$);

r_c– the plant canopy resistance (s m^{-1});

r_a – the diffusion resistance of the air layer (aerodynamic resistance) (s m^{-1}).

7.2.1.5 Channel Water Routing Method – Variable Storage

In SWAT flow rate and flow velocity are calculated by Manning's equation. The channel water routing is done through the channel network using the variable storage or the Muskingum

river routing approach (Neitsch et al., 2002a). The rate and flow velocity in the reach segment for a given time step is defined using the following equations:

$$q_{ch} = \frac{A_{ch}.R_{ch}^{2/3}.slp_{ch}^{1/2}}{n}$$

(eq. 7.2.1.5-1)

$$v_c = \frac{R_{ch}^{2/3}.slp_{ch}^{1/2}}{n}$$

(eq.7.2.1.5-2)

Where

q_{ch} – the rate of flow in the channel (m^3/s);
A_{ch} – the cross-sectional area of flow in the channel (m^2);
R_{ch} – the hydraulic radius for a given depth of flow (m);
Slpch – the slope along the channel length (m/m)
n – Manning's "n" coefficient for the channel;
v_c – the flow velocity (m/s).

The daily value of flow for cross-sectional area, A_{ch}, is defined as:

$$A_{ch} = \frac{V_{ch}}{1000_{ch}}$$

(eq. 7.2.1.5-3)

Where

A_{ch}- cross-sectional area of flow in the channel for a given depth of water (m^2);
V_{ch} – the volume of water stored in the channel (m^3);
L_{ch}–the channel length (km).

The depth of flow for a given time step is:

$$depth = \sqrt{\frac{A_{ch}}{Z_{ch}} + \left(\frac{W_{btm}}{2.Z_{ch}}\right)^2} - \frac{W_{btm}}{2.Z_{ch}}$$

(eq. 7.2.1.5-4)

Where

depth – the depth of flow (m);

A_{ch}– the cross-sectional area of flow in the channel for a given depth of water (m^2);

W_{btm} – the bottom width of the channel (m);

Z_{ch}– the inverse of the channel side slope.

Equation 7.2.1.5-4 is valid only when all water is contained in the channel. For the case that the volume of water in the reach segment has filled the channel and is in the flood plain, the depth is calculated as:

$$depth = depth_{bnkful} + \sqrt{\frac{A_{ch} - A_{ch,bnkfull}}{Z_{fld}} + \left(\frac{W_{btm.fld}}{2.Z_{fld}}\right)^2} + - \frac{W_{btm.fld}}{2.Z_{fld}}$$

(eq. 7.2.1.5-5)

Where

depth– the depth of flow (m);

$depth_{bnkfull}$– the depth of water filled to the top of the bank in the channel (m);

A_{ch} – the cross-sectional area of flow in the channel for a given depth of water (m^2);

$A_{ch,bnkful}$– the cross sectional area of flow when filled to the top of the bank (m^2);

W_{btmfld}– the bottom width of the flood plain (m);

Z_{fld} – the inverse of the flood plain side slope.

7.2.1.6 Storage Routing Methods

A continuity equation (William, 1969) is used to compute the storage routing for a given reach segment. The continuity equation is:

$$V_{in} - V_{out} = \Delta V_{stored} \quad \text{(eq. 7.2.1.6-1)}$$

Where

V_{in} – the volume of inflow during the timestep (m^3 H_2O);

V_{out} - the volume of outflow during the timestep (m^3 H_2O);

ΔV_{stored}– the change in volume of storage during the time step (m^3 H_2O).

Equation eq. 7.2.1.6-1 can be derived as

$$\Delta t.\left(\frac{q_{in.1}-q_{in.2}}{2}\right)-\ \Delta t.\left(\frac{q_{out.1}-q_{out.2}}{2}\right)=\ V_{stored.2}-V_{stored.1}$$

(eq. 7.2.1.6-2)

Where

Δt – the length of timestep (s);

$q_{in,1}$ – the inflow rate at the beginning of the time step (m^3/s);

$q_{in,2}$ - the inflow rate at the end of the time step (m^3/s);

$q_{out,1}$ – the outflow rate at the beginning of the time step (m^3/s);

$q_{out,2}$ - the outflow rate at the end of the time step (m^3/s);

$V_{stored,1}$– the storage volume at the beginning of the time step (m^3 H_2O);

$V_{stored,2}$– the storage volume at the end of the time step (m^3 H_2O).

The equation 7.2.1.6-2 can be rearranged as:

$$q_{in,ave}+\ \frac{V_{stored,1}}{\Delta t}-\frac{q_{ot,1}}{2}=\frac{v_{stored,2}}{\Delta t}+\frac{q_{out,2}}{2}$$

(eq. 7.2.1.6-3)

Where $q_{in,ave}$is the average inflow rate during the time step:

$$q_{in,ave}=\frac{q_{in,1}+q_{in,2}}{2}$$

(eq. 7.2.1.6-4)

Travel time can be calculated by dividing volume of water in the channel by the flow rate. The travel time equation is:

$$TT=\ \frac{v_{stored}}{q_{out}}=\frac{V_{store,1}}{q_{out,1}}=\frac{V_{stored\ ,2}}{q_{out,2}}$$

(eq. 7.2.1.6-5)

Where

TT – the travel time (s);

V_{stored}– the storage volume (m^3 H_2O);

q_{out} – the discharge rate (m^3/s).

The relationship between travel time (*TT*) and storage coefficient can be calculated by substituting eq.7.2.1.6-5 into eq. 7.2.1.6-3:

$$q_{in,ave} + \frac{V_{stored,1}}{\left(\frac{\Delta t}{TT}\right).\left(\frac{V_{stored,1}}{q_{out,1}}\right)} - \frac{q_{out,1}}{2} = \frac{V_{stored,2}}{\left(\frac{\Delta t}{TT}\right).\left(\frac{V_{stored,2}}{q_{out,2}}\right)} + \frac{q_{out,2}}{2}$$

(eq. 7.2.1.6-6)

Equation 7.2.1.6-5, can be simplified to

$$q_{out,2} = \left(\frac{2.\Delta t}{2.TT + \Delta t}\right).q_{in,ave} + \left(1 - \frac{2.\Delta t}{2.TT + \Delta t}\right).q_{out,1}$$

(eq. 7.2.1.6-7)

Equation 7.2.1.6-7 is similar to the coefficient method equation:

$$q_{out,2} = SC.q_{in,ave} + (1 - SC).q_{out,1}$$

(eq. 7.2.1.6-8)

Equation 7.2.6-8 is the basis for the CSC convex routing (SCS, 1964), where SC is the storage coefficient.

The storage coefficient is defined as

$$SC = \frac{2.\Delta t}{2.TT + \Delta t}$$

(eq. 7.2.1.6-9)

It can be simplified as:

$$(1 - SC).q_{out} = SC.\frac{V_{stored}}{\Delta t}$$

Replace that into eq. 7.2.1.6-8:

$$q_{out,2} = SC.\left(q_{in,ave} + \frac{V_{stored,1}}{\Delta t}\right)$$

(eq. 7.2.1.6-10)

Equation 7.2.1.6-10 can be expressed in units of volume by multiplying both by time step:

$$V_{out,2} = SC.(V_m + V_{stored,1})$$

(eq. 7.2.1.6-11)

7.2.1.7 Parameter Range Used in Sediment Simulation

The Manning's "n" value for all the main channel and tributary channels was set to the default value of 0.014. The growth heat units were estimated for each land cover using local climatic data and were set to default values contained in the US database.

7.2.1.7.1 CN Curve Number (.mgt)

CN curve numbers are stored in the *.mgt* input file and are summarize in Table 7-5.

Table 7-5. CN2 values used in sediment simulations.

SUBBASIN	2005 LU	1970's LU
1	83.00	72.00
2	83.00	72.00
3	67.00	31.00
4	83.00	72.00
5	77.00	59.00
6	83.00	72.00
7	59.00	59.00
8	78.00	59.00
9	83.00	72.00
10	83.00	72.00
11	83.00	72.00
12	83.00	72.00
13	83.00	72.00
14	77.00	59.00
15	83.00	72.00
16	83.00	72.00
17	83.00	72.00
18	83.00	72.00
19	83.00	72.00
20	83.00	72.00
21	83.00	72.00
22	87.00	79.00
23	85.00	72.00
24	89.00	79.00
25	83.00	83.00
26	85.00	72.00
27	83.00	83.00
28	89.00	89.00
29	89.00	79.00
30	85.00	85.00
31	89.00	79.00

7.2.1.7.2 Erodibility Factor (USLE_K) (.sol)

Erodibility factor values are stored in the .sol input file. The same values were used for both the 1970's and 2005 land uses, and the values are listed in Table 7-6.

Table 7-6. Soil erodibility factors used in the model simulations.

SUBBASIN	2005 LU	1970's LU
1	0.37	0.37
2	0.37	0.37
3	0.10	0.10
4	0.37	0.37
5	0.32	0.32
6	0.37	0.37
7	0.32	0.32
8	0.32	0.32
9	0.37	0.37
10	0.37	0.37
11	0.37	0.37
12	0.37	0.37
13	0.37	0.37
14	0.32	0.32
15	0.37	0.37
16	0.37	0.37
17	0.37	0.37
18	0.37	0.37
19	0.37	0.37
20	0.37	0.37
21	0.37	0.37
22	0.49	0.49
23	0.37	0.37
24	0.49	0.49
25	0.49	0.49
26	0.37	0.37
27	0.49	0.49
28	0.49	0.49
29	0.49	0.49
30	0.49	0.49
31	0.49	0.49

7.2.1.7.3 Slope Length (SLSUBBSN)(.hru)

Values of the slope length factor are stored in the *.hru* input file. It is noted that a large amount of uncertainty in the slope length measurement may occur as it is affected by support practices used in HRU (Neitsch et al, 2002b). The values of slope length factors used in model simulations were the same for the both the 1970's and 2005 land uses as shown in Table 7-7.

Table 7-7. Slope length factor used in model simulations.

SUBBASIN	2005 LU	1970's LU
1	121.951	121.951
2	121.951	121.951
3	121.951	121.951
4	121.951	121.951
5	121.951	121.951
6	121.951	121.951
7	121.951	121.951
8	121.951	121.951
9	121.951	121.951
10	121.951	121.951
11	121.951	121.951
12	121.951	121.951
13	121.951	121.951
14	121.951	121.951
15	121.951	121.951
16	121.951	121.951
17	121.951	121.951
18	121.951	121.951
19	121.951	121.951
20	121.951	121.951
21	121.951	121.951
22	121.951	121.951
23	121.951	121.951
24	121.951	121.951
25	121.951	121.951
26	121.951	121.951
27	121.951	121.951
28	121.951	121.951
29	121.951	121.951
30	0.050	0.050
31	121.951	121.951

7.2.1.7.4 Support Practice Factor (USLE_P) (.mgt)

Support practice factor (USLE_P) values are stored in the *.mgt* input file. A USLE_P value of " 1" was used in the model simulation for both the 1970's and 2005 land uses.

7.2.1.7.5 Cover and Management Factor (USLE_C) (crop.dat)

In some cases, the minimum cropping practice (*C*) value reported for the plant cover may not be accurate for the study area (Neitsch et al, 2002b). The cover and management factor values are stored in the crop.dat file, which can be viewed as a text file. Crop and management factor values used vary upon type of land cover/plant growth. The different values of USLE_C for different land cover are listed in Table 7-8.

Table 7-8. Cover and management factor for different land covers.

Land Cover Types	Crop Management Factor (USLE_C)
Forest-mixed (bush)	0.001
Ever Green Forest	0.001
Deciduous Forest	0.001
Water	0
Wetland Forested	0.001
Wetland Nonforested	0.003
Agriculture and cropland	0.2

7.3 Results and Discussion

7.3.1 Discharge Results at the Upstream and Downstream Sites

The same rainfall data were used for simulating the output for both the 1970's and 2005 land uses. The daily and monthly results indicate that discharge at the downstream site is somewhat higher than the upstream site (Figure7-10, Figure 7-11, and Figure 7-12). The daily data show that there are seven or eight large events per year at both sites. For the 1970's land

use, the highest peaks of daily discharge are approximately 32.2 ft^3/s (0.91 m^3s^{-1}) and 17.1ft^3/s (0.48 m^3s^{-1}) at the downstream and upstream sites respectively. For the flow results of 2005 land use, the maximum daily flows are about 47.8 ft^3/s (1.35 m^3s^{-1}) and 31.3 ft^3/s (0.88 m^3s^{-1}) downstream and upstream sites respectively (Figure 7-10 and Figure 7-11).

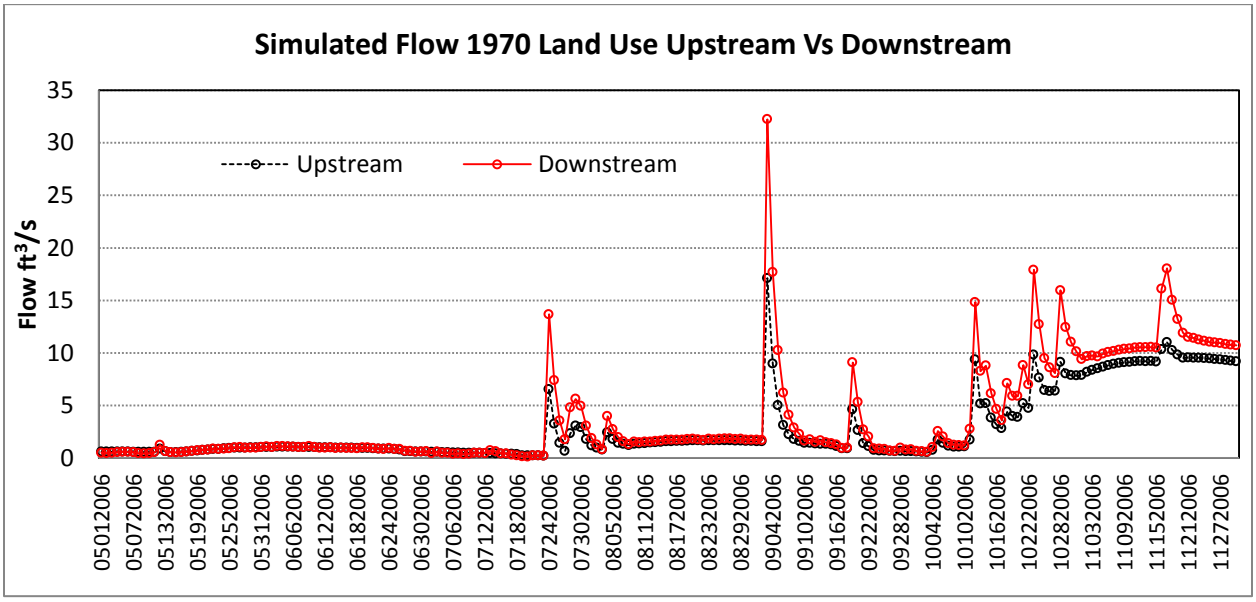

Figure 7-10. Daily simulated flows at both sites for 1970's land use.

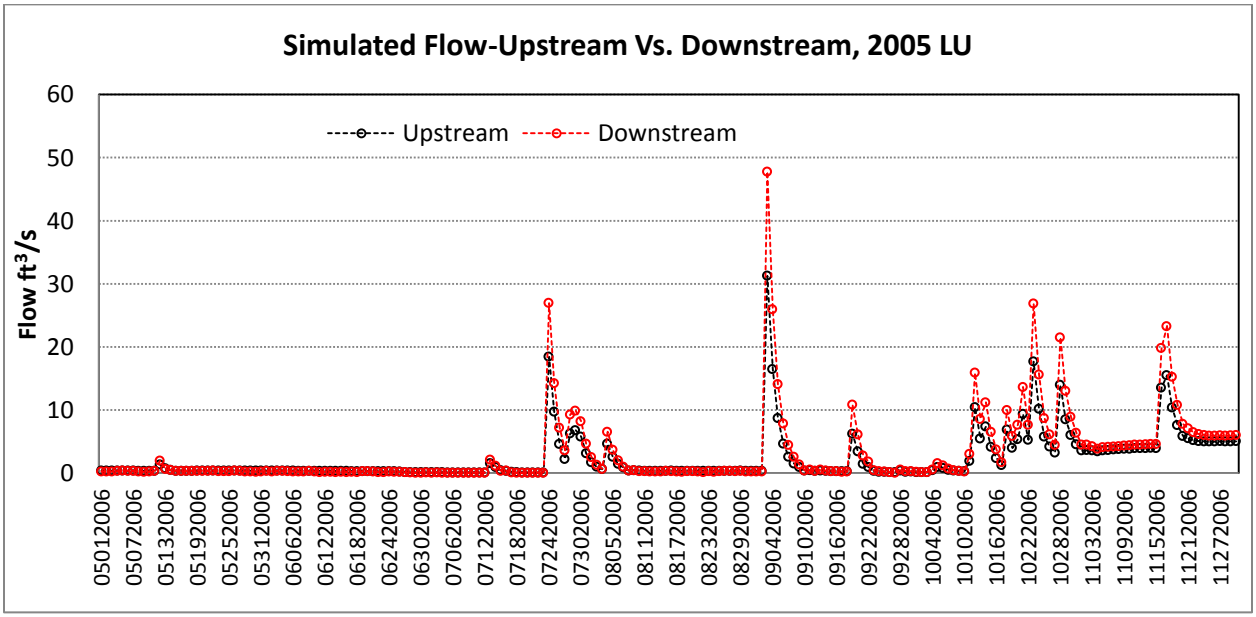

Figure 7-11. Daily simulated flow at both sites for 2005 land use.

The discharge data at both sites are quite low. At the upstream site, the mean monthly discharge ranges from 0.7 ft^3/s (0.02 m^3s^{-1}) to 9.6ft^3/s (0.27 m^3s^{-1}) and from 0.3 ft^3/s (0.01m^3s^{-1}) to 5.5 ft^3/s (1.5m^3s^{-1}) for 1970's and 2005 land uses respectively (Figure7-12). At the downstream site, the mean monthly discharge ranges from 0.8 ft^3/s (0.02 m^3s^{-1}) to 11.7 ft^3/s (0.33 m^3s^{-1}), and from 0.2 ft^3/s (0.005 m^3s^{-1}) to 7 ft^3/s (0.2 m^3s^{-1}) for 1970's and 2005 land uses respectively (Figure 7-12). These results seem to reflect the fact that the flow at the upstream site should be low and it increases in the downstream direction due to the increase in catchment areas, which results in an increase in runoff and flow at the downstream site.

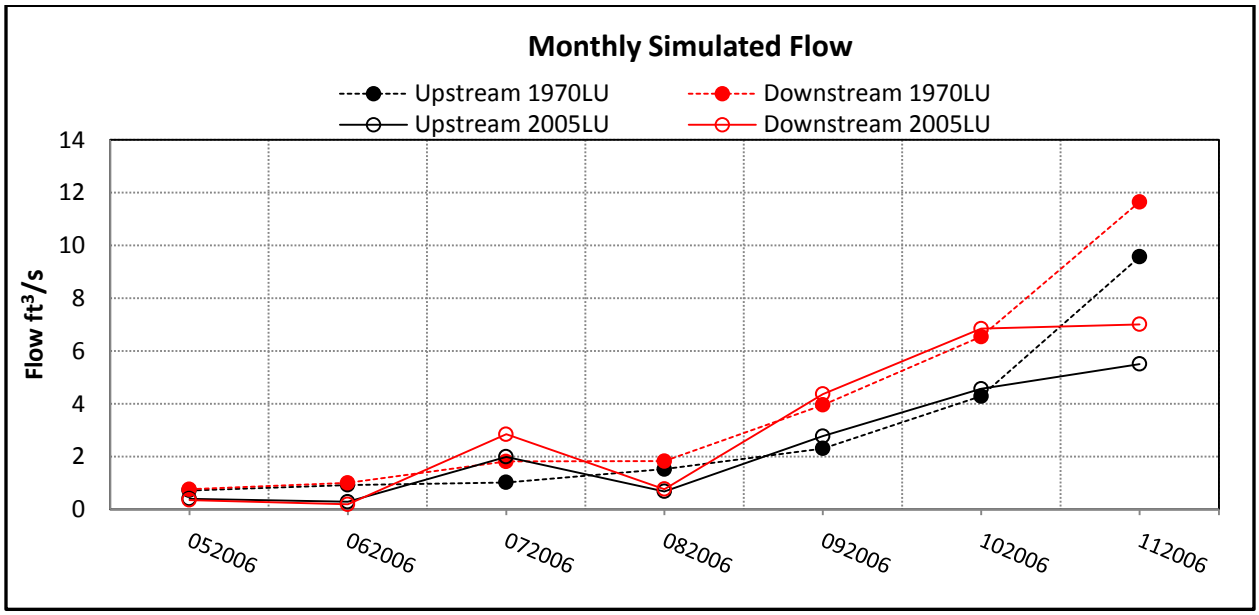

Figure 7-12. Monthly simulated flow for the upstream and downstream sites for 1970's land use and 2005 land use.

Flow was quite low in April and May as there was limited amount of rainfall. The increase in discharge is a function of input (precipitation), output (evaporation, interception, infiltration, and runoff), and storage within the basin. The peaks of monthly discharge are high in October and November as the wet period starts in August and it fills up the storage that has emptied out

over the dry months: May, June and July (Figure 7-7), which then results in the increase in runoff. Plus, the temperature and evapotranspiration decline in October and November due to low incoming insolation. As a result, the flow increases in October and November.

7.3.2 Impact of Land Use Change on Discharge Data

Figure 7-10 and Figure 7-11 suggest greater imperviousness in 2005 land use as the storm events have higher peak daily flows in 2005 than in the 1970's. Based on Figure 7-12, it is obvious that change of land use from 1970's to 2005 has impact on flow in the Cayuga Creek. The total discharges (wet and dry months) decrease by 20% and 19% at upstream and downstream sites respectively between 1970's and 2005. In reality the discharge should increase with the change of land uses as urban development has increased from the 1970's to 2005. Hence the discharge should increase due to urban runoff as the same rainfall data was used in running the model, and the increase in impervious surface would limit the available storage in soil; and therefore the infiltration rate decreases and overland flow increases (Brooks et al., 2003). However, the applied 1970's land use classification contains a huge error with the commercial and service land use, which in fact should be classified as agriculture. As a result of misclassification of land use, the 1970's land use has higher percentage of urban land use (includes industrial, residential, transportation and utilities, and commercial land use). Consequently the percent of impervious surface for 1970's land use is higher than the 2005 land use (Table 6-4). Conclusively, the misclassification of 1970's land use plays an important role in this error.

7.3.3 Spatial Variation of Sediment Concentration at the Upstream and Downstream Sites

The monthly sediment results are represented in Figure 7-13. The results indicate that sediment concentration at the upstream site is higher than the downstream site for 2005 land use and the sediment concentration at the downstream site was higher than that of the upstream site for 1970's land use. This result reflects the spatial variation of runoff and/or the spatial variation of erosion in the uplands areas since the sediment concentration is controlled by runoff. Since the model suggests that there is no deposition between the two sites, hence sediment results for 2005 land use do not match the TSS results which indicate the sediment at the downstream site is higher than the upstream site. The reason behind this error may be due to the fact that the values of CN2 used were the same (83) for both sites. The error may be fixed by calibrating the model after the simulation.

7.3.4 Impacts of Land Use Changes on Sediment Concentration

The sediment concentration increases with change in land use from 1970's to 2005 (Figure 7-12). At the upstream site, the sediment concentration ranges from 0.1 mg/l to 7.5 mg/l and 0.01 mg/l to 91.3 mg/l for 1970's land use and 2005 land use respectively. Whereas at the downstream site, it ranges from 0.4 mg/l to 7.9 mg/l and 0.01 mg/l to 66.9 mg/l for 1970's land use and 2005 land use respectively. The soil erodibility is controlled by the properties of the soil (Wischmeier and Smith, 1978). The same soil data were used in the simulation for both land uses, therefore the increase in sediment concentrations from 1970's land use to 2005 land use may be explained by the land use type used for model simulations. Change in land use from 1970's to 2005 caused more soil erosion. MUSLE equation (eq. 3.6.1-2) in the Chapter 3 explains the change in sediment concentration with the change of land use. The parameters that

can influence erosion include surface runoff volume, peak runoff rate, HRU area, soil erodibility factor, cover and management factor, support practice, topographic factor and coarse fragment factor, land use change affect cover and management factor (see Table 7-8 for *USLE_C* values for different land/cover), and *CN* curve number (see Table 7-5 for *CN* curve number for different land use). *CN2* number is the initial SCS runoff curve number of moisture condition II. The values of *CN2* at the upstream site were 72 for 1970's land use and 83 for 2005 land use (Table 7-5, subbasin17). This explains why the sediment concentration increases at the upstream site with the change of land uses. However, at the downstream site, same value of 83 of *CN2* was used for both land uses (Table 7-5, subbasin27).

Another land use change factor that contributes to the increase in sediment concentration is the crop management factor (*USLE_C*). There was an increase of approximately 42% (2493 hectares) of agriculture and cropland in 2005 while the agricultural land use was 0 hectare in 1970's, which was due to mis-coding of the 1970's land use (Table 6-4). This huge increase of agricultural land use leads to the increase in sediment concentration at both upstream and downstream sites as the values of USLE_C for agricultural land is fairly high (0.2, Table 7-8). Consequently the sediment for 1970's land use is low since the large amount of agricultural land is classified as commercial land use. However, the increase in sediment concentration may vary if the classification of the land use is reliable.

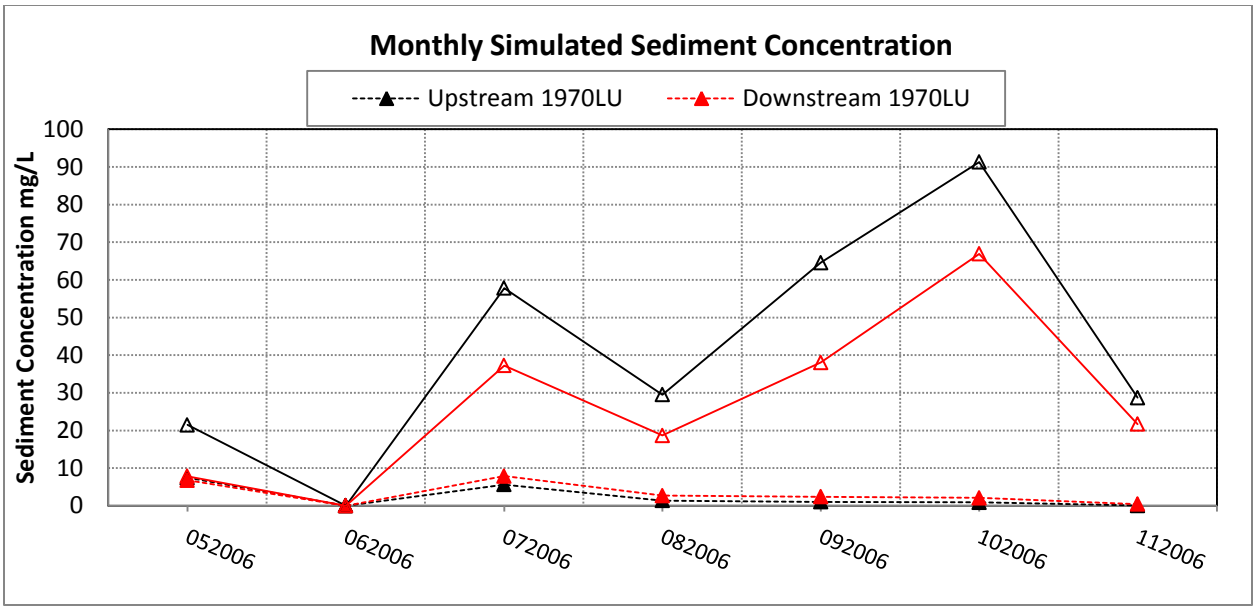

Figure 7-13. Summary of sediment results at upstream and downstream sites for 1970's and 2005 land uses.

CHAPTER 8

8 CONCLUSION

The overall conclusions for this research project are presented in the basis of the objectives stated in the Introduction (Chapter 1). The conclusions are drawn in the context of 10 weeks period of water quality assessment of the Cayuga Creek, the land use change from 1970's to 2005, the impact of land use change on discharge and sediment concentrations at the upstream and downstream sites.

8.1 Water Quality Assessment of Cayuga Creek Watershed

The 10-week results obtained from the Hydrolab Datasonde 4a indicated that weekly mean water temperature of the Cayuga Creek exhibits the diurnal pattern and the water at the upstream site is colder than that of the downstream site. The daily temperature ranged from 9 °C to 21 °C at the upstream site and 11 °C to 25 °C at the downstream site. The weekly mean dissolved oxygen data ranged from 6.05 mg/L (standard deviation was 1.56) at the upstream site and 6.0 mg/L at the downstream site (standard deviation was 0.67). The conductivity of the Cayuga Creek water is quite high. The 15 minute time step conductivity data indicated a diurnal pattern at both sites. The weekly mean conductivity values ranged from 0.4-2.2 mS/cm at the upstream site and 1.24-1.69 mS/cm at the downstream site. The Hydrolab's weekly data showed that the pH values at the upstream site appeared to be good throughout the 10 weeks of assessment.

Turbidity and TSS results showed that the sediment concentration at the downstream site was quite high. The weekly mean turbidity values ranged from 280 NTU to 880 NTU at the downstream site and from 0.1-14 NTU at the upstream site. The 15 minutes time step data indicated that frequently the sensors reached the maximum reading of 1000 NTU at the downstream site. Results from lab analysis showed that the TSS concentration at the downstream

site ranged from 4.4 mg/L to 49.65 mg/L and from 0 mg/L to 4.41 mg/L at the upstream site. The regression analysis of turbidity and TSS revealed the coefficient of correlation of 0.8153 at the upstream site and 0.5339 at the downstream site.

8.2 Land Use Change Evaluation

1970's land use and 2005 land use were used in SWAT simulations to identify the impacts of land use change on flow and sediment concentration at the upstream and downstream site. These two land uses classifications were based on the Anderson Level II system. The 1970's land use (GIRAS land use) was done by the USGS in late 1970's and early 1980's. The 2005 land use was obtained by digitizing the digital orthoimagery (1 ft (0.3 m) resolution) of watershed area. The result of this assessment indicated that the 1970's land use data for the Cayuga Creek watershed contained coding and topological errors. Based on a visual examination, a portion of land of the watershed was mis-coded because a big portion of agricultural area (approximately 4471 hectares) of the 1970's land use was misclassified as commercial and services. The rest of the 1970's land use was classified as deciduous forest land (about 6 % of the watershed area), transportation and utilities (about 7 % of the watershed area), residential (about 8.8 % of the watershed area), industrial (about 1 % of the watershed area), and other agricultural land (about 0.3 % of the watershed area), and other urban/built up land (about 0.7 % of the watershed area).

The 2005 land use is predominantly agricultural land use which covered about 42 % of the watershed area. About 10% of the watershed area was found to be commercial and services and another 10% was deciduous forest land with approximately 3% classified as brush. Industrial land use tended to be the same from the 1970's, which covered approximately 1% of the watershed area. The 2005 land use appeared to have some portion of wetlands forest and wetland

non-forest (about 4%), and water/stream/reservoir/lake (2%), which did not exist in the 1970's land use. It was noted that residential land use was double of the 1970's land use (about 16 %). The rest of the land uses are other agricultural land (about 1.6%), other urban or built-up/mixed built-up (about 2.3 %), strip mines (0.6 %), and transportation and utilities (about 6%).

8.3 Discharge Results and Effects of Land Use Change on Discharge

To assess the spatial distribution of flow and sediment concentration and the effects of land use change on flow and sediment at the upstream and downstream site, the same data of rainfall were used in model simulation for both scenarios of land use type. The simulation period was from May 2005 to November 2005.

The modeling results indicated that the flow at the upstream site was lower than the downstream site for both land use periods. For the 1970's land use, the highest peaks of daily discharges are approximately 32.2 ft^3/s (0.91 m^3s^{-1}) and 17.1 ft^3/s (0.48 m^3s^{-1}) at the downstream and upstream sites respectively and for the 2005 land use, the maximum daily flows are about 47.8 ft^3/s (1.35 m^3s^{-1}) and 31.3 ft^3/s (0.88 m^3s^{-1}) at the downstream and upstream sites respectively. The monthly data suggested that the flows at both sites were quite low and the flow at the downstream site was higher than the upstream site for 1970's land use and 2005 land use due the increase in catchment size as moving downstream. The peaks of discharge were found in the October and November.

The land use change from 1970's to 2005 caused the flow to decrease by 20% and 19% in terms of total flows at the upstream and downstream sites respectively. These results could not be taken as the correct findings since the flow should increase as there has been the urban development over the years and therefore flow should increase. This error in my finding was due to the mis-coding of the agricultural land use for the 1970's land use.

8.4 Sediment Results and Impacts of Land Use Change Effects on Sediment Concentration

Results showed that the sediment concentration at the upstream site was higher than the downstream site for 2005 land use while with the 1970's land use, the sediment concentration at the upstream site was lower than that of the downstream site.

The change in land use from the 1970's to 2005 causes the sediment concentration to increase at both upstream and downstream sites. These increases in sediment concentration are affected by the different temporal land use distributions of CN2 values plus the cover management factor also changed with different land cover.

8.5 Future Work Needed

There are several aspects of further research in this thesis. Firstly, more field work should be conducted to collect flow data in order to calibrate to model. Secondly, additional water samplings are required for TSS analysis to achieve a better correlation between turbidity and TSS. Thirdly, a better field probe for a replacement of Hydrolab Datasonde 4a may be considered since the turbidity data were not properly read at the downstream site due to high turbidity. An alternative site may be considered. Lastly, the model may be run with other land use data, which are accurately classified in order to observe response of erosion and flow to the change of land use.

LIST OF REFERENCES

Anderson, J.R., E.E. Hardy, J.T. Roach, and R.E. Witmer. 1976. *A land use and land cover classification system for use with remote sensor data*. U.S. Geological Survey Professional Paper 964. Washington, DC: U.S. Government Printing Office.

Arnold, J.G., J.R. Williams and D.R. Maidment. 1995. Continuous-time water and sediment-routing model for large basins. *Journal of Hydraulic Engineering* 121(2):171-183.

Arnold, C.A, Jr., and C.J., Gibbons. 1996. Impervious surface coverage: the emergence of a key urban environmental indicator. *Journal of the American Planning Association* 62(2):243-258.

Arnold, J.G., R. Srinivasan, R.S. Muttiah, and J.R. Williams. 1998. Large area hydrologic modeling and assessment part I: model development. *Journal ofAmerican Water Resources Association* 34(1):73-89.

Batie, S.S. 1983. *Soil erosion: crisis in America's croplands?* Washington, DC: Conservation Foundation.

Baird W. F. & Associates Coastal Engineers Ltd. 2005.*Shoreline erosion and sedimentation assessment study upstream and downstream of the Power Project*. Prep. for the New York Power Authority.

Bagnold, R.A.1977. Bed-load transport by natural rivers. *Water Resources Research* 13(2):303-312.

Beasley, D. B., E. J. Monke, and L. F. Huggins. 1980. ANSWERS: a model for watershed planning. *Transactions of the ASAE* 23(4):938-944.

Blackburn, W.H. 1975. Factors influencing infiltration and sediments production of semi-arid rangelands in Nevada.*Water Resources Research*. 11(6):929-937.

Buckman, H.O., and N.C. Brady. 1974. *The nature and properties of soils*. New York: Macmillan.

Chapman, L.J., and D.F. Putnam. 1973. *The physiography of Southern Ontario*. 2 ed. Ontario: University of Toronto Press.

Chaubey, I., A.S.Cotter, T.A. Costello, and T.S. Soerens. 2005. Effect of DEM data resolution on SWAT output uncertainty. *Hydrological Processes*19: 621–628.

Chen, S., D. Stechey, and R. F. Malone. 1994. Suspended solids control in recirculating aquaculture systems. In *Developments in aquaculture and fisheries sciences 27, aquacultine water reuse system: Engineering design and management*, ed. M.B. Timmons and T.M Losordo, 61-100. Amsterdam: Elsevier.

Chow, V.T. 1959. *Open-channel hydraulics*.McGraw-Hill civil engineering series. New York: McGraw-Hill.

CH2M HILL, 2001.*PLOAD Version 3 AnArcView GIS tool to calculate nonpoint sources of pollution in watershed and stormwater projects, User's Manual*. U.S. EPA Report.

Di Luzio, M., J.G. Arnold, and R. Srinivasan. 1998. Watershed oriented non-point pollution assessment tool. In *Computers in Agriculture - 7th international conference*. *October 26-30th 1998,* 233-241. Sponsored by ASAE, Orlando, FL.

Droppo, I.G., G.G. Leppard, D.T. Flannigan, and S.N. Liss. 1997. The freshwater floc: A functional relationship of water and organic and inorganic floc constituents affecting suspended sediment properties. *Water, Air & Soil Pollution* 99 (1/4):43-53.

Droppo, I.G, D.E. Walling, and E.D. Ongley. 1999. Suspended sediment structure: Implications for sediment and contaminant transport modelling. NWRS Contribution No. 99-098, National Water Research Institute. Burlington, Ontario, Canada.

Droppo, I.G, D.E. Walling, and E.D. Ongley. 2000. The influence of floc size, density and porosity on sediment and contaminant transport. In*The role of erosion and sediment transport in nutrient and contaminant transfer,* ed. M. Stone, 141-147.IAHS Publication No. 263.

Droppo, I.G. 2001.Rethinking what constitutes suspended sediment. *Hydrological Processes 1*5:1551-1564.

du Boys, P. 1879. *Le Rhone et les rivieres a lit affouillable, Annals des Ponts Chaussees*5(18):141-195.

Eisma, D. 1993. *Suspended matter in the aquatic environment*. Berlin: Springer-Verlag.

Elliott, E. T., I. C. Burke, C. A. Monz, and S. D. Frey. 1994. Terrestrial carbon pools in grasslands and agricultural soils: Preliminary data from the Corn Belt and Great Plains regions. *SSSA Special Publication* 35:179-191.

Elwell, H. A. 1977. *A soil loss estimation system for Southern Africa: fourth Rhodesian science congress 1977*. Salisbury: Department of Conservation and Extension.

ENCRPB 1975.Water quality study of Cayuga Creek. Erie and Niagara Counties Regional Planning Board.

Foster, G.R. 1986. *Understanding ephemeral gully erosion (concentrated Flow Erosion).* In *soil conservation: Assessing the National Resources Inventory,* vol. 2, ed. Committee on Conservation Needs and Opportunities. Board on Agriculture, 90-128 Washington, DC:National Academy Press.

Foster G. R. 1988. Modeling soil erosion and sediment yield. In *Soil erosion research methods (2 ed),* ed. R. Lal, 97-118. Soil and Water Conservation Society, Iowa: Ankeny.

Foster, G. R., L.J. Lane, M.A. Nearing, S.C. Finkner, and D.C. Flanagan. 1989. *Erosion component.* In*USDA-Water erosion prediction project: Hillslope profile version:profile model Documentation NSERL Report No. 2*, ed. L.J. Lane and M.A. Nearing, 10.1-10.2. W. Lafayette, Ind: National Soil Erosion Research Laboratory, USDA, Agricultural Research Service.

Free, G. R. 1960. Erosion characteristics of rainfall.*Agricultural Engineering* 41:447-455.

Govers, G. and J. Poesen. 1986. A field-scale study of surface sealing and compaction on loam and sandy loam soils. Part I. Spatial variability of soil surface sealing and crusting. In*Assessment of soil surface sealing and crusting: proceedings of the symposium held in Ghent, Belgium, 1985,* ed. F. Callebaut, D. Gabriels and M. de Boodt, 171-182. Ghent: University of Ghent.

Graf, W. H. 1971. *The hydraulics of sediment transport*. New York: McGraw-Hill.

GreenW.H., and G.A. Ampt.1911. Studies on soil physics, part I, the flow of air and water through soils. *The Journal of Agricultural Science* 4(1):1-24.

Guy, H.P. 1964. An analysis of some storm period variables affecting stream sediment transport.US Geological Survey Professional Paper 462-E.

Hadley, R.F., and L. M. Shown. 1976. Relation of erosion to sediment yield. In *Proceedings, Third Federal Inter-Agency Sedimentation conference: March 22-25, 1976, Denver, Colorado,* 132-139.Washington, DC: U.S. Government Printing Office.

Hanson, G.J. 1990. Surface erodibility of earthen channels at high stresses.PartII-Developing an in situ testing device.*Transactions of the ASAE* 33(1):132-137.

Hanson, G.J. 1991. Development of a jet index method to characterize erosion resistance of soils in earthen spillways.*Transaction of the ASAE* 36(5):2015-2020.

Horton, R.E. 1933. The role of infiltration in the hydrologic cycle.*Transactions of the American Geographical Union* 14:446-460.

Howard A. 1984. Sufficient conditions for river meandering: a simulation approach. *Water Resources Research* 20(11): 1659–1667.

Irvine, K., and M. Perrelli. 2006. *Synthesis/Mapping Environmental Data of the Niagara River Tributaries*. Report to the U.S. Environmental Protection Agency, Region 2, 8 p. with 4 Interactive CDs.

Julien, P.Y. 1995. *Erosion and Sedimentation*. New York: Cambridge University Press.

Kelly, J., I. Thornton, and P. R. Simpson. 1996. Urban geochemistry: a study of the influence of anthropogenic activity on the heavy metal content of soils in traditionally industrial and non-industrial areas of Britain. *Applied Geochemistry: Journal of the International Association of Geochemistry and Cosmochemistry* 11(1/2):363-70.

Kirkby, M. J. 1980. *Modelling water erosion processes.* In *Soil Erosion,* ed. M. J. Krikby and R. P. C. Morgan, 183-216. New York: John. Wiley & Sons.

Klimpel, R.C., R. Hogg. 1986. Effects of flocculation conditions on agglomerate structure. *Journal of Colloid Interface Science* 113:121-131.

Krishnappan, B.G. 2000.In-situ size distribution of suspended particles in the Fraser River.*Journal of Hydraulic Engineering* 126(8):561-569.

Krishnappan, B.G. 2000.Modelling cohesive sediment transport in rivers.In *The role of erosion and sediment transport in nutrient and contaminant transfer,* ed. M. Stone, 269-276.IAHS Publication No. 263. Wallingford: IAHS.

Lal, R. 1994. *Soil erosion researchmethods*. 2nd ed. Delray Beach, Fl: St. Lucie Press.

Lambe, T.W., and R.V. Whitman. 1969. *Soil mechanics*. New York: John Wiley & Sons.

Lavelle, P., and A.V. Spain. 2001. *Soil ecology*. Dordrecht ; Boston: Kluwer Academic Publishers.

Lawler, D.F. 1993. Physical aspects of flocculation: from microscale to macroscale. *Water Science and Technology* 27(10):165-180.

Laws, J.O. 1941.Measurement of the fall velocity of water drops and raindrops.*Transactions of the American Geographical Union* 22:709-721.

Li, J., M. Chen, and F. Zheng. 1997.Diffusion theory of slow responses. *Science in China Series a Mathematics Physics Astronomy* 40 (3):290-296.

Li, D. H. and J. Ganczarczyk.1987.Stroboscopic determination of settling velocity, size, porosity of activated sludge flocs. *Water Research* 21:257-262.

Lick, W., H. Huang, and R. Jespen. 1993. Flocculation offline-grained sediment due to differential settling. *Journal of Geophysical Research* 98(6):10279–88.

Linsley, R.K., M.A. Kahler, and J.L.H. Paulhus.1958. *Hydrology for Engineers*. New York: McGraw-Hill.

Linsley, R.K., M.A. Kahler., and J.L.H.Paulhus. 1982. *Hydrology for engineers.* 3rd ed. New York: McGraw-Hill.

Lorup, J.K., and M. Styczen.1996. Soil Erosion Modelling. In *Distributed Hydrological Modelling,* ed. M.B. Abbott and J.C. Refsgaard, 93-120. The Netherlands: Kluwer Academic Publishers.

Meyer, L.D., and E.J. Monke. 1965.Mechanics of soil erosion by rainfall and overland flow. *Transactions of ASAE* 8:572–580.

Meyer, L.D., and W.H. Wischmeier.1969. Mathematical simulation of the process of soil erosion by water. *Transactions of the American Society of Agricultural Engineers* 12:654-762.

Meyer, L. D., G.R. Foster, and M. J.M. Romkens. 1975b. Sources of soil ended by water from upland slopes. In *Present and Prospective Technology for Predicting Sediment Yields and Sources*, USDA-Agricultural Research Service Publication ARS-S-40, 177-189.

Meyer, L. D., and K.G. Renard. 1991. How research improves land management. In *Agriculture and the Environment,USDA Yearbook of Agriculture,* 20-27, Washington, DC: U.S. Government Printing Office.

Mielke H.W., C.R. Gonzales, M.K. Smith, and P.W. Mielke. 1999. The urban environment and children's health: soils as an integrator of lead, zinc, and cadmium in New Orleans, louisiana, USA. *Environmental Research*81(2):117-29.

Mielke, H.W., G. Wang, C.R. Gonzales, E.T. Powell, B. Le, and V.N. Quach. 2004. PAHs and metals in the soils of inner-city and suburban. New Orleans, Louisiana, USA. *Environmental Toxicology And Pharmacology* 18(3):243-248.

Miller J.J., E.C. Olson, D.S. Chanasyk, B.W. Beasley, F.J. Larney, and B.M. Olson. 2006. Phosphorus and nitrogen in rainfall simulation runoff after fresh and composted beef cattle manure application. *Journal of Environmental Quality* 35(4):1279-1290.

Mutchler, C. K., C.E. Murphree, and K. C. McGregor. 1988. Laboratory and field plots for soil erosion studies. In *Soil erosion research methods,* ed. R. Lal, 9-36.Soil and Water Conservation Society, IA: Ankeny.

Mutchler, C.K., C.E. Murphree, and K.C. McGregor. 1994. Laboratory and field plots for erosion studies. In *Soil Erosion Research Methods,* ed. R. Lal, 11-38. Delray Beach, FL: St. Lucie Press.

Nearing, M. A., L.J. Lane, and V.L. Lopes. 1994. Modelling soil erosion. In *Soil Erosion Research Methods,* ed. R. Lal, 127-156. Delray Beach, FL: St. Lucie Press.

Neitsch, S., J.G. Arnold, and J.R. Williams.2002b. *Soil and Water Assessment Tool User's Manual Version 2000.* http://www.brc.tamus.edu/swat/downloads/doc/swatuserman.pdf.(last accessed 12 January 2009).

Neitsch, S.L., J. G. Arnold, J.R. Kiniry, and J. R. Williams.2002a. *Soil and Water Assessment Tool theoretical documentation version 2000*.http://www.brc.tamus.edu/swat/downloads/doc/swat2000theory.pdf(last accessed 12 January 2009).

New York Power Authority. 2006. *Cayuga Creek Watershed Assessment: Summary Report.*Niagara Power Project.New York Power Authority and Gomez and Sullivan Engineers, P.C.

New York State Department of Environmental Conservation. 2005b. *The Niagara River-Lake Erie Drainage Basin*. Sampling Years 2000-2001. February 2005. Division of Water.

New York State Department of Health. 2005. Chemicals in Sportfish and Game: 2005-2006 Health Advisories.

Niagara County Department of Planning, Development, and Tourism.1997. *Cayuga Creek Management Study*. Niagara County, New York: Research Report.

Nicholas, A.P., and D.E. Walling. 1996. The significance of particle aggregation in the overbank deposition of suspended sediment on river floodplains. *Journal of Hydrology* 186(1-4):275.

Nichols, G. 1999. *Sedimentology and stratigraphy*. Oxford: Blackwell Science.

Osterkamp, W.R., P. Heilman, and L.J. Lane. 1998. Economic considerations of a continental sediment monitoring program. *International Journal of Sediment Research* 13(4):12-24.

Ottesen R.T., and M. Langedal. 2001. Urban geochemistry in Trondheim, Norway. *NGU-Bulletin* 438:63-9.

Sharma, P.P., S.C. Gupta, and G.R. Foster. 1993. Predicting soil detachment by raindrops. *Soil Science Society of America Journal* 57:674-680.

Park, S.W., J.K. Mitchell, and J.N. Scarborough. 1982. Soil erosion simulation on small watersheds: A modified answer model. *Transactions of the ASAE* 25:1581-1588.

Patra, K.C. 2001. *Hydrology and water resources engineering*. Pangbourne, UK: Alpha Science International.

Phillips, J.M., and D.E. Walling. 1999. The particle size characteristics of fine-grained channel deposits in the River Exe Basin, Devon, UK. *Hydrological Processes* 13(1):1-19.

Pirsson, L.V., and A. Knopf. 1929. *Rocks and rock minerals; a manual of the elements of petrology without the use of the microscope*. New York: John. Wiley & Sons.

Prest, J.M. 1981. *The Garden of Eden: the botanic garden and the re-creation of paradise.* New Haven: Yale University Press.

Price, C., N. Naomi, K.J. Hitt, and R.M. Clawges. 2003. Mining GIRAS: Improving on a national treasure of land use data. In *Proceedings of the 23rd ESRI International Users Conference, July 7-11, 2003, Redlands Calif.*http://gis.esri.com/library/userconf/proc03/p0904.pdf (last accessed 12 October 2008).

Refsgaard, J. C. 1996. Terminology, modelling protocol and classification of hydrological model codes.In *Distributed hydrological modelling*, ed. M.B. Abbott and J.C. Refsgaard, 17-39. Dordrecht: Kluwer Academic.

Renard, K.G., G.R. Foster, D.C. Yoder, and D.K. McCool. 1994. RUSLE revisited: Status, questions, answers, and the future. *Journal of Soil and Water Conservation* 49(3):213.

Renard, K.G., G.R. Foster, G.A. Weesies, D.K. McCool, and D.C. Yoder. 1997. *Predicting soil erosion by water: a guide to conservation planning with the revised universal soil loss equation (RUSLE)*. USDA-ARSAgriculture Handbook No. 703.Washington, DC: U.S. Department of Agriculture, Agricultural Research Service.

Reeve, J.S. 1982.Bond Percolation and the Yang-Lee Edge Singularity Problems in Three Dimensions.*Journal of Physics A-Mathematical and General* 15(9):521-524.

Reynolds, O. 1883.An experimental investigation of the circumstances which determine whether the motion of water shall be direct or sinuous, and of the law of resistance in parallel channels.*Philosophical Transactions of the Royal Society of London* 174:935-982.

Richman, L. 1999. *Niagara River Mussel Biomonitoring Program, 1997*. Toronto: Ontario, Ministry of the Environment.

Rose, J. H., J. R. Smith, and J.Ferrante. 1983. Universal features of bonding in metals.*Physical Review Series B* 28:1835-1845.

Savat, J. 1981. Work done by splash: laboratory experiments. *Earth Surface Process-Landforms* 6:275-283.

Schueler, T.R. 1994. The importance of imperviousness.*Watershed Protection Techniques* 1(3):100-110.

Schumm, S.A. 1977. *The Fluvial System.*New York: John. Wiley & Sons.

Scoging H. 1989. Runoff generation and sediment mobilization by water.In *Arid Zone Geomorphology*, ed. D.S.G. Thomas, 87-116. Bell Haven: London.

Sharma, M.M.,M.A. Nagarajan, and P. Ring. 1993. Rho meson coupling in the relativistic mean field theory and description of exotic nuclei. *Physics Letters Series B* 312 (4):377-381.

Shields, A. J., M. Pepper, M.Y. Simmons, and D.A. Ritchie. 1995. Spin-triplet negatively charged excitons in GaAs quantum wells. *Physical Review Series B*52(11):7841-7844.

Skidmore, E.L. 1994. Wind erosion. In *Soil erosion research methods*,ed. R. Lal, 265-293.Delray Beach, FL: St. Lucie Press.

Smoot, G. F., C.L.Bennett, A. Kogut, et al. 1992. Structure in the COBE differential microwave radiometer first-year maps.*The Astrophysical Journal*396 (1): L1-L5.

Soil and Conservation Service. 1972. *National engineering handbook, section 4, Hydrology.* U.S. Department of Agriculture,Washington, DC: U.S. Government Printing Office.

Stantec Consulting Services, Inc., URS Corporation, Gomez and Sullivan Engineers, P.C., and E/PRO Engineering & Environmental Consulting, LLC. 2005. *Effect of Water Level and Flow Fluctuations on Aquatic and Terrestrial Habitat*. prep. for the New York Power Authority.

Stone, M., and B.G. Krishnappan. 2003. Floc morphology and size distributions of cohesive sediment in steady-state flow. *Water Research* 37(11): 2739-2747.

Temple, P.H. and A. Sundborg. 1972. The Rufiji River, Tanzania: hydrology and sediment transport. *Geografiska Annaler Serie A* 54:345-68.

Toy, T.J., G.R. Foster, and K.G. Renard. 2002. *Soil erosion: processes, prediction, measurement, and control*. New York: John Wiley & Sons.

Thomas, A.W., R. Welch, and T.R. Jordan. 1986. Quantifying concentrated flow erosion on cropland with aearial photogrammetry. *Journal of Soil Water Conservation* 41(40):249-252.

Trimble, S.W. 1977. The fallacy of stream equilibrium in contemporary denudation studies.*American Journal Science* 277:876-887.

Troeh, R.F., J. A. Hobbs, and R. L. Donahue. 1980. *Soil and water conservation for productivity and environmental protection*. Englewood Cliffs, NJ: Prentice-Hall.

Troeh, R.F., J.A. Hobbs, and R.L. Donahue. 1991. *Soil and Water Conservation.*2ed.Upper Saddle River, NJ: Prentice Hall.

Truman, C.C. and J.M. Bradford. 1990. Effect of antecedent soil moisture on splash detachment under simulated rainfall. *Soil Science* 150:787-798.

U.S. Army Corps of Engineers - Buffalo District.2002. *Cayuga Creek, Niagara County, New York, Flooding and Related Water Resources*. Section 905(b) (WRDA 86) Analysis Reconnaissance Report.

URS Greiner Consultants, Inc. 2000.Town of Lewiston Comprehensive Plan, Draft Generic Environmental Impact Statement.

URS Corporation and Gomez and Sullivan Engineers, P.C. 2005. *Surface Water Quality of the Niagara River and its U.S. Tributaries*. Prep. for the New York Power Authority.

URS Corporation, Gomez and Sullivan Engineers, P.C., and E/PRO Engineering & Environmental Consulting, LLC. 2005a. *Groundwater Flow Investigations in the Vicinity of the Niagara Power Project.*Prep. for the New York Power Authority.

URS Corporation, Gomez and Sullivan Engineers, P.C., and E/PRO Engineering & Environmental Consulting, LLC. 2005b. *Ecological Condition of Gill, Fish, and Cayuga Creeks.* Prep. for the New York Power Authority.

U.S. Fish and Wildlife Service. 2005a. *Impacts of Storm Water Discharge from Niagara Falls Air Reserve Station on Cayuga Creek.* Prep. For the Niagara Falls Air Reserve Station, Niagara Falls, NY.

U.S. Fish and Wildlife Service.2005b. *Restoration Plan and Environmental Assessment for the Love Canal, 102nd Street, and Forest Glen Mobile Home Subdivision Superfund Sites*. Cortland, NY.

U.S. Environmental Protection Agency, 2000. U.S. Geological Survey GIRAS land use and land cover data in ArcInfo format, http://www.epa.gov/ngispgm3/spdata/EPAGIRAS/ Tool theoretical documentation version 2000. (last accessed 22 August 2008).

Ward, R.C., and M. Robinson. 1990. *Principles of Hydrology*. 3rded. New York: McGraw-Hill International Editions.

Williams, J. R., 1975. Sediment-Yield Prediction with Universal Equation Using Runoff Energy Factor.In Present and Prospective Technology for Predicting Sediment Yields and Sources, Agricultural Research Service, ARS-S-40, 244-252. Washington, DC: U.S. government Printing Office.

Williams, J.R. 1980. SPNM, a model for predicting sediment, phosphorus, and nitrogen yields from agricultural basins. *Water Resource Bulletin* 16:843-848.

Williams, J.R. 1995. The EPIC Model.In *Computer models of watershed hydrology,*ed.V.P. Singh, 909–1000. Highlands Ranch, CO: Water Resources Publications.

Walling, D.E. 1988. Measuring sediment yield from river basins.In*Soil erosion research methods,* ed.R.Lal, 39-82.Soil and Water Conservation Society, IA: Ankeny.

Webster, J.R., S.W. Golladay, E.F. Benfield, D.J. D'Angelo, and G.T. Peters. 1990. Effects of Forest Disturbance on Particulate Organic Matter Budgets of Small Streams. *Journal of the North American Benthological Society* 9(2):120-140.

Wischmeier, W.H. 1959. A rainfall erosion index for a universal soil loss equation.*Soil Science Society of America Proceeding* 23(3): 246-249.

Wischmeier, W.H., and D.D. Smith. 1965. *Predicting rainfall-erosion losses from cropland east of the Rocky Mountains: A guide for selection of practices for soil and water conservation.*Agricultural Handbook No. 282. U.S. Department of Agriculture, Washington, DC:Agricultural Research Service.

Wischmeier, W.H., and D.D. Smith. 1978. *Predicting rainfall erosion losses: a guide to conservation* planning. Agriculture Handbook No. 537. U.S. Department of Agriculture, Washington, DC: U.S. Government Printing Office.

Whittemore RC, and J. Beebe. 2000. EPA's BASINS model: good science or serendipitous modeling? *Journal of the American WaterResources Association* 36(3): 493–499.

Wolman, M.G. and A.P. Schick. 1967.Effects of construction on fluvial sediment, urban and suburban areas of Maryland. *Water Resources Research* 3:451-464.

Young, R.A., C.A. Onstad, D.D. Bosch and W.P. Anderson. 1989. AGNPS: A nonpoint source pollution model for evaluating agricultural watersheds.*Journal of Soil Water Conservation* 44:168-173.

Zachar, D. 1982. *Soil Erosion: Developments in Soil Science 10*. Amsterdam: Elsevier Scientific. 547